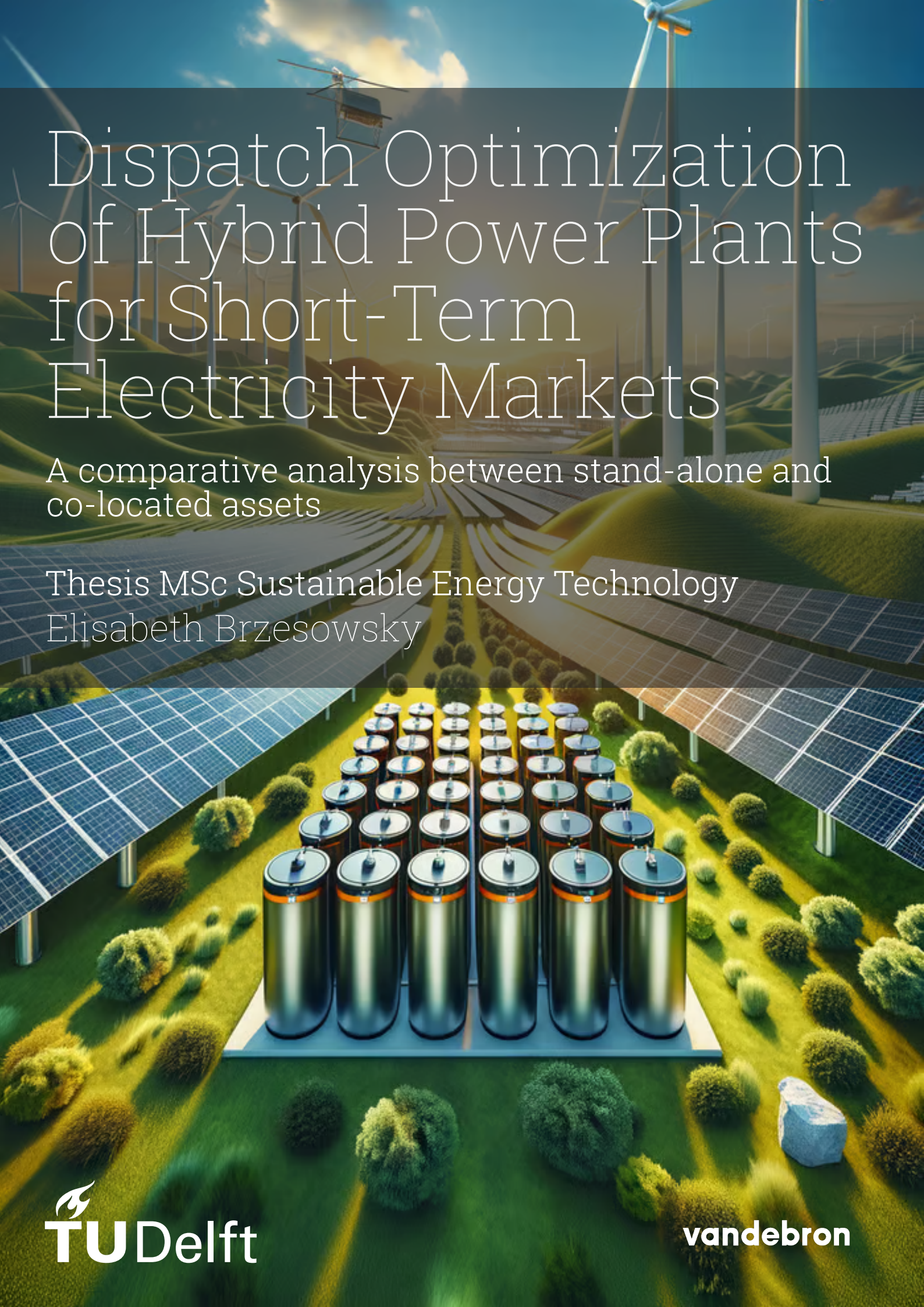

Dispatch Optimization of Hybrid Power Plants for Short-Term Electricity Markets

A comparative analysis between stand-alone and co-located assets

Thesis MSc Sustainable Energy Technology

Elisabeth Brzesowsky

TU Delft

vandebron

Dispatch Optimization of Hybrid Power Plants for Short-Term Electricity Markets

A comparative analysis between stand-alone and co-located assets

by

Elisabeth Brzesowsky

To obtain the degree of Master of Science in Sustainable Energy Technology
at Delft University of Technology

Wind Energy Group, Faculty of Aerospace Engineering
Faculty of Electrical Engineering, Mathematics and Computer Science
Delft University of Technology

Vandebron Energie B.V.

Student Number:	4865383
Project duration:	December 1, 2024 - July 16, 2025
Electronic version:	http://repository.tudelft.nl
Publicly defended:	July 16, 2025, Faculty of Aerospace Engineering
Thesis Comittee:	Prof.dr. D.A. von Terzi, TU Delft, Chair
	Dr.ir. K. Bruninx, TU Delft, Second member
	Dr.ir. J. Iori, TU Delft, Third member and supervisor
	ir. N. van den Bos, Vandebron, External member and supervisor

Preface

In 2018, I began my academic journey at Delft University of Technology. Fresh out of high school, I chose to start the BSc in Systems Engineering, Policy Analysis and Management. Although this program placed technology in a broader context, I found myself missing the in-depth technical aspects. After completing my propaedeutic year, I decided to switch to the BSc in Mechanical Engineering. I thoroughly enjoyed the challenging courses and the various group projects.

After finishing my bachelor's degree, I once again felt the urge to connect the technical knowledge I had gained with a broader perspective. This led me to go on an exchange to the University of British Columbia in Vancouver, Canada. There, I gained new insights into the role of technology in today's world, and made memories for life, especially during time spent with new friends in the breathtaking Canadian nature.

These experiences further sparked my passion for sustainability and motivated me to begin the MSc in Sustainable Energy Technology the following year. This program offered everything from solar cells at the nanoscale to energy systems at the gigawatt scale, combining in-depth technological understanding with system behavior. It aligned perfectly with my interest in both technical details and the societal, political, and economic aspects of energy. From this, I take with me an analytical way of thinking and a drive fueled by passion and curiosity.

Beyond academic growth, the past seven years have shaped me personally. Through many group projects, I encountered new people, perspectives, and ideas. While they broadened my view of the world, they also challenged my own beliefs and working style, teaching me that there's more than one path to success. More importantly, I made many new friends along the way.

Now that my time at TU Delft is coming to an end, I look back with joy and gratitude. Especially over the past eight months, I have learned a great deal. Working on one project for such an extended period has been a true eye-opener. I've enjoyed the variety and excitement that came with each stage of the research, while deepening my understanding of hybrid power plants, electricity markets, and coding.

This whole process would not have been possible without the people around me. First of all, I want to thank Jenna Iori, who guided me closely during our meetings and provided in-depth feedback on my report. Your open and critical attitude has truly helped me. I also want to thank my colleagues at Vandebron for welcoming me and making my time there so enjoyable and fun. In particular, I'd like to thank Niek van den Bos, without your guidance, ideas, and brainstorming sessions, this thesis and the road leading up to it would not have been the same. Lastly, I want to thank my family and friends for always supporting me.

I am truly proud of the final result of this thesis project. I've learned a lot and hope it provides valuable insights into the functioning of electricity markets and systems, and how hybrid power plants can contribute to a reliable and sustainable energy system.

Elisabeth Brzesowsky
Amsterdam, July 2025

Executive Summary

The transition to a sustainable energy system has accelerated the integration of renewable energy sources (RES), such as wind and solar power, into electricity markets and infrastructures. While these sources contribute significantly to the decarbonization of the energy sector, their inherent variability and limited predictability introduce operational challenges for maintaining system balance and ensuring cost-effective grid utilization. Additionally, the geographic distribution of RES, often located in remote areas, has exacerbated issues of grid congestion, leading to limitations in grid access, rising curtailment levels, and deferred renewable projects. In response to these challenges, Hybrid Power Plants (HPPs), which co-locate RES with Battery Energy Storage Systems (BESS), have emerged as a viable solution offering increased operational flexibility, improved forecast error mitigation, and enhanced economic performance, while utilizing one grid connection point.

This study evaluates the added economic and energetic value of co-locating a BESS with a RES under the Dutch electricity market structure. A multi-stage stochastic optimization framework is developed to simulate HPP participation across the day-ahead, intraday, and imbalance markets. The model incorporates power forecast uncertainty through scenario generation and reduction techniques, and captures the physical constraints of energy systems, including battery operations and capacity, RES capacity, and restricted grid connection capacity. Optimization is conducted on a rolling horizon to reflect the sequential nature of market decision-making.

Three configurations are analyzed: a standalone RES system, a standalone BESS, and a co-located HPP. These systems are evaluated based on simulated operations over four weeks each representing a season using real market prices and wind power data. The co-located HPP demonstrates superior performance in terms of both economic return and renewable energy utilization. By enabling time-shifting of generation, reducing curtailment, and participating more effectively in short-term markets, the HPP captures additional value that standalone systems cannot access. Moreover, the ability to operate flexibly within a fixed grid export limit allows the HPP to relieve grid congestion, using storage to shift energy dispatch in line with the needs of the electricity system, indicated by price signals, thereby reducing strain on network infrastructure.

A comprehensive analysis investigates the impact of key assumptions regarding price and power forecasts and operational parameters, such as battery size, technology characteristics, grid connection capacity, and reoptimization frequency. Results indicate that system performance is highly dependent on the quality of imbalance price forecasts and the ability to respond dynamically to power forecast updates and market prices. This has been demonstrated by a comparison between no foresight, perfect foresight and using the day-ahead clearing price as imbalance forecast. Moreover, allowing the HPP to withdraw energy from the grid, results in signficant economic gains, however, this comes at the cost of renewable energy utilization. Although the study excludes capital and degradation costs, the findings underscore the operational advantages of co-locating RES and BESS under uncertainty and grid limitations.

Overall, this research contributes to a deeper understanding of how flexible, market-responsive HPPs can support the transition to a resilient and economically efficient low-carbon power system. It highlights the importance of integrated modeling approaches for optimizing renewable dispatch strategies in evolving electricity markets, while also demonstrating how HPPs can contribute to better utilizing grid connection capacity and enabling greater renewable integration.

Contents

List of Figures

List of Tables

Nomenclature

Abbreviations

Abbreviation	Definition
aFRR	Automatic Frequency Restoration Reserve
ARMA	Auto-Regressive Moving Average
BESS	Battery Energy Storage System
BRP	Balance Responsible Party
BSP	Balance Service Provider
CAPEX	Capital Expenditures
D	Day of energy delivery
D-1	Day before energy delivery
D+1	Day after energy delivery
DA	Day-Ahead Market
DoD	Depth of Discharge (minimum allowable battery energy level)
EMS	Energy Management System
ENTSO-E	European Network of Transmission System Operators for Electricity
ESS	Energy Storage System
FCR	Frequency Containment Reserve (primary reserve service)
HPP	Hybrid Power Plant (co-location of RES and BESS under one grid connection)
ID	Intraday Market
IDA	Intraday Auction
ISP	Imbalance Settlement Period (typically 15 minutes)
MAC	Marginal Avoided Cost (used in day-ahead bidding)
MILP	Mixed Integer Linear Programming
mFRR	Manual Frequency Restoration Reserve (tertiary reserve service)
MLE	Maximum Likelihood Estimation
NEMO	Nominated Electricity Market Operator
OPEX	Operational Expenditures
PV	Photovoltaic (solar energy technology)
RES	Renewable Energy Sources
RMSE	Root Mean Square Error
RO	Robust Optimization (worst-case based decision-making under uncertainty)
SO	Stochastic Optimization (probabilistic decision-making under uncertainty)
SoC	State of Charge (energy level of the battery)
TSO	Transmission System Operator
VRFB	Vanadium Redox Flow Battery
VPP	Virtual Power Plant
WF	Wind Farm
XBID	Cross-Border Intraday Market (European continuous trading platform)

Symbols

Symbol	Definition	Unit
$P_{\text{DA},t}$	Power committed in the day-ahead market at time step t	[MW]
$P_{\text{ID},t}$	Power traded in the intraday market at time step t	[MW]
$P_{\text{IM-forecast},j,t}$	Expected power imbalance in scenario j at time t	[MW]
$P_{\text{IM},t}$	Realized power imbalance in scenario at time t	[MW]
$\hat{P}_{\text{source},j,t}$	Forecasted renewable generation in scenario j at t	[MW]
$P_{\text{HPP},j,t}$	Net hybrid power plant output in scenario j at t	[MW]
$P_{\text{battery},j,t}$	Net battery power (positive = discharging, negative = charging)	[MW]
$P_{\text{charge},j,t}$	Battery charging power	[MW]
$P_{\text{discharge},j,t}$	Battery discharging power	[MW]
$P_{\text{curtail},t}$	Curtailed renewable generation	[MW]
$P_{\text{realized,curtail},t}$	Realized curtailed power due to grid or storage limits	[MW]
$P_{\text{max-source}}$	Installed renewable capacity	[MW]
$P_{\text{max-battery}}$	Battery charge/discharge power limit	[MW]
$P_{\text{grid-feed-in}}$	Maximum export capacity to the grid	[MW]
$P_{\text{grid-withdraw}}$	Maximum import capacity from the grid	[MW]
$E_{\text{battery},j,t}$	Battery energy (SoC) in scenario j at time t	[MWh]
$E_{\text{start},i}$	Battery energy at start of iteration i	[MWh]
E_{initial}	Initial SoC at beginning of simulation	[MWh]
$E_{\text{max-battery}}$	Maximum battery energy capacity	[MWh]
E_{DoD}	Minimum energy (depth of discharge limit)	[MWh]
η_{battery}	Round-trip battery efficiency	[–]
C	C-rate — reciprocal of time to fully (dis)charge battery at max power	[h^{-1}]
t	Timestep index	[–]
dt	Duration of a timestep	[h]
$N_{t,i}$	Number of time steps of optimization window i	[–]
T_{sim}	Total simulation time horizon	[h]
t_{update}	Update interval between optimizations	[–]
$t_{\text{current},i}$	Time step at which the i^{th} optimization of intraday bidding and expected imbalance is performed	[–]
i	Optimization iteration index (re-optimization loop)	[–]
N_i	Total number of re-optimization iterations	[–]
s	Scenario index	[–]
N_s	Total number of generated forecast scenarios	[–]
j	Scenario cluster index	[–]
N_c	Number of representative scenario clusters	[–]
M	Big-M constant for binary constraint enforcement	[–]
$u_{\text{charging},j,t}$	1 if battery is charging in j, t; 0 otherwise	[–]
$u_{\text{regulation},t}$	1 if system is in surplus; 0 if in shortage at t	[–]
$u_{\text{ID},t}$	1 if intraday trade executed at t; 0 otherwise	[–]
$u_{\text{buy-possible},t}$	1 if intraday buying is possible at t	[–]
$u_{\text{sell-possible},t}$	1 if intraday selling is possible at t	[–]
$\varepsilon_{j,t}$	Forecast error in scenario j at time t (ARMA residual)	[MW]
$\varepsilon_{\text{historical},t}$	Historical forecast error used for ARMA training	[MW]
ϕ_i	i-th AR coefficient in ARMA(p, q), $i = 1, ..., p$	[–]
θ_i	i-th MA coefficient in ARMA(p, q), $i = 1, ..., q$	[–]
μ	Mean level of ARMA forecast error process	[–]
p	Order of autoregressive process in ARMA(p, q)	[–]
q	Order of moving average process in ARMA(p, q)	[–]
$\lambda_{\text{ID},t}$	Intraday market price	[€/MWh]
$\lambda_{\text{IM},j,t}$	Realized imbalance price in scenario j at t	[€/MWh]

Symbol	Definition	Unit
$\lambda_{\text{IM,long},t}$	Imbalance price in surplus (long) direction	[€/MWh]
$\lambda_{\text{IM,short},t}$	Imbalance price in shortage (short) direction	[€/MWh]
$\Pi_{\text{DA},i,t}$	Day-ahead revenue at time t in iteration i	[€]
$\Pi_{\text{ID},i,t}$	Intraday revenue at time t in iteration i	[€]
$\Pi_{\text{IM-forecast},j,t}$	Expected imbalance revenue in scenario j at time t	[€]
$\Pi_{\text{IM},t}$	Realized mbalance revenue in scenario at time t during real time operation	[€]
$\Pi_{\text{DA,realized}}$	Cumulative realized day-ahead revenue	[€]
$\Pi_{\text{ID,realized}}$	Cumulative realized intraday revenue	[€]
$\Pi_{\text{IM,realized}}$	Cumulative realized imbalance revenue	[€]
$\Pi_{\text{total,realized}}$	Total realized revenue from all markets	[€]

1

Introduction

This chapter introduces the context and motivation for the research, offering a foundation for understanding the challenges and opportunities related to hybrid power plant (HPP) operation in electricity markets. Section 1.1 outlines the background and key developments driving the need for HPP integration in the current energy system. This is followed by a literature review in Section 1.2, which summarizes recent advancements and identifies gaps in current research. Based on these insights, the research objectives are defined in Section 1.3, and the scope and limitations of the study are detailed in Section 1.4.

1.1. Context and Background

In recent years, the energy transition has gained significant momentum, driven by climate goals and the push toward sustainable energy systems. As a result, electricity production is shifting away from fossil fuels toward renewable energy sources (RES), such as wind and solar power [1]. In the Netherlands and surrounding countries, this has led to the large-scale development of wind farms (WF) and photovoltaic (PV) parks. While the integration of these technologies contributes to a cleaner energy mix, it also introduces a set of challenges that must be addressed to ensure a reliable and cost-effective electricity system [2].

One of the central challenges stems from the mismatch between where and when electricity is generated versus when and where it is needed. Geographically, wind and solar installations are typically built in remote locations with favorable weather conditions, far from the urban or industrial centers where electricity demand is concentrated. This increases the strain on transmission networks and contributes to growing grid congestion [3]. Temporally, RES generation does not always align with demand. As illustrated in Figure 1.1, wind and solar profiles follow natural patterns that rarely match consumption load profiles. This mismatch leads to inefficient use of grid infrastructure, which must be sized for peak capacity but is often underutilized.

As more RES are connected to the grid, grid access becomes a limiting factor. In many regions, network operators are unable to approve new RES projects due to lack of capacity. Moreover, curtailment of renewable generation is already occurring, and grid tariffs are rising as network upgrades struggle to keep pace. At the same time, market volatility increases: prices fluctuate more sharply due to the variability of weather conditions, and power forecasts become more uncertain [5]. This uncertainty results in deviations between day-ahead forecasts and actual production, leading to system imbalances that require costly balancing services and increase the need for flexible, controllable resources [6].

A promising solution to address these interconnected challenges is the deployment of HPPs, where renewable generation assets are co-located with battery energy storage systems (BESS). This system design can help mitigate several of the previously mentioned problems. First, by combining generation and storage under one grid connection, infrastructure can be used more efficiently, reducing peak loads and relieving grid congestion. Second, the BESS component provides steerable capacity, allowing operators to shift energy in time and balance short-term mismatches between supply and demand. Third,

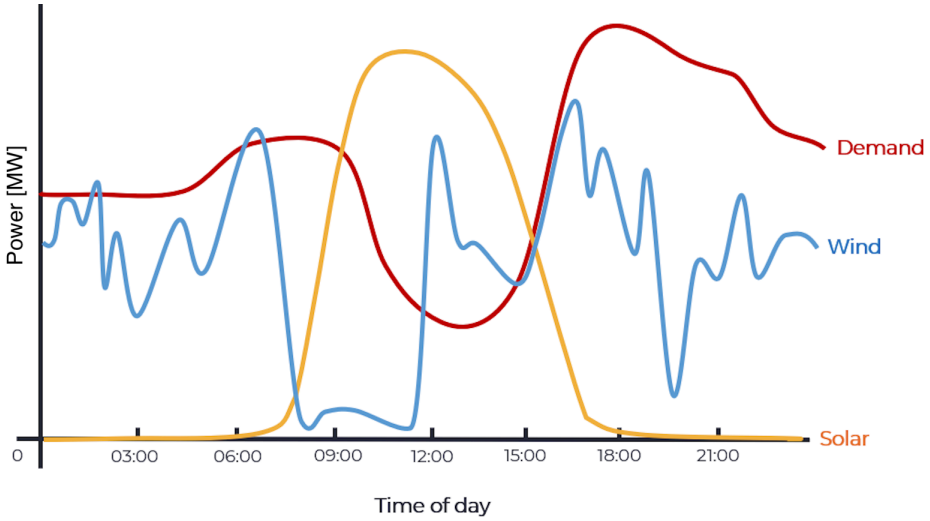

Figure 1.1: Example of variable load profiles for wind, solar, and demand over one day, showing the temporal mismatch between demand and supply of renewable energy sources [4]

batteries enable compensation for forecast errors, allowing the plant to manage its own imbalance position and reduce reliance on, and cost associated with, external reserve capacity.

In addition to technical innovations, the design of electricity markets is evolving to better accommodate the characteristics of intermittent generation. One important development is the transformation of the intraday market, where trading is now allowed up to the moment of delivery. Previously, cross-border intraday trading was restricted to one hour before delivery, but recent reforms have extended trading closer to real-time. This enables market participants to continuously update their positions based on the latest forecasts and price signals, thereby reducing forecast errors and improving operational efficiency [7]. Figure 1.2 illustrates the increasing trading volumes and liquidity in the intraday market, emphasizing its growing relevance for flexible assets such as HPPs.

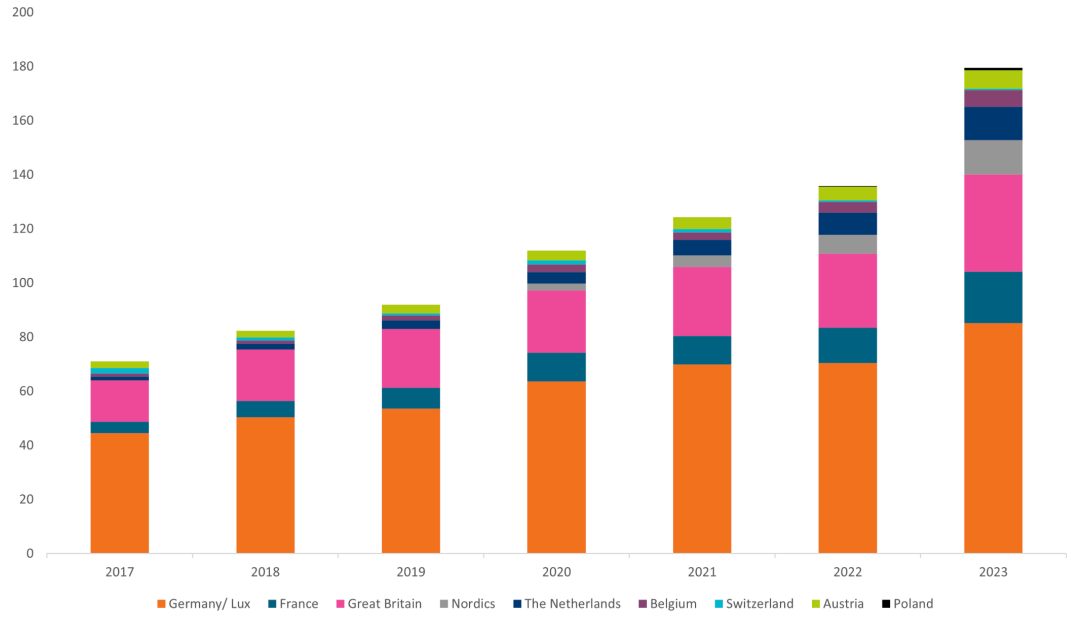

Figure 1.2: Traded volume on the intraday market per country [TWh/year] [7]

In parallel, the day-ahead market design is also undergoing changes. One anticipated shift is the transition from hourly bids to quarter-hourly bids, a reform aimed at aligning market operation more closely with the fluctuating nature of renewable energy production [8]. Such developments highlight

the increasing importance of forecasting accuracy and operational flexibility, further reinforcing the role that HPPs can play in supporting a reliable and efficient electricity system.

These developments highlight a clear need for renewable energy systems that are not only clean, but also flexible, responsive, and grid-compatible. HPPs offer a promising pathway to meet these requirements. However, their value depends on how well they can operate under uncertainty, manage grid constraints, and exploit market opportunities. This study investigates the operational and economic potential of HPPs by modelling their behavior in a stochastic optimization framework and evaluating their performance in realistic market conditions.

1.2. Literature Review

The integration of BESS with a RES, forming a HPP, has been extensively studied in recent years. The literature identifies several core themes in optimizing the economic and operational performance of HPPs: the role of BESS in operations and in multi-market participation strategies, the modeling of uncertainty, and scenario-based approaches for decision-making. This section reviews each theme, highlights current trends, and identifies remaining research gaps.

1.2.1. Operational and Economic Role of BESS in Hybrid Power Plants

The integration of a BESS with a RES into HPP enhances both operational flexibility and economic value. BESS technology enables HPPs to shift energy delivery in time, thereby increasing operational flexibility, offering services such as forecast error mitigation, energy arbitrage, and participation in reserve markets. The ability to provide several services simultaneously with a single asset is commonly referred to as value stacking.

A consistent theme across the literature is that value stacking substantially improves the profitability of BESS systems [9, 10, 11, 12]. For instance, Gomes et al. [9] investigate a combined wind and solar HPP and find that using BESS solely in the day-ahead market to mitigate imbalance does not yield an economically viable outcome. They stress the importance of exploiting additional services to fully realize the potential of hybrid systems. In a related study, Heredia, Cuadrado, and Corchero [10] show that while imbalance mitigation is essential for operational feasibility, further economic value is unlocked through energy arbitrage and the provision of balancing capacity. Their results indicate a 10.4% increase in profit due to arbitrage, with even greater gains when balancing services are included.

Other studies further support the positive impact of stacking services. Zhu et al. [11] and Ledro et al. [12] confirm that participating in multiple markets increases revenue, but also highlight the technical and operational constraints that limit this potential. Notably, the grid connection capacity plays a pivotal role in determining the dispatch flexibility of an HPP. A restricted export limit may cause overproduction and curtailment, increase battery cycling, and lead to accelerated degradation. The interaction between grid constraints and optimal BESS scheduling introduces trade-offs between economic gain and asset wear. Overplanting, where the combined output of the RES and BESS exceeds the nominal grid connection capacity, can further complicate this balance.

Beyond technical operation, the market participation strategy of HPPs is a major determinant of their economic value. Several studies evaluate participation across multiple electricity markets, including the day-ahead, intraday, and balancing markets, an elaborate explanation of these markets can be found in Chapter 2. In the day-ahead market, producers submit bids based on forecasted generation, but deviations in real-time introduce imbalances. BESS systems enable HPPs to compensate for these deviations, reducing imbalance costs and increasing revenue. Das et al. [13] report a 10% increase in day-ahead market revenue through BESS-supported forecast error compensation, though they do not consider degradation costs. Similarly, Ledro et al. [12] find that joint HPP operation reduces imbalances by 35.6%, but results in a 2.37% decrease in profit compared to separate operation, highlighting the complexity of co-optimizing multiple value streams.

Participation in the intraday market offers additional flexibility, as trading closer to the time of delivery allows actors to adjust schedules based on updated forecasts. Studies by Martinez-Rico et al. [14], Ayón, Moreno, and Usaola [15], Crespo-Vazquez et al. [16], and Silva, Pousinho, and Estanqueiro [17] demonstrate that intraday trading can significantly reduce imbalances and improve profitability. For example, Crespo-Vazquez et al. [16] show a 6.2% income increase with intraday trading, while

Silva, Pousinho, and Estanqueiro [17] report a 63.8% imbalance reduction and a 10.1% profit increase. Importantly, the impact of intraday participation increases with higher forecast uncertainty, as shown by Martinez-Rico et al. [14] and Ayón, Moreno, and Usaola [15].

Among all market types, balancing markets typically offer the highest revenue potential for flexible assets. Both Heredia, Cuadrado, and Corchero [10] and Gonzalez-Garrido et al. [18] find that balancing market participation leads to substantially higher profits compared to wholesale markets. Heredia, Cuadrado, and Corchero [10] observe that the inclusion of balancing services increases profit by nearly four times, with returns scaling proportionally to BESS capacity. Likewise, Gonzalez-Garrido et al. [18] report profit increases up to ten times higher in balancing markets compared to the auction-based intraday market.

While the literature firmly establishes the value of BESS-enabled flexibility and multi-market participation, several important gaps remain. Most existing studies focus on auction-based intraday trading, while the continuous intraday market, particularly as implemented in the Dutch system, has received little attention. Given the shift toward continuous trading with shorter gate closure times and higher liquidity, this market represents a critical and underexplored opportunity for HPPs.

Another underdeveloped area is the interaction between forecast uncertainty, value stacking, and grid constraints. While most models include basic grid export limits, few explicitly analyze how uncertainty and grid limitations jointly affect optimal dispatch and economic outcomes. This interaction is especially relevant in systems with overplanting and limited grid capacity. Further research is needed to capture these complexities and to assess the economic and operational sustainability of HPPs under real-world conditions.

1.2.2. Modeling and Mitigating Uncertainty

Uncertainty is a critical challenge market participation of HPPs. The operational schedule is based upon forecasts for both power production and market prices, which are associated with uncertainty. Logically, research has been done on the gains of a stochastic, over the deterministic approach. Across literature both Stochastic Optimization (SO) and Robust Optimization (RO) have been explored.

The objective of robust optimization is to find a solution that is feasible for all possible realizations of uncertain parameters, gathered in an uncertainty set. To establish such an uncertainty set the variety of stochastic parameters is described by their distributional bounds, therefore this set represents all the possible values the parameters can take [19]. To ensure feasibility for all these possible realizations, the optimization finds the solution for the worst case making it robust. While being an effective method to incorporate stochastic behavior into the decision making process, it leads to a more conservative market participation strategy. Therefore, it ensures reliability, but performs less on profitability compared to other optimization techniques [20].

In the research of Mohamed, Jin, and Su [21] the optimal operation of a wind park with BESS from a system operator point of view, showing an increased robustness when using the of a RO approach compared to the conventional approach. The increased robustness results in a 95% power output increase and additionally a 11.5% profit increase for the wind park and energy storage operators, compared to the conventional approach. Rahimiyan and Baringo [22] investigated a wind farm, energy storage and demand cluster with an energy management system ruled by a robust optimization. Two case studies have been conducted demonstrating the impact of risk taking on bidding strategy, power traded and utility. Based upon the risk appetite, the uncertainty set is defined. The article concludes the optimal risk strategy depends on the difference between day-ahead and real-time markets. With a correct prediction of this difference less conservative strategy yields higher results.

Another widely adopted optimization method is stochastic optimization (SO). SO assumes that uncertain parameters follow a probability distribution, which is used to describe the possible realizations of the system. By weighing these realizations according to their probability, often represented as discrete scenarios, the optimal solution to the problem is determined [23]. While SO emphasizes profitability, this can come at the cost of feasibility across all realizations [20].

In the context of HPPs this would come down to profit maximization at the cost of adhering operational and market constraints, which lead to deviations from trade commitments. Studies like [12, 10, 9,

17] demonstrate the effectiveness of SO in incorporating uncertainties in power generation and market prices. These uncertainties are typically represented by scenarios, which enable adaptive bidding strategies that optimize expected economic value across multiple markets. For example, Ledro et al. [12] evaluate an HPP with limited grid capacity and show that using a stochastic model reduces curtailed energy by 35% compared to a deterministic approach.

When optimizing across multiple electricity markets, multi-stage stochastic optimization has proven to be especially effective [10, 24, 15, 25]. This approach models different decision moments, such as day-ahead and intraday bidding, as separate stages. Each stage reflects the information available at that time, based on the realization of uncertain parameters. For instance, day-ahead market bids are made under price and acceptance uncertainty, whereas intraday decisions can incorporate updated forecasts and known day-ahead outcomes. Additionally, different market rules apply at each stage, further justifying the use of a multi-stage framework.

SO is particularly well-suited for supporting decision-making in dynamic and uncertain environments [26]. However, its effectiveness depends on the quality of the underlying probability distributions and scenario generation methods, which can be difficult to define accurately in high-uncertainty settings [23].

1.2.3. Scenario Modeling

Scenario-based stochastic optimization is a widely used approach to capture uncertainty in system behavior by representing possible realizations of stochastic variables through a finite set of scenarios with associated probabilities [26]. The main objective is to model uncertainty accurately while maintaining computational tractability. However, increasing the number of scenarios improves the representation of uncertainty but significantly raises the computational complexity of multi-stage optimization problems, as each scenario path must be evaluated at every decision stage [10].

To address this trade-off, scenario reduction techniques are employed to retain representative system behavior while limiting the number of scenarios. A commonly used approach in the literature is clustering, particularly k-means clustering [27, 28, 16]. This technique groups similar scenario trajectories into clusters and selects a representative centroid for each cluster. The resulting reduced scenario set preserves the key statistical properties of the original ensemble while reducing computational burden. For instance, Gulotta et al. [27] first generate a large ensemble of wind power scenarios using an ARMA model and then apply k-means clustering to extract a limited number of representative profiles. The reduced scenario set allows for a real-time rolling horizon dispatch with only a marginal increase (12 seconds per timestep) in computational effort compared to a deterministic model.

Similarly, Wozabal and Rameseder [28] apply k-means clustering to renewable energy production data, assigning probabilities to clusters using maximum likelihood estimation. Their results demonstrate that the resulting high-dimensional stochastic optimization problem can be solved within minutes, well within operational timeframes for intraday auction trading, highlighting the practicality of such scenario modeling techniques in time-constrained market environments.

Moreover, scenario generation methods have also evolved through the integration of machine learning. For example, Crespo-Vazquez et al. [16] propose a hybrid framework combining multivariate k-means clustering algorithm with recurrent neural networks to generate energy generation and energy price scenarios that better capture temporal dependencies and uncertainty. These advanced methods demonstrate the growing importance of both accurate scenario generation and computational efficiency in the design of stochastic optimization frameworks for power system applications.

1.2.4. Conclusion of Literature Review

The existing literature demonstrates substantial progress in modeling and optimizing the operation of HPPs within electricity markets. It is broadly acknowledged that a BESS participating only in the day-ahead market is insufficient to justify its investment economically. To fully exploit the BESS's flexibility, it must engage in multiple markets, thereby enabling value stacking across multiple services.

Furthermore, incorporating uncertainty through stochastic optimization has been shown to significantly improve operational decision-making in short-term electricity markets. However, the resulting increase in model complexity poses a computational challenge. To address this, k-means clustering is widely applied as a scenario reduction technique, allowing the construction of representative yet computationally

manageable scenario sets.

Grid connection constraints are also identified in the literature as a critical factor influencing HPP operation. Yet, their effect on bidding behavior and market performance under uncertainty is not sufficiently explored. While many studies examine auction-based markets, continuous intraday markets, despite their growing relevance, remain underrepresented in current research. Additionally, few studies offer a comparative perspective on different asset configurations (e.g., standalone RES, standalone BESS, and co-located HPPs) under forecast uncertainty. These gaps highlight the need for further research into the interaction between uncertainty, market dynamics, and grid constraints in short-term HPP operations.

1.3. Research Objective

As outlined in this chapter, the growing integration of renewable energy sources into the energy system introduces significant reliance on uncertain generation forecasts. This creates a need for advanced dispatch strategies, in which the co-location of a BESS with RES can enhance flexibility, support market participation, and mitigate the impact of forecast errors.

The primary objective of this research is to quantify the economic and energetic added value of co-locating a BESS with a wind or photovoltaic (PV) asset. The analysis is conducted under conditions of forecast uncertainty and limited grid connection capacity, and considers participation in the Dutch day-ahead, intraday, and imbalance markets. A comparative analysis is carried out across three configurations: standalone RES, standalone BESS, and a co-located HPP, with the aim of identifying optimal operational strategies.

This objective is addressed through the following sub-objectives:

- Develop a multi-stage stochastic optimization framework that integrates power forecast uncertainty into market bidding strategies.
- Validate the framework by testing the influence of assumptions regarding imbalance price forecasts and power forecast scenarios.
- Compare the economic performance and energy utilization of a co-located HPP with standalone RES and standalone BESS systems.
- Perform a sensitivity analysis on key HPP parameters, including grid connection capacity, battery size, battery technology, and optimization frequency.

These efforts aim to answer the overarching research question:

What is the added energetic and economic value of BESS co-location for a Hybrid Power Plant participating in the Dutch day-ahead, intraday, and imbalance markets, when using a bidding strategy that accounts for power forecasting uncertainty?

To address this question, the research builds upon the existing literature by:

- Implementing a multi-stage stochastic optimization framework for HPP participation in multiple short-term electricity markets.
- Providing a mathematical definition of the optimization problem.
- Modeling forecast uncertainty using scenario generation and reduction techniques.

The proposed approach aims to offer a realistic and flexible framework for HPP bidding strategies, with the goal of maximizing economic returns and quantifying energy performance while accounting for physical constraints such as grid export limits, BESS and RES operations.

1.4. Scope

This study focuses on the operational and economic potential of a HPP participating in the Dutch electricity markets, specifically, the day-ahead, intraday, and imbalance markets. For the intraday market only 15-minute products are considered. The analysis is conducted from the perspective of an individual HPP located in the Netherlands, excluding portfolio effects and aggregated bidding strategies.

The HPP is modeled as a price taker, assuming its bidding volume is too small to influence market prices or dynamics. The renewable energy source used in this study is wind, and stochastic behavior is incorporated for its power forecast using scenario-based uncertainty modeling. A similar approach could also be implemented for PV power source. Stochastic behavior is considered only for power generation, while electricity prices are treated deterministically.

Bidding in the day-ahead market is based on a deterministic forecast without the BESS. In contrast, the BESS is included in the intraday and imbalance markets, where it can be used to mitigate forecast errors and perform arbitrage. Battery operation is subject to technical constraints, such as power limits, energy capacity, and round-trip efficiency, although battery degradation and lifecycle costs are not modeled.

The model accounts for grid connection limitations by enforcing a fixed export limit on the HPP. Overplanting is permitted, which may result in curtailment of renewable output or restricted battery (dis)charging. The time resolution used in the optimization corresponds to the market granularity (e.g., 15-minute intervals), and simulations are performed over one week per season.

This study does not consider capital or operational expenditures, policy incentives, or participation in ancillary services beyond the imbalance market. As such, the results are interpreted in terms of operational revenue potential rather than full techno-economic feasibility.

2

Electricity Markets

This chapter provides an overview of the structure and functioning of the electricity markets relevant to this study. Section 2.1 introduces the key market participants and their roles within the electricity system. Section 2.2 describes the operation of the Dutch short-term wholesale markets, including the day-ahead and intraday markets. This is followed by a discussion of the balancing markets in Section 2.3, and the imbalance settlement mechanism in Section 2.4. A thorough understanding of these market mechanisms is essential for designing effective bidding strategies and optimizing the participation of hybrid power plants.

2.1. Actors within the Electricity Market

In the Dutch electricity market, various actors play crucial roles, each with distinct responsibilities to maintain balance within the system. This section focuses on three key roles: the Transmission System Operator (TSO), the Balance Responsible Party (BRP), and the Balance Service Provider (BSP).

First, the Transmission System Operator (TSO) is responsible for operating and maintaining the electricity transmission network. In the Netherlands, this role is carried out by TenneT, which manages the high-voltage transmission system. TenneT ensures a continuous balance between electricity demand and supply in the Netherlands while working with other European TSOs to harmonize the European electricity market [29]. Furthermore, TenneT manages the infrastructure in terms of transmission capacity, voltage control, reactive power and congestion.

Second, Balance Responsible Parties (BRPs) are electricity producers or consumers connected to the transmission grid. They are required to provide the TSO with an energy program (e-program) containing their position, which is a forecast for 24-hours of the electricity they expect to feed into or withdraw from the grid during each Imbalance Settlement Period (ISP), a 15-minute interval. The TSO monitors the actual consumption or production against this forecast to identify any imbalances. BRPs are held accountable for not adhering their e-program [29].

Finally, Balance Service Providers (BSPs) offer their capacity or energy to TenneT to address unforeseen imbalances. These imbalances can arise from factors such as inaccurate forecasts or power plant failures. Balancing services provided by BSPs are traded in the balancing markets, which are further discussed in 2.3.

In this research, the HPP will exclusively take on the role of a BRP. As such, the HPP is responsible for generating power forecasts and to form its energy program. Although outside the scope of this study, the HPP could potentially operate as a BSP by offering balancing services such as battery (dis)charging or renewable curtailment.

2.2. Wholesale Markets

The purpose of wholesale electricity markets is to provide a platform that connects electricity producers with consumers to buy and sell their energy. The energy is traded in three different markets: forward

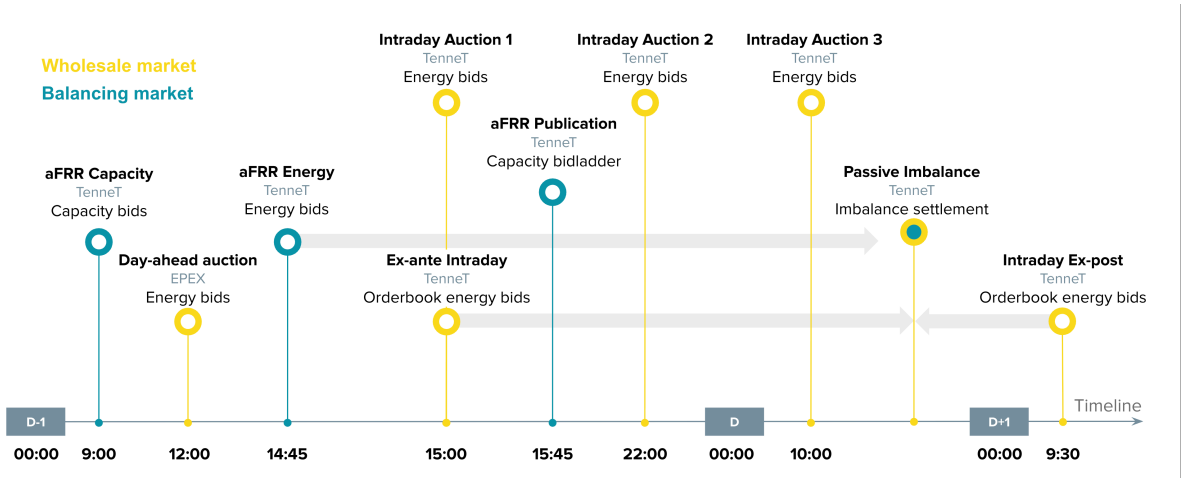

Figure 2.1: Overview of the timeline for relevant Dutch short-term electricity markets, showing the auction closing times, order book opening times, market operators, and accepted bid types.

and futures market, day-ahead market and intraday market. Consecutively, these markets are closer to the time of delivery. In this study the focus will be on short term electricity markets, leaving the forward and futures market out of scope.

2.2.1. Day-ahead Market

In the day-ahead market, all BRPs can participate by submitting hourly bids for electricity consumption or production for the following day. The auction closes at 12:00 noon one day before delivery, as can be seen in Figure 2.1. Next, all the bids are combined into a merit order, putting bidded volumes for demand in descending price order and for supply in ascending price order. After this process, the market clearing point is determined, which is the point where supply meets demand as shown in Figure 2.2. All supply and demand bids to the left of the market clearing point are accepted against the market clearing price.

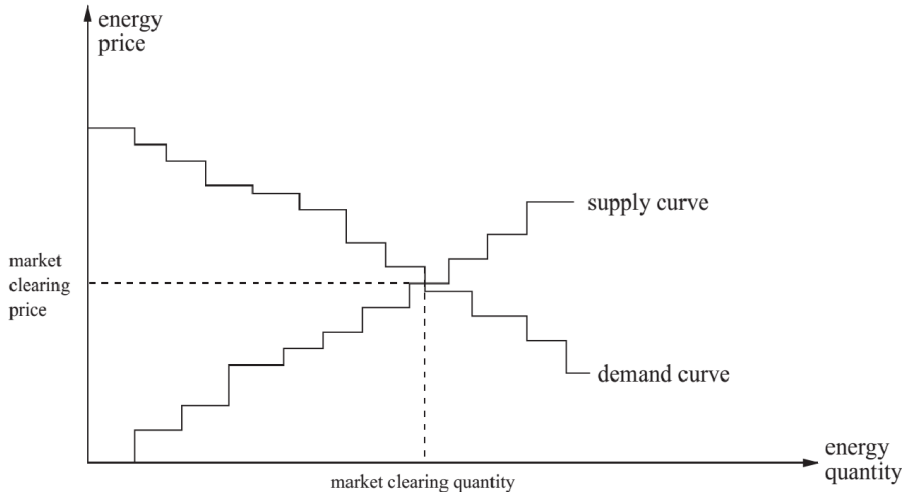

Figure 2.2: Example of market clearing principal for day-ahead market with supply and demand curves, the market clearing point is indicated together with the market clearing price and quantity [30]

Participants whose bids are accepted must buy or sell electricity at the market clearing price and are required to adhere to their submitted energy program in terms of power output for the specified period. Failing to comply with the agreed-upon program results in imbalances, which typically incur unfavorable costs to offset the discrepancy, which will be discussed in Section 2.4.

2.2.2. Intraday Market

On the intraday market, BRPs can make trades after the day-ahead market is cleared. Since forecasts typically become more accurate closer to the time of delivery, it is often beneficial to adjust purchased or sold volumes based on these updated forecasts.

In the Netherlands, there are two types of intraday markets: the intraday auction and the continuous intraday market. In both markets, quarter-hourly, half-hourly, and hourly contracts can be traded. Cross-border intraday trading is facilitated through the XBID platform, with bids submitted via Nominated Electricity Market Operators (NEMOs) such as Nordpool and EPEX [31].

In the continuous intraday market, trades are executed immediately once a supply bid matches a demand bid. Transactions are settled on a pay-as-bid basis, ensuring prompt execution [32]. The ex-ante market allows to adjust the position before the moment of the delivery, whereas the ex-post allows BRPs to balance imbalance positions with other BRPs, which can be particularly useful during a regulation state 2 (discussed further in Section 2.3). Figure 2.1 shows the time at which continuous intraday trades can be made:

- **Ex-ante market:** Open from 15:00 D-1 until the start of the delivery ISP.
- **Ex-post market:** Opens immediately after physical delivery and remains active until 09:30 on D+1.

The intraday auction (IDA) market operates on a pay-as-cleared principle, providing structured trading opportunities. Three auction gates are held daily as depicted in Figure 2.1, each covering specific timeframes [32]:

- **IDA 1:** Closes at 15:00 D-1, accepting bids for delivery from 00:00 to 24:00 on the following day.
- **IDA 2:** Closes at 22:00 D-1, accepting bids for delivery from 00:00 to 24:00 on the following day.
- **IDA 3:** Closes at 10:00 D, accepting bids for delivery from 12:00 to 24:00 on the same day.

The continuous intraday market offers the advantage of immediate execution and the transparency of order books, which enables dynamic and responsive trading. Conversely, the auction-based intraday market facilitates more structured trading strategies.

For the HPP, fast and adaptive trading is particularly relevant due to the uncertain nature of renewable generation. The battery enables the system to react quickly to new forecasts and market opportunities. Therefore, this study focuses on the continuous ex-ante intraday market as part of the trading strategy. Only the 15-minute product is considered in this analysis, leaving trading opportunities for 30-minute and hourly products underexplored.

2.3. Balancing Markets

The purpose of balancing markets is to maintain the grid frequency stable at 50 Hz at all times. As mentioned before, BRPs put in an e-program one day before delivery. However, deviations from these schedules occur often and can create imbalance. Such an imbalance between demand and supply will disturb the grid frequency, driving the frequency up in case of power surplus and down in case of power shortage. Too large deviations from 50 Hz could lead to outages or damage to the grid. Therefore, separate markets have been established, varying in response time, minimum capacity and traded product, being either energy or capacity as shown in Table 2.1. As can be seen in Figure 2.3, the first market to be activated is Frequency Containment Reserve (FCR) being operational for a short time, followed by automatic Frequency Restoration Reserve (aFRR) and thereafter manual Frequency Restoration Reserve (mFRR). Only BSPs can participate in these markets.

Although balancing markets are essential for maintaining system stability, they are not included in this study, as the HPP is assumed to operate solely as a BRP. Participating in FCR, aFRR, or mFRR requires capacity bids to be submitted one day in advance, often over a longer period of time (e.g. 4 hours, full day). This time frame presents challenges due to the uncertainty in power forecasts from renewable energy sources. However, since the aFRR market influences the settlement of imbalance prices, which directly affect BRPs, it is included in this overview.

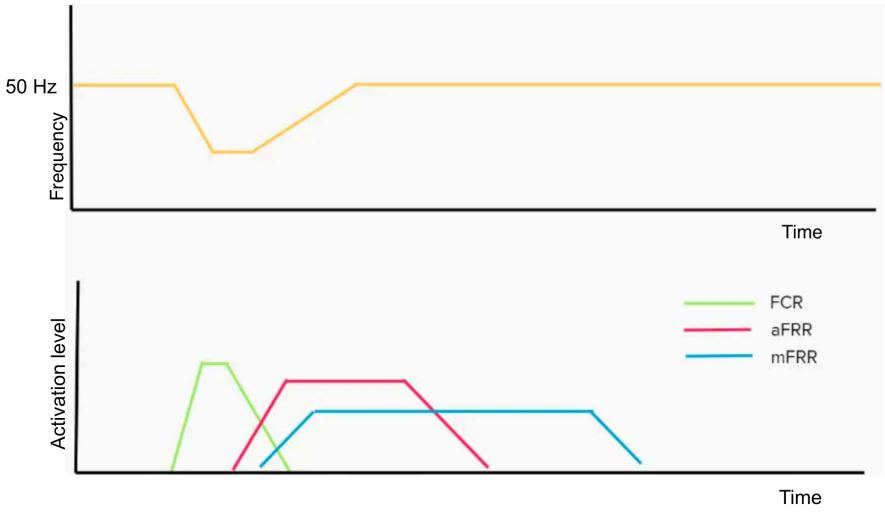

Figure 2.3: Timeline of activation of balancing markets after occurrence of imbalance, indicated by a frequency deviation from 50 Hz [33]

Market	Response time	Minimum capacity	Traded product
FCR (primary)	<30 sec	1 MW upward **and** downward	contracted capacity
aFRR (secondary)	1 – 15 min	1 MW upward **or** downward	contracted capacity & activated energy
mFRR (tertiary)	>15 min	1 MW upward **or** downward	contracted capacity

Table 2.1: Balancing market types and their properties regarding response time, minimum capacity and direction, and traded product [33]

2.3.1. Automatic Frequency Restoration Reserve

The Automatic Frequency Restoration Reserve is designed to handle imbalances over a longer time horizon than FCR market but shorter than mFRR market. This reserve is the second product activated to restore balance in the event of system deviations. The aFRR market consist out of two auctions, the aFRR capacity and aFRR energy market.

The aFRR capacity market is auctioned one day before delivery as is shown in Figure 2.1. BSPs submit bids for upward and/or downward aFRR capacity to TenneT. These bids form the basis for two separate merit orders, one for upward regulation and another for downward regulation. The volume of capacity required determines which bids are accepted. The auction for aFRR capacity operates under a pay-as-bid mechanism, meaning BSPs receive payment based on the price they specify in their accepted bids. Accepted BSPs are contracted for the full 24-hours of the next day, during which they must ensure the availability of the agreed-upon capacity.

In addition to capacity bidding, BSPs also submit energy bids to participate in the aFRR energy market. BSPs accepted in the aFRR capacity auction are obligated to make bids for the whole day, while other BSPs can make bids voluntarily up to 25 minutes before delivery (Figure 2.1). For each ISP, separate merit orders are created for upward and downward energy bids, as can be seen in Figure 2.4. Upward bids (yellow) are sorted in increasing price order, while downward bids (blue) are arranged in decreasing price order. The activation of energy bids within the ISP follows a pay-as-cleared pricing principle. This means all accepted upward bids are paid the price of the highest accepted upward bid, while all accepted downward bids receive the price of the lowest accepted downward bid.

The establishment of the balancing price in the aFRR market is illustrated in Figure 2.4. Additionally, a mid-price is calculated by averaging the highest downward bid and the lowest upward bid. This mid-price is occasionally used to determine the imbalance price, which will be discussed in Section 2.4.

Overall, the aFRR market plays a critical role in maintaining system stability, ensuring that imbalances are addressed efficiently while providing economic incentives for BSPs to participate [34]. While the

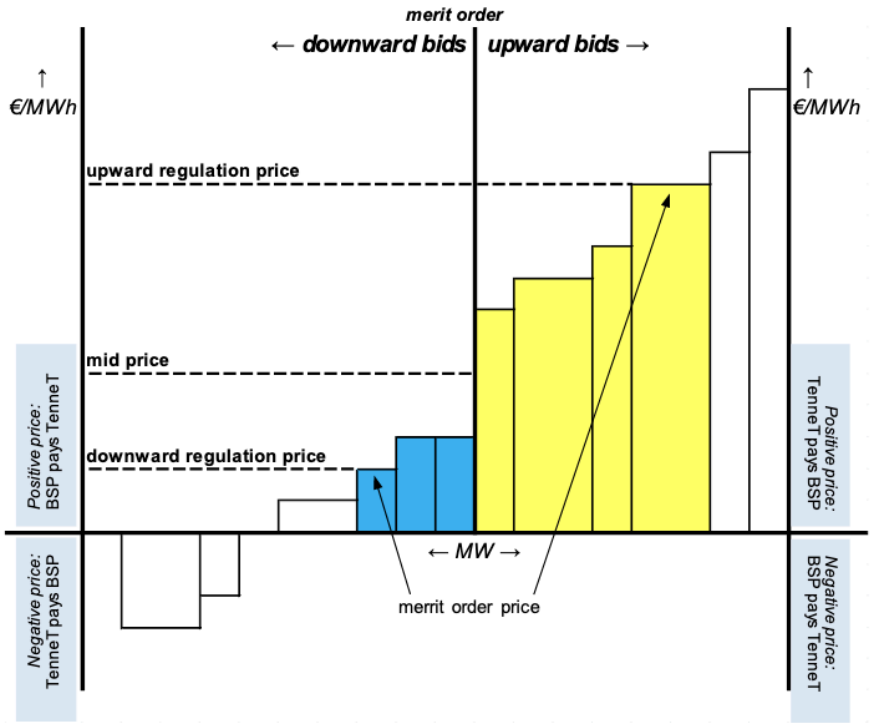

Figure 2.4: Example of balance price setting for a single ISP. Activated downward bids are shown in blue and upward bids in yellow, each representing a combination of volume (MW) and price (€/MWh). The merit order is established per direction, and the clearing price determines the payment flow: either from the BSP to TenneT or vice versa, depending on the sign. [35]

aFRR market is essential for system operations, its capacity product presents a challenge for HPPs due to long commitment periods and forecast uncertainty. The aFRR energy product, traded closer to delivery and over shorter durations, would better suit an HPP. However, because the plant is modeled purely as a BRP, participation in this market falls outside the scope of this study.

2.4. Imbalance Market

In the occasion that a BRP does not follow its e-program, these deviations are financially settled via the imbalance market. This is not a real market but provides a settlement of imbalances. TenneT publishes the balance delta containing the imbalance volume, direction and price every minute, with 5 minute-delay. This determines the regulation state and accordingly the imbalance price.

Imbalance prices are closely linked to aFRR prices within the same ISP and vary depending on the regulation state. The regulation state reflects whether upward or downward balancing energy was activated during the ISP, or if both directions were required. The regulation state and a BRP's position jointly influence whether a BRP's imbalance is penalized or rewarded.

The regulation state is determined by the type of steering the TSO activates within one ISP:

- Regulation state **0** occurs when TenneT does not perform any upward or downward regulation during an ISP.
- Regulation state **+1** occurs when TenneT exclusively regulates upward during an ISP.
- Regulation state **-1** occurs when TenneT exclusively regulates downward during an ISP.
- If both upward and downward regulation occur within an ISP, the progression of balance deltas within the ISP determines the regulation state:
  - If the balance deltas within the ISP consistently increase or remain unchanged, regulation state **+1** is assigned.

- If the balance deltas within the ISP consistently decrease or remain unchanged, regulation state **-1** is assigned.
- If the balance deltas within the ISP show both increasing and decreasing trends, regulation state **2** is assigned.

A BRP's position can be either as surplus (injecting more or withdrawing less power than planned) or as shortage (injecting less or withdrawing more power than planned). This determines the direction of financial settlement. In general, positions that help restore grid balance may be rewarded, while positions that worsen grid imbalance are penalized [35]. The payment mechanics are described in Table 2.2.

BRPs can engage in a strategy known as passive imbalance steering, where they adjust their positions to align with favorable imbalance prices. For instance, during upward regulation, a BRP with a battery asset could discharge power to create a surplus position, earning the upward balancing price while helping mitigate grid imbalances. Conversely, BRPs with shortage positions during upward regulation are required to pay the upward balancing price, reflecting their negative contribution to grid stability.

However, excessive reliance on passive imbalance steering can destabilize the system. If many BRPs react simultaneously, overcompensation may occur, leading to frequent oscillations between upward and downward regulation triggering a regulation state 2 and resulting in extreme imbalance price volatility. To discourage such behavior, the upward and downward price are flipped. For example if a BRP has a shortage position during regulation state 2, it receives the upward price (instead of the downward price), as shown in Table 2.2. In this way any imbalance of an BRP during regulation state 2 is unfavorable. During regulation state 2, the surplus and shortage price are not the same, and therefore it can be beneficial to trade away imbalances in the ex-post intraday market since both BRP surplus and shortage can mitigate their losses [35].

The imbalance market thus serves as an essential mechanism for maintaining grid stability. It incentivizes BRPs to minimize deviations while providing financial signals that align with operational requirements, ensuring a balanced and reliable electricity system.

The imbalance market is relevant for HPPs when they commit to positions in the day-ahead market based on forecasts. Uncertainties are inherent to forecasts and can cause HPPs to deviate from their initial positions. If these deviations are not compensated for by taking a position in other markets, such as the intraday market, the imbalance price will apply. Consequently, passively steering on imbalance emerges as a viable strategy to compensate for forecasting errors or by providing flexibility with the BESS.

Table 2.2: Overview of imbalance settlement rules as defined by TenneT for each regulation state. The figure outlines how the imbalance price and payment direction depend on the BRP's imbalance position (shortage or surplus), the prevailing regulation state (0, $\pm$1, or 2), and the condition and resulting imbalance price including sign (derived from the aFRR balance price). The sign of the price determines the payment direction, either from the BRP to the TSO or vice versa. [35]

Regulation State	BRP Position	Imbalance Price		Direction of Payment
		Condition	Applied aFRR Price (sign)	
State 0	Shortage	–	$P_{\text{mid}}(+)$	BRP $\rightarrow$ TSO
		–	$P_{\text{mid}}(-)$	TSO $\rightarrow$ BRP
	Surplus	–	$P_{\text{mid}}(+)$	TSO $\rightarrow$ BRP
		–	$P_{\text{mid}}(-)$	BRP $\rightarrow$ TSO
State +1	Shortage	–	$P_{\text{up}}(+)$	BRP $\rightarrow$ TSO
		–	$P_{\text{up}}(-)$	TSO $\rightarrow$ BRP
	Surplus	–	$P_{\text{up}}(+)$	TSO $\rightarrow$ BRP
		–	$P_{\text{up}}(-)$	BRP $\rightarrow$ TSO
State -1	Shortage	–	$P_{\text{down}}(+)$	BRP $\rightarrow$ TSO
		–	$P_{\text{down}}(-)$	TSO $\rightarrow$ BRP
	Surplus	–	$P_{\text{down}}(+)$	TSO $\rightarrow$ BRP
		–	$P_{\text{down}}(-)$	BRP $\rightarrow$ TSO
State 2	Shortage	$P_{\text{up}} \geq P_{\text{mid}}$	$P_{\text{up}}(+)$	BRP $\rightarrow$ TSO
			$P_{\text{up}}(-)$	TSO $\rightarrow$ BRP
		$P_{\text{up}} < P_{\text{mid}}$	$P_{\text{mid}}(+)$	BRP $\rightarrow$ TSO
			$P_{\text{mid}}(-)$	TSO $\rightarrow$ BRP
	Surplus	$P_{\text{down}} \leq P_{\text{mid}}$	$P_{\text{down}}(+)$	TSO $\rightarrow$ BRP
			$P_{\text{down}}(-)$	BRP $\rightarrow$ TSO
		$P_{\text{down}} > P_{\text{mid}}$	$P_{\text{mid}}(+)$	TSO $\rightarrow$ BRP
			$P_{\text{mid}}(-)$	BRP $\rightarrow$ TSO

3

Methodology

This chapter outlines the methodological approach used to evaluate the economic and energetic value of co-locating a BESS with a renewable energy asset. Section 3.1 introduces the overall optimization framework, followed by the model structure and its mathematical formulation in Sections 3.2 and 3.3. Scenario generation and reduction techniques used to model power forecast uncertainty are discussed in Section 3.4. Section 3.5 defines the performance metrics used to assess outcomes, while Section 3.6 describes the case study configurations. Model evaluation methods are detailed in Section 3.7, and implementation aspects are addressed in Section 3.8.

3.1. Modeling Framework

To effectively address the research question, a multi-stage stochastic optimization framework is adopted. This approach is well-suited for modeling the sequential and uncertain nature of HPP operations in electricity markets. It enables the integration of multiple trading stages, each governed by different rules, timeframes, and uncertainties, into an optimization model. Additionally, it captures the stochastic behavior of renewable energy generation, such as wind power, through probabilistic scenario modeling. By formulating the problem as an optimization, the model ensures optimal operation aimed at maximizing economic value.

The multi-stage structure of the optimization model mirrors the sequential nature of market participation, aligning with the operational timelines of the day-ahead, intraday, and imbalance markets as detailed in Chapter 2. Each stage represents a distinct market environment with its own constraints, prices, and decision rules, and depends on decisions made in preceding stages. In Section 3.2 an in depth description of each stage is given.

The optimization problem is formulated as a Mixed Integer Linear Program (MILP), allowing the system dynamics to be expressed through a set of linear constraints, integer variables and objective function. MILP offers a computationally efficient framework while accommodating binary decisions, such as the (dis)charging status of the battery. Physical properties of the system such as power limits, energy storage capacity, and efficiency, as well as market participation rules are captured using linear equations. The objective of the optimization is to maximize market revenues. The full mathematical formulation of the MILP, including all decision variables and constraints, is provided in Section 3.3.

To represent forecast uncertainty, the model utilizes a scenario-based stochastic framework. Power forecasts are modeled as discrete probabilistic scenarios, each associated with a likelihood of occurrence, as described in Section 3.4. This enables the model to evaluate a range of possible future outcomes and derive an operational strategy that generates most economic value weighing all realizations. By incorporating stochastic elements, the model becomes more robust to deviations in forecasts, improving its ability to adapt to real-world volatility.

3.2. Model Definition

This section details the structure of the proposed model, including the configuration of the HPP, the sequential market stages, and their interdependencies. The operational logic of each stage is described, after which the full system is formulated as a MILP problem. The aim is to provide a comprehensive mathematical representation that captures the physical constraints, market rules, and optimization objectives defined in the methodology. An overview of key characteristics of each optimization stage are given in Table 3.1

3.2.1. Model Configuration

The operation of the HPP determines the power flows within the system, as illustrated in Figure 3.1. In this model, a distinction is made between physical and traded power, intersecting at the HPP's grid connection point (P_{HPP}). The stochastic variable $\hat{P}_{\text{source}}$ represents the forecasted power output of renewable energy source, which is modeled through discrete scenarios. The actual power generation can be controlled by curtailment, with $P_{\text{generated}}$ representing the controllable output. This energy can either be injected into the grid or used to charge the battery. Charging is denoted by a negative P_{battery}, discharging by a positive value. The battery can only draw power from the RES. The total output to or from the grid is denoted by P_{HPP}.

All power exchanged with the grid must be settled via market transactions. Power sold or bought through the day-ahead (DA) and intraday (ID) markets is represented by P_{DA} and P_{ID} respectively, while any deviation is resolved through the imbalance (IM) market via P_{IM}. By convention, feed-in to the grid is positive and withdrawal is negative. As a result sold power on an electricity market is considered positive, whereas power bought is negative.

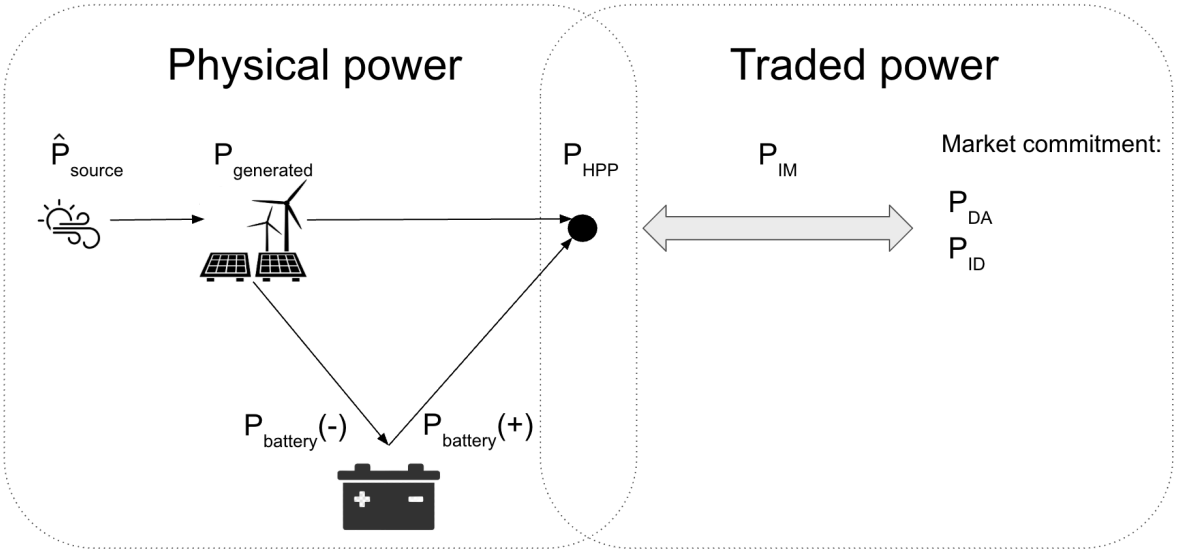

Figure 3.1: Definition hybrid power plant (HPP) configuration with the definition of physical and traded power flows consisting of day-ahead (DA), intraday (ID) commitments and resulting imbalance position (IM)

To determine the optimal flow of power within the HPP and trading activities the model optimizes using 3 stages as depicted in Figure 3.2. Each stage with its own decision variables, objective function and constraints. The definition of each stage will be discussed next.

3.2.2. Day-ahead Bidding

The first stage captures participation in the day-ahead market. The bids are put in against marginal cost of the asset, since the day-ahead market operates under a pay-as-cleared principle. The day-ahead auction takes place once a day, therefore this optimization is also performed one time a day. In Figure 3.3 the evolution of the optimization time horizons for one day have been illustrated. Figure 3.4 shows a more detailed picture of the timelines associated with two different optimizations. Hourly bids are submitted before day-ahead market closure at 12:00 on the day before delivery, represented by the

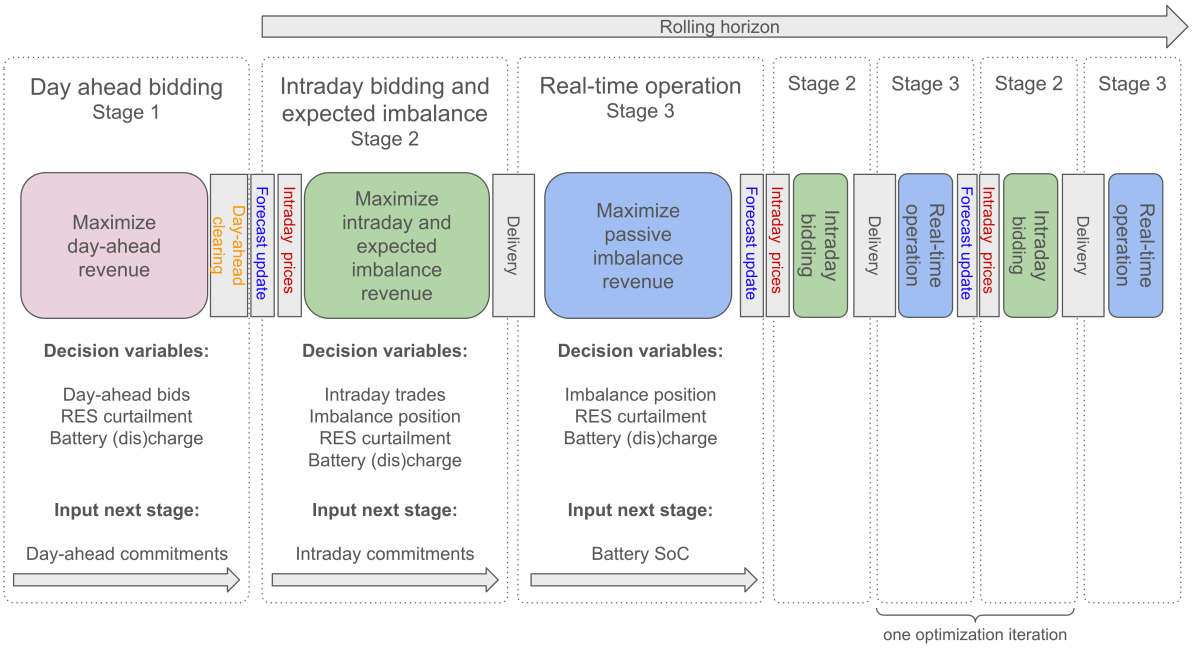

Figure 3.2: Three stages in the multi-stage stochastic optimization, showing the objective (blue boxes), the decision variables, the input for the next stage, events separating the stages (vertical boxes). The intraday bidding and real time operation stages are repeatably performed adopting a rolling horizon.

yellow box/dot in Figure 3.3 and 3.4.

In this stage the acceptance of hourly day-ahead bids ($u_{\text{accepted},t}$) as a result of the market clearing is the decision variable, this time horizon is denoted by the pink box in Figure 3.3 and 3.4 spanning from 00:00 - 23:45. This time horizon starts 11 hours after the publication of day-ahead results, thus $\frac{11}{dt}$ time steps.

The day-ahead bids are submitted as if the RES operates independently, excluding the BESS from day-ahead market bidding. This approach is supported by literature, which indicates that battery storage systems generate greater economic value through participation in intraday and balancing markets [9, 10]. The bids are put in against its marginal cost (MAC_{RES}) of the RES, excluding subsidies. Moreover, this stage considers the power forecast as a deterministic and does not consider strategic bidding (e.g. reserving energy to trade in other markets).

The objective in this stage is to to maximize expected day-ahead revenue. Therefore, the full forecasted generation is bid into the day-ahead market, based upon the latest available forecast at 12:00 D-1. Once the market clears at approximately 13:00 D-1 (orange box/dot in Figure 3.3 and 3.4), the model evaluates whether the bids are accepted, assuming the RES to be a price-taker, meaning the price bid does not impact the market clearing price. Thus, in the case that the marginal cost of the asset are equal to or below the clearing price, the bid is accepted. The accepted volumes $P_{\text{DA},t}$ form the foundation for subsequent decision-making.

3.2.3. Intraday Bidding and Expected Imbalance

The second stage involves HPP participation in the continuous intraday market, which opens at 15:00 on the day before delivery (D-1). In this stage, both the RES and the BESS are engaged. The objective is to maximize combined revenue from intraday trading and expected passive imbalance settlement by dynamically adjusting to updated forecasts and real-time market signals.

Intraday and expected imbalance revenues are related because trades executed on the intraday market can alter the system's imbalance position relative to its day-ahead commitments. Consequently, any intraday trading action must consider the potential imbalance settlement outcome. While intraday prices are available at the time of optimization, the actual imbalance price is still unknown. As accurate imbalance price forecasting lies outside the scope of this study, the day-ahead market clearing price is

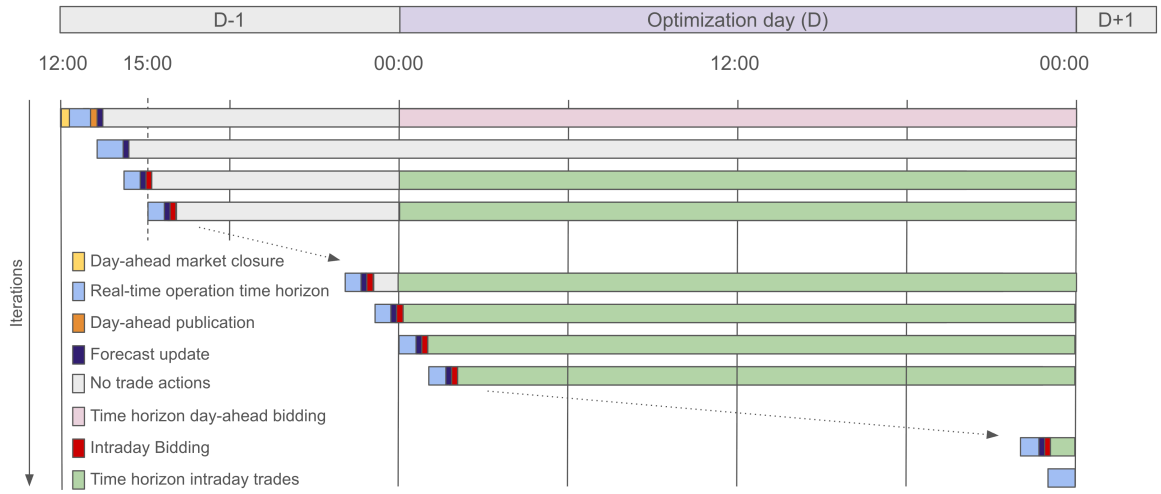

Figure 3.3: Time line of rolling horizon of optimization shifting forward one hour per iteration and dynamically adjusting optimization window length. Demonstrating the open markets and market events considered in the each optimization iteration.

used as a forecast for the imbalance price ($\lambda_{\text{IM-forecast},t}$) to incorporate the expected economic impact of imbalance positions. The implications of this approximation are further discussed in Section 4.3. During this stage, the dual-pricing scheme of the imbalance market is simplified: the model assumes symmetrical pricing (i.e., the same value for upward and downward regulation), with only the payment direction varying. This corresponds to assuming only Regulation States -1 and +1, as outlined in Chapter 2.

To avoid excessive speculative behavior arising from simplified imbalance price forecasts, the model applies imbalance constraints following the approach of Heredia, Cuadrado, and Corchero [10]. This limits the volume of allowed imbalance positions to reflect physical feasibility and market realism.

The BESS plays a crucial role in this phase by leveraging its operational flexibility for short-term arbitrage, mitigating RES forecast errors, and responding to real-time market opportunities. This optimization evaluates the trade-offs between economic gains from market participation and physical constraints, such as state-of-charge (SoC) limits, grid export capacity, and battery efficiency. Notably, the model assumes that the battery only charges from the RES and not from the grid. Battery degradation is also neglected at this stage, an assumption that simplifies the analysis but may result in an overestimation of the BESS's long-term arbitrage potential.

Because the intraday market operates in close proximity to the delivery time, with trading allowed up until the start of the Imbalance Settlement Period (ISP), forecast accuracy improves substantially. This enhanced precision increases the operational value of the BESS and enables the HPP to refine its market position using more accurate and timely data. To exploit this feature, the model employs a rolling horizon optimization strategy. At fixed intervals (t_{update}), hourly in this study, the model incorporates the most recent renewable generation forecasts along with updated data from the intraday market order book. These are indicated in Figure 3.3 and 3.4 by the purple and red boxes/dots respectively.

The order book provides real-time information on the best available trading prices. It is assumed that the HPP can transact at the most advantageous prices available at the time of bidding. More precisely, the lowest available sell price is used for buying transactions, and the highest available buy price is used for selling. This assumption reflects an ideal but plausible execution scenario.

In Figure 3.4 the bottom bar presents one optimization from the rolling horizon, including the intraday bidding and expected imbalance stage. Such an optimization consist of three sequential steps: first, the realization of real-time operation (Section 3.2.4) indicated by the blue bar, second, the integration of updated forecast (purple) and intraday market data (red), and third, a re-optimization horizon of future intraday trades (green), constrained by prior market commitments and physical limitations. Depending on the current time ($t_{\text{current},i}$), it is determined which markets are open, and thus the length of the optimization horizon ($N_{t,i}$). This iterative process enables the HPP to continuously adapt its operational strategy to evolving system conditions.

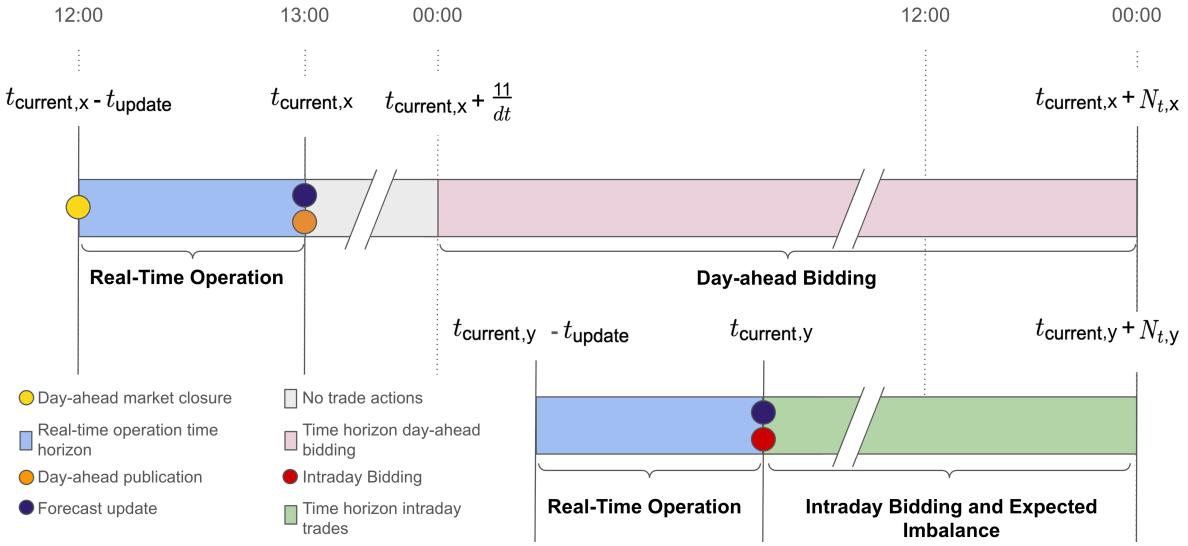

Figure 3.4: Illustrative time horizons (bars) and events (dots) of two optimization iterations. The upper optimization (bar) consist of the Real time operation optimization (bar) and the Day-ahead bidding optimization. The bottom optimization consist of the Real time operation optimization and Intraday bidding and expected imbalance optimization.

While Figure 3.3 illustrates a single operational day, which causes the optimization window to shrink with each passing iteration, the actual model implements a rolling multi-day horizon. After t_{current} has passed 13:00, when the results of the day-ahead market for the next day are published, the window expands to include new commitments until the following midnight to schedule its operations accordingly. Similarly, from 15:00 onward, intraday trading for the next day becomes available. This dynamic adjustment of the horizon reflects the real operational environment of an HPP engaging in sequential market participation.

3.2.4. Real-time Operation

The third stage of the optimization framework concerns real-time operation and imbalance settlement. During this stage, market positions from earlier bidding stages are fixed, but actual renewable energy production may deviate from forecasts, leading to imbalances. The objective is to steer real-time power flows to maximize imbalance market revenue while maintaining feasibility under technical and market constraints. The real-time delivery window is covering the time between the start of the current ($t_{\text{current},i}$) and previous optimization ($t_{\text{current},i-1}$). This interval consist of t_{update} time steps and is illustrated as the blue bar in Figure 3.3 and 3.4.

Within this stage, the model performs strategic curtailment and battery (dis)charging to exploit favorable imbalance prices or mitigate penalties. Since the intraday market is closed during real-time delivery, all adjustments are executed physically and are financially settled through the imbalance market.

This stage assumes perfect foresight of imbalance prices within the real-time delivery window. Although this assumption simplifies the optimization and allows for price-responsive dispatch, it introduces a degree of optimism in estimated imbalance revenues. In practice, TenneT publishes upward and downward regulation prices with a five-minute delay, offering operators only a partial indication of the final imbalance price used for settlement. While this reduces uncertainty, the actual settlement price depends on the regulation state, which is determined only after the Imbalance Settlement Period (ISP) has ended. To prevent unrealistic arbitrage under perfect foresight, speculative behavior is restricted in earlier stages of the model. In the real-time stage, however, these constraints are lifted since trades are no longer speculative: the intraday market has closed, and operational actions must be based on physical delivery within the current ISP.

The real-time operation stage and the intraday bidding and expected imbalance stage are solved simultaneously. Therefore, decisions during the real-time operation stage take the scheduling for the expected future timesteps into account. This design ensures continuity across decision stages: the realized operation not only determines the actual imbalance revenues, but also sets the initial conditions

for subsequent intraday bidding, particularly the battery's state of charge (E_{start}). Thus, consistency is maintained between short-term execution (real-time operation stage) and longer-term planning horizons (intraday bidding and expected imbalance stage).

In summary, this final stage completes the three-stage stochastic MILP framework. By integrating real-time realizations with forecast-based decision-making and market constraints, the model provides a comprehensive and realistic representation of HPP participation in short-term electricity markets. It enables robust operational strategies that balance profitability with system reliability, while acknowledging the inherent uncertainties of renewable generation.

3.3. Mathematical Formulation

This section presents the mathematical formulation of the model introduced previously. The problem is formulated as a MILP. An overview of the input variables, type of power forecast, objective, decision variables, output variables and optimization frequency and timelines of the three optimization stages are given in Table 3.1 at the end of this section. Next follows a description of the decision variables, and the mathematical formulation of the objective functions and associated constraints for each stage of the optimization in dedicated subsections.

3.3.1. Day-ahead Bidding

The objective of the day-ahead bidding stage is to maximize revenues from the day-ahead market, as defined in Equation 3.1. The decision variable is the acceptance of day-ahead bids ($u_{\text{accepted},t}$) for each hour. This is determined based on the bid volume $P_{\text{DA-bid},t}$, which is set equal to the deterministic forecast ($P_{\text{forecast},t}$) available at 12:00 on the day prior to delivery (Equation 3.2). Since day-ahead market clearing happens at 13:00 one day before delivery, the next day will be 11 hours later. Thus the number of time steps from the current time to the start of day-ahead bidding time horizon is defined as $t_{\text{current},i} + \frac{11}{dt}$ as indicated in Figure 3.4. The acceptance of the bids determines the commitment to the day-ahead market as described in Equation 3.3.

The RES has a marginal cost MAC_{RES}, and bids are accepted if the market clearing price $\lambda_{\text{DA},t}$ exceeds this cost. This is enforced through the binary variable $u_{\text{accepted},t}$ and the big-M formulation provided in Equation 3.4.

$$\text{maximize} \quad \sum_{t=11/dt}^{N_t} \Pi_{\text{DA}} = \sum_{t=11/dt}^{N_t} P_{\text{DA},t} \cdot \lambda_{\text{DA},t} \tag{3.1}$$

w.r.t. u_{accepted}

$$\text{subject to} \quad P_{\text{DA-bid},t} = P_{\text{forecast},t} \qquad t = \frac{11}{dt}, ..., N_t \tag{3.2}$$

$$P_{\text{DA},t} = P_{\text{DA-bid},t} \cdot u_{\text{accepted},t} \qquad t = \frac{11}{dt}, ..., N_t \tag{3.3}$$

$$-M \cdot (1 - u_{\text{accepted},t}) \leq \lambda_{\text{DA},t} - MAC_{\text{RES}} \leq M \cdot u_{\text{accepted},t} \qquad t = \frac{11}{dt}, ..., N_t \tag{3.4}$$

The accepted volumes $P_{\text{DA},t}$ are carried forward as fixed parameters into the intraday bidding and expected imbalance stage. Additionally, the clearing prices $\lambda_{\text{DA,t}}$ are used as a forecast for the imbalance price.

3.3.2. Intraday Bidding and Expected Imbalance

This stage models the intraday bidding strategy of the HPP under forecast uncertainty and evaluates the economic impact of passive imbalance exposure. At each iteration, the model makes decisions based on the current system state, which includes the existing intraday market commitments $P_{\text{ID-commit},t}$ and the battery state of charge $E_{\text{battery},t=t_{\text{current}}}$ inherited from previous iterations. The MILP of this stage is defined by Equations 3.5–3.20.

$$\text{maximize} \quad \mathbb{E}_{j\in[1,N_c]}\left[\sum_{t=1}^{N_t}(\Pi_{\text{IM-forecast},j,t}+\Pi_{\text{ID},t})\right] \tag{3.5}$$

$$\text{w.r.t.} \quad \Pi_{\text{ID}},\ \Pi_{\text{IM-forecast}},\ P_{\text{generated}},\ P_{\text{ID}},\ P_{\text{IM-forecast}},\ P_{\text{charge}},\ P_{\text{discharge}},\ E_{\text{battery}},\ P_{\text{HPP}},\ u_{\text{charging}},\ u_{\text{ID}}$$

$$\text{subject to} \quad -M(1-u_{\text{ID},t})u_{\text{buy-possible},t} \le P_{\text{ID},t} \le Mu_{\text{ID},t}u_{\text{sell-possible},t} \qquad t=1,...,N_t \tag{3.6}$$

$$-Mu_{\text{ID},t} \le \Pi_{\text{ID},t} - \lambda_{\text{ID-buy},t}P_{\text{ID},t}dt \le Mu_{\text{ID},t} \qquad t=1,...,N_t \tag{3.7}$$

$$-M(1-u_{\text{ID},t}) \le \Pi_{\text{ID},t} - \lambda_{\text{ID-sell},t}P_{\text{ID},t}dt \le M(1-u_{\text{ID},t}) \qquad t=1,...,N_t \tag{3.8}$$

$$P_{\text{generated},j,t} - P_{\text{DA},t} \le P_{\text{IM-forecast},j,t} \le P_{\text{DA},t} - P_{\text{generated},j,t} \qquad t=1,...,N_t \wedge j=1,...,N_c \tag{3.9}$$

$$\Pi_{\text{IM-forecast},j,t} = P_{\text{IM-forecast},j,t}\cdot\lambda_{\text{IM-forecast},t} \qquad t=1,...,N_t \wedge j=1,...,N_c \tag{3.10}$$

$$0 \le P_{\text{generated},j,t} \le \hat{P}_{\text{source},j,t} \qquad t=1,...,N_t \wedge j=1,...,N_c \tag{3.11}$$

$$E_{\text{battery},j,t+1} = E_{\text{battery},j,t} + P_{\text{charge},j,t}dt\cdot\eta_{\text{battery}} - \frac{P_{\text{discharge},j,t}dt}{\eta_{\text{battery}}} \qquad t=1,...,N_t+1 \wedge j=1,...,N_c \tag{3.12}$$

$$0 \le P_{\text{charge},j,t} \le u_{\text{charging},j,t}P_{\text{max-battery}} \qquad t=1,...,N_t \wedge j=1,...,N_c \tag{3.13}$$

$$0 \le P_{\text{discharge},j,t} \le (1-u_{\text{charging},j,t})P_{\text{max-battery}} \qquad t=1,...,N_t \wedge j=1,...,N_c \tag{3.14}$$

$$P_{\text{battery},j,t} = P_{\text{discharge},j,t} - P_{\text{charge},j,t} \qquad t=1,...,N_t \wedge j=1,...,N_c \tag{3.15}$$

$$E_{\text{DoD}} \le E_{\text{battery},j,t} \le E_{\text{max-battery}} \qquad t=1,...,N_t \wedge j=1,...,N_c \tag{3.16}$$

$$E_{\text{battery},j,t_{\text{current}}} = E_{\text{start}} \qquad j=1,...,N_c \tag{3.17}$$

$$P_{\text{HPP},j,t} = P_{\text{generated},j,t} + P_{\text{battery},j,t} \qquad t=1,...,N_t \wedge j=1,...,N_c \tag{3.18}$$

$$-P_{\text{grid-withdraw}} \le P_{\text{HPP},j,t} \le P_{\text{grid-feed-in}} \qquad t=1,...,N_t \wedge j=1,...,N_c \tag{3.19}$$

$$P_{\text{IM-forecast},j,t} = P_{\text{HPP},j,t} - (P_{\text{DA},t} + P_{\text{ID-commit},t} + P_{\text{ID},t}) \qquad t=1,...,N_t \wedge j=1,...,N_c \tag{3.20}$$

The objective of each optimization problem is to maximize the expected value of passive imbalance revenue forecast ($\Pi_{\text{IM-forecast},j,t}$) and intraday revenue ($\Pi_{\text{ID},t}$), aggregated across all time steps $t = 1,..,N_t$ and scenarios $j = 1,\ldots,N_c$, as shown in Equation 3.5, while satisfying all operational and market constraints across all considered scenarios.

The decision variables in this stage include the realized intraday traded power ($P_{\text{ID},t}$), expected power imbalance ($P_{\text{IM-forecast},j,t}$), and the resulting realized intraday revenue ($\Pi_{\text{ID},t}$) and expected imbalance revenue ($\Pi_{\text{IM-forecast},j,t}$). Additionally, the model forecasts the physical power flows: forecast for RES generation accounting for curtailment ($P_{\text{generated},j,t}$), charging and discharging powers ($P_{\text{charge},j,t}$ and $P_{\text{discharge},j,t}$), the battery state of charge ($E_{\text{battery},j,t}$), and the total power output of the hybrid power plant ($P_{\text{HPP},j,t}$). Binary variables $u_{\text{charging},j,t}$ and $u_{\text{ID},t}$ ensure correct battery operation and pricing logic, respectively, based on power flow directions. It is important to note that in this optimization stage only the intraday trades and revenues are fixed and realized, while all other decisions are based on forecasts and thus expected values. This is explicitly defined in Table 3.1.

The constraints are organized into intraday market participation, imbalance settlement, generation, battery operation, and power balance categories, as detailed below.

Intraday Market Constraints

Market liquidity limitations are captured using binary variables $u_{\text{sell-possible},t}$ and $u_{\text{buy-possible},t}$, which are defined during data pre-processing. These variables indicate whether buying or selling is possible in a given time step based on the order book and are enforced by Equation 3.6.

Intraday revenue is computed as the product of traded power $P_{\text{ID},t}$ and the applicable market price $\lambda_{\text{ID,buy},t}$ or $\lambda_{\text{ID,sell},t}$, multiplied by the duration of the market product, one timestep of 15 minutes in this study (dt). A binary variable $u_{\text{ID},t}$ determines whether a trade is a buy or a sell, ensuring the correct price is applied via big-M formulations in Equations 3.7 and 3.8.

Imbalance Market Constraints

To prevent speculation based upon a simplistic imbalance price forecast, the power traded on the imbalance market is restricted following the same logic as Heredia, Cuadrado, and Corchero [10]. This limits the expected imbalance power to the difference between actual generation and previously committed trades, as formulated in Equation 3.9.

The imbalance market handles discrepancies between actual power delivery and committed trades. Using the day-ahead clearing prices as an imbalance price forecast ($\lambda_{\text{IM-forecast},t}$) results in approximated imbalance revenues ($\Pi_{\text{IM-forecast},j,t}$), as described in Equation 3.10.

Power Generation Constraints

The generated RES output in each scenario is defined by Equation 3.11. This defines the expected curtailed generation, where the upper bound for each scenario is set by the expected available RES power of that scenario ($\hat{P}_{\text{source},j,t}$).

BESS Operation Constraints

Battery energy dynamics are governed by Equation 3.12, which accounts for charging and discharging losses represented by the battery efficiency (η_{battery}). The expected charging and discharging power flows are separately defined in Equations 3.13 and 3.14. A binary variable $u_{\text{charging},j,t}$ ensures that charging and discharging do not occur simultaneously, while Equation 3.15 computes the net battery power.

The state of charge is bounded between the minimum depth of discharge (E_{DoD}) and the maximum capacity ($E_{\text{max-battery}}$) (Equation 3.16). The initial battery state at the beginning of each iteration is specified in Equation 3.17.

Power Balance Constraints

The physical power expected to be exchanged with the grid ($P_{\text{HPP},j,t}$) must match the net output of the RES and the battery, as specified in Equation 3.18. This output must lie within the grid connection capacity limits defined in Equation 3.19. Here, the power to withdraw from the grid ($P_{\text{grid-withdraw}}$) and to feed into the grid ($P_{\text{grid-feed-in}}$) are defined separately as the grid connection can be asymmetrical.

Finally, the market balance constraint is given in Equation 3.20, which states that the residual between physical output and total market commitments constitutes the imbalance volume.

The above formulation is applied at each optimization iteration. For simplicity, the mathematical formulation is not explicitly indexed by the optimization iteration ($i = 1, \ldots, N_i$). However, input variables follow from previous optimization iterations. From the intraday bidding and expected imbalance stage, the resulting intraday commitments ($P_{\text{ID, commit},i,t}$) from each optimization serve as input for the subsequent real-time imbalance optimizations as well as the next intraday bidding and expected imbalance optimizations. The updated intraday commitment is defined as the intraday trade actions from the most recent optimization ($P_{\text{ID},i,t}$), added to the commitments made in the previous iterations ($P_{\text{ID-commit},i-1,t}$), as shown in Equation 3.21.

$$P_{\text{ID-commit},i,t} = P_{\text{ID-commit},i-1,t} + P_{\text{ID},i,t} \quad i = 1, \ldots, N_i \wedge t = 1, ..., N_{t,i} \tag{3.21}$$

3.3.3. Real-time Operation

The final stage of the multi-stage optimization framework addresses the real-time operation of the HPP, during which physical power delivery occurs. Therefore, the model decisions result in realized output, rather than expected output. At this point, no further trades can be made in the intraday market. The mathematical formulation of the MILP is described by Equation 3.11–3.19 and 3.22 – 3.23. This stage is implemented over the most recent delivery window, as represented by the blue box in Figure 3.3 and 3.4. Mathematically this is defined as $t = t_{\text{current}} - t_{\text{update}}, \ldots, t_{\text{current}}$, where t_{current} is the current time and t_{update} is the interval between rolling iterations. Within this window, actual physical generation and battery operations are decided. As these values are known, scenario-based forecasting is no longer used.

$$\text{maximize} \quad \sum_{t=t_{\text{current}}-t_{\text{update}}}^{t_{\text{update}}} \Pi_{\text{IM},t} \tag{3.22}$$

$$\text{w.r.t.} \quad \Pi_{\text{IM}},\ P_{\text{IM}},\ P_{\text{generated}},\ P_{\text{charge}},\ P_{\text{discharge}},\ E_{\text{battery}},\ P_{\text{HPP}},\ u_{\text{regulation}}$$

$$\text{subject to} \quad P_{\text{IM},t} = P_{\text{HPP},t} - (P_{\text{DA},t} + P_{\text{ID-commit},t}) \qquad t = t_{\text{current}} - t_{\text{update}}, \ldots, t_{\text{current}} \tag{3.23}$$

$$-M(1 - u_{\text{regulation},t}) \leq P_{\text{IM},t} \leq M u_{\text{regulation},t} \qquad t = t_{\text{current}} - t_{\text{update}}, \ldots, t_{\text{current}} \tag{3.24}$$

$$-M(1 - u_{\text{regulation},t}) \leq \Pi_{\text{IM},t} - \lambda_{\text{IM,long},t} P_{\text{IM},t} dt \leq M(1 - u_{\text{regulation},t}) \qquad t = t_{\text{current}} - t_{\text{update}}, \ldots, t_{\text{current}} \tag{3.25}$$

$$-M u_{\text{regulation},t} \leq \Pi_{\text{IM},t} - \lambda_{\text{IM,short},t} P_{\text{IM},t} dt \leq M u_{\text{regulation},t} \qquad t = t_{\text{current}} - t_{\text{update}}, \ldots, t_{\text{current}} \tag{3.26}$$

$$\text{Eq. (3.11)–(3.19)} \qquad t = t_{\text{current}} - t_{\text{update}}, \ldots, t_{\text{current}}$$

The objective of this stage is to steer real-time power flows to maximize realized revenue on the imbalance market ($\Pi_{\text{IM},t}$), as formulated in Equation 3.22. This optimization is based on realized physical output and the most recent system information available at the time of delivery. The dual pricing mechanism of the Dutch imbalance market is considered, assuming perfect foresight of imbalance prices.

The decision variables include the imbalance power ($P_{\text{IM},t}$) and the regulation direction ($u_{\text{regulation},t}$), which together determine the imbalance revenue ($\Pi_{\text{IM},t}$). Additional real-time decisions include for curtailment corrected RES output ($P_{\text{generated},t}$), battery charging and discharging powers ($P_{\text{charge},t}$) and ($P_{\text{discharge},t}$), the battery state of charge ($E_{\text{battery},t}$), and the total HPP output ($P_{\text{HPP},t}$).

The realized imbalance volume is calculated as the difference between physical output and prior market commitments from the day-ahead and intraday stages, as shown in Equation 3.23.

The Dutch imbalance market uses a dual pricing mechanism where the applicable imbalance price depends on the HPP's system position, as described in Chapter 2. The binary variable $u_{\text{regulation},t}$ indicates this: $u_{\text{regulation},t} = 1$ for surplus and $u_{\text{regulation},t} = 0$ for shortage. This relationship is enforced by the big-M formulation in Equation 3.24.

The realized imbalance revenue also depends on the imbalance price associated with the regulation position. When in surplus, the long imbalance price ($\lambda_{\text{IM,long},t}$) is applied; in shortage, the short imbalance price ($\lambda_{\text{IM,short},t}$) is applied. These cases are captured by Equations 3.25 and 3.26.

All physical constraints on generation and storage, originally defined in Equations 3.11–3.19, remain applicable in this stage but are enforced deterministically based on realized trajectories. Thus the decision on power flows are executed during this stage, rather than used as a forecast as in the intraday bidding and expected imbalance stage.

Crucially, the realized operation in this stage not only determines imbalance revenues, but also establishes the initial conditions for the next intraday bidding (Equation 3.28) and real-time operation stages. For the real-time operation stage, the battery state of charge ($E_{\text{start},i}$) at the beginning of the real-time operation optimization ($t = t_{\text{current,i}} - t_{\text{update}}$) must match the final battery energy level from the previous

iteration ($i-1$). This consistency is enforced by Equation 3.27, which ensures that energy trajectories align across successive optimization windows.

$$E_{\text{start,RTO},i} = E_{\text{start},i,t=t_{\text{current,i}}-t_{\text{update}}} = E_{\text{battery},i-1,t=t_{\text{current},i-1}} \quad i = 1,\ldots,N_i \tag{3.27}$$

Moreover, the energy in the battery at the start of the intraday bidding and expected imbalance stage (IDB) is defined by the real-time operation within the same iteration (i), as is given by Equation 3.28. Since the two stages are solved simultaneously this is carried over to the next stage within the same optimization iteration.

$$E_{\text{start,IDB},i} = E_{\text{battery},i,t=t_{\text{current}}} \quad i = 1,\ldots,N_i \tag{3.28}$$

Table 3.1: Stage-wise overview of the multi-stage optimization framework. For each stage the table details the input variables and their sources, forecast type, objective, decision and output variables (distinguishing realized from forecasted), as well as the optimization frequency and time horizon.

	Day-ahead bidding stage	**Intraday bidding and expected imbalance stage**	**Real-time operation stage**
Input variables	External: MAC_{RES} $\lambda_{\text{DA},t}$ $P_{\text{forecast, }t_{\text{current}}} = P_{\text{DA,bid}}$	DA bidding stage: $P_{\text{DA},t}$ Real-time IM stage: $E_{\text{start,IDB}}$ External: $\lambda_{\text{IM-forecast},t} = \lambda_{\text{DA},t}$ $\lambda_{\text{ID,buy},t}$ $\lambda_{\text{ID,sell},t}$ $u_{\text{ID-buy-possible},t}$ $u_{\text{ID-sell-possible},t}$ $P_{\text{forecast,t}}$ $ARMA(2,2)$	DA bidding stage: $P_{\text{DA},t}$ ID bidding and IM forecast stage: $P_{\text{ID-commit},t}$ Previous real-time IM optimization stage: $E_{\text{start,RTO}}$ External: $P_{\text{forecast},t}$ $\lambda_{\text{IM,short},t}$ $\lambda_{\text{IM,long},t}$
Type of power forecast	Deterministic	Stochastic	Perfect foresight
Objective	Maximize DA revenue	Maximize ID revenue and forecasted IM revenue	Maximize IM revenue
Decision variables	$u_{\text{accepted},t}$	$\Pi_{\text{ID},t}$ $\Pi_{\text{IM-forecast},j,t}$ $P_{\text{generated},j,t}$ $P_{\text{ID},t}$ $P_{\text{IM-forecast},j,t}$ $P_{\text{battery},j,t}$ $E_{\text{battery},j,t}$ $P_{\text{HPP},j,t}$ $u_{\text{charging},j,t}$ $u_{\text{ID},t}$	$\Pi_{\text{IM},t}$ $P_{\text{IM},t}$ $P_{\text{generated},t}$ $P_{\text{battery},t}$ $E_{\text{battery},t}$ $P_{\text{HPP},t}$ $u_{\text{regulation},t}$ $u_{\text{charging},t}$
Output variables	Realized: $\Pi_{\text{DA},t}$ $P_{\text{DA},t}$	Realized: $\Pi_{\text{ID},t}$ $P_{\text{ID-commit},t}$ $u_{\text{ID},t}$ Forecasted: $\Pi_{\text{IM-forecast},j,t}$ $P_{\text{IM-forecast},j,t}$ $P_{\text{generated},j,t}$ $P_{\text{battery},j,t}$ $E_{\text{battery},j,t}$ $P_{\text{HPP},j,t}$ $u_{\text{charging},j,t}$	Realized: $\Pi_{\text{IM},t}$ $P_{\text{IM},t}$ $P_{\text{generated},t}$ $P_{\text{battery},t}$ $E_{\text{battery},t}$ $P_{\text{HPP},t}$ $u_{\text{regulation},t}$ $u_{\text{charging},t}$
Optimization frequency	Once per day	Every '$t_{\text{update}} \cdot dt$' hours	Every '$t_{\text{update}} \cdot dt$' hours
Time horizon	$[t_{\text{current},i} + \frac{11}{dt},$ $t_{\text{current},i} + N_{t,i}]$	$[t_{\text{current},i},\ t_{\text{current},i} + N_{t,i}]$	$[t_{\text{current,i}} - t_{\text{update},i}, t_{\text{current},i}]$

3.4. Scenario Generation and Reduction Methodology

The uncertainty associated with power forecasts is addressed by introducing stochastic variables into the model. A widely adopted method to represent these variables is through discrete set of scenarios associated with probability of realization. To comprehensively capture the stochastic behavior of a system, a large set of scenarios is required. However, with an increasing number of scenarios, the computational burden grows, demanding a careful trade-off between accuracy and computational efficiency. Therefore, clustering of scenarios is often used.

In this study, power generation forecast ($\hat{P}_{\text{source}j,t}$) is treated as a stochastic variable for the intraday bidding and expected imbalance optimization stage. Each scenario cluster is represented by a representative scenario that corresponds to a realization of this stochastic variable. In the optimization decision variables are determined depending on the power available. These decision variables are defined in Section 3.3.2. To generate representatives for scenario clusters first scenarios must be generated. The generation and clustering of these scenarios will be discussed next.

3.4.1. Scenario Generation

To account for the uncertainty in renewable power production, this study uses historical data to generate stochastic scenarios for future generation. The scenario generation is based on a combination of a deterministic forecast and a statistical model of historical forecasting errors as described by Conejo, Carrión, and Morales [26].

The historical forecasting error is defined as the difference between the day-ahead forecast used to submit market bids and the actual realized power generation. In this study, the day-ahead forecast is based on weather data published at 9:00 on the day prior to delivery ($t = 9{:}00\ D-1$), representing a realistic operational setting where approximately three hours are required to generate a power forecast from the published weather data. As a result, the forecast used spans delivery periods from 00:00 to 23:45 on day D, implying a lead time range of approximately 15 to 39 hours depending on the specific delivery time. The historical forecast error $\epsilon_{\text{historical},t}$ is then computed as the difference between this fixed day-ahead forecast and the realized generation at time t, as shown in Equation 3.29:

$$\epsilon_{\text{historical},t} = P_{\text{forecast,DA-bids}} - P_{\text{realized},t} \tag{3.29}$$

While this method does not explicitly model the effect of lead time on forecast accuracy, it captures the realistic operational error associated with day-ahead bidding. Given that the emphasis of this study lies in optimizing market participation under forecast uncertainty rather than developing a detailed forecasting model, this approximation is considered sufficient for generating representative stochastic input scenarios.

To represent the statistical properties of the forecast error, an autoregressive moving average (ARMA) model is employed, similar to methods used by Gulotta et al. [27] and Ayón, Moreno, and Usaola [15]. The ARMA model is well-suited to describe time series data with temporal dependencies and residual structure, making it an appropriate choice for modeling forecasting error dynamics.

An ARMA model consists of two key components and is mathematically defined by Equation 3.30. The Autoregressive (AR) component captures the relationship between the current value of the error and its previous values (lags). The number of lag terms included is denoted by the parameter p. Additionally, the Moving Average (MA) component captures the relationship between the current error and past white noise terms (i.e., residuals from a lagged error process). The number of these terms is denoted by the parameter q.

$$y_t = \mu + \sum_{m=1}^{p} \phi_m y_{t-m} + \varepsilon_t - \sum_{n=1}^{q} \theta_n \varepsilon_{t-n} \tag{3.30}$$

In Equation 3.30, y_t represents the forecast error at time t, and μ is the constant mean level around which the process fluctuates. The parameters ϕ_m are the autoregressive (AR) coefficients that quantify the influence of past errors y_{t-m} on the current value, with $m = 1, \ldots, p$. The term ε_t denotes a white

noise error term at time t, assumed to be independently and identically distributed with zero mean. The parameters θ_n are the moving average (MA) coefficients that capture the influence of past shock terms ε_{t-n}, where $n = 1, \ldots, q$. Together, these elements allow the ARMA model to describe both the temporal structure of the error process and its stochastic fluctuations.

To apply the ARMA(p, q) model for scenario generation, the appropriate model order is selected based on the historical error series, sampled over a full year with 15 minute time intervals. The values of p and q are determined using the Akaike Information Criterion (AIC), which balances model fit with complexity. Next, the ARMA model is fitted to the historical forecast errors. The model parameters are estimated by performing a maximum likelihood estimation (MLE), resulting in values for μ, ϕ_m, and θ_n.

The calibrated ARMA model is then used to simulate multiple future realizations of forecast errors ($\epsilon_{\text{simulated}}$). These simulated error paths are added on the deterministic forecast (P_{forecast}) to construct a set consisting of N_s stochastic power generation scenarios ($\hat{P}_{\text{source},s,t}$), as defined in Equation 3.31. Each realization represents a plausible trajectory of future power output that reflects both forecast uncertainty and temporal error structure. To ensure the power forecast scenarios adhere the physical bounds of the RES, the upper and lower bounds are defined by Equation 3.32, where $P_{\text{max-power-source}}$ is the maximum power of the RES.

$$\hat{P}_{\text{source},s,t} = P_{\text{forecast},t} + \epsilon_{\text{simulated},s,t} \qquad t = 1, ..., N_t \wedge s = 1, ..., N_s \tag{3.31}$$

$$0 \leq \hat{P}_{\text{source},s,t} \leq P_{\text{max-power-source}} \qquad t = 1, ..., N_t \wedge s = 1, ..., N_s \tag{3.32}$$

An example of the generated power forecast scenarios is shown in Figure 3.5. These scenarios are created by superimposing ARMA(2,2)-simulated forecast errors onto the latest available deterministic forecast, which in this case is based on weather data published at 05:00 and processed into a forecast by 08:00. This results in a lead time ranging from 3 to 19 hours. The deterministic forecast is shown in orange, five stochastic scenarios in blue, and the realized power in green.

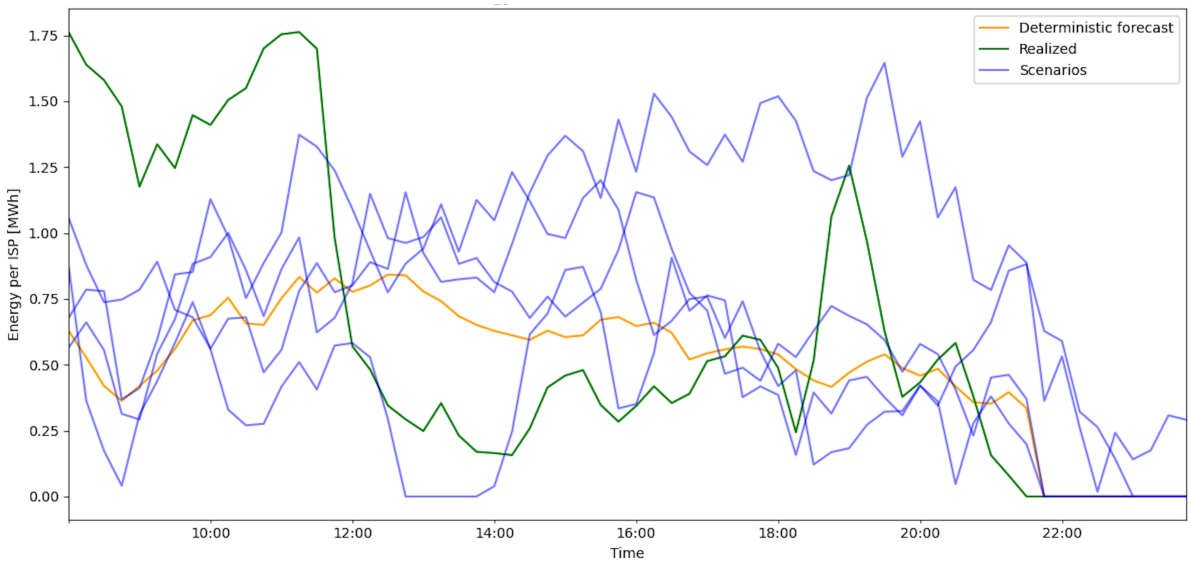

Figure 3.5: Five forecast scenarios with a lead time of 3-19 hours generated by imposing ARMA(2,2) sampled errors. The deterministic forecast is taken as one scenario. The realized power output is also shown.

Figure 3.5 illustrates a key limitation of the scenario generation process: the realized power falls outside the bounds of the scenario ensemble during multiple periods. This underrepresentation of extreme values suggests that, although the ARMA model captures central tendencies and temporal structure, it fails to represent distribution tails adequately. As a result, the stochastic optimization may overlook high-impact deviations, potentially leading to suboptimal bidding decisions, increased imbalance costs, or missed trading opportunities.

Capturing rare but impactful events is essential for robust scenario design. One strategy is to generate a larger pool of scenarios and apply clustering to select a representative subset. This can broaden the range of outcomes considered while keeping the problem computationally tractable. The clustering procedure used in this study to address this trade-off is discussed in the next section.

While the ARMA approach offers transparency and low computational cost, several caveats should be noted. It assumes stationarity and linearity, which may not hold in practice, especially under rapidly changing weather conditions. The model also treats forecast error characteristics as uniform across lead times, potentially underestimating short-term accuracy and overstating longer-term variability. Finally, applying errors directly to power output, rather than to underlying meteorological inputs like wind speed, can distort physical realism, particularly in non-linear regions of the power curve.

Despite these limitations, the ARMA-based scenario generation remains a pragmatic approach for representing forecast uncertainty in the context of market-based optimization.

3.4.2. Scenario Clustering

To manage computational complexity while preserving the essential variability in forecast uncertainty, this study applies scenario clustering to reduce the dimensionality of the generated scenario set. Specifically, k-means clustering is used to group similar power trajectories and select a representative scenario for each cluster, which is then assigned a corresponding probability.

K-means clustering is widely used in energy system modeling due to its simplicity and computational efficiency [28, 27, 16]. Each scenario is treated as a time series vector, where each time step is a feature. The algorithm partitions the full set of N_s generated scenarios into N_c clusters by minimizing the total within-cluster variance, using Euclidean distance as a similarity metric. This ensures that scenarios within the same cluster exhibit similar temporal patterns, which is important for capturing consistent operational dynamics over the optimization horizon.

Let p_j denote the probability assigned to cluster j, defined as the proportion of scenarios allocated to it. The representative scenario $\hat{P}_{\text{source},j,t}$ is then the centroid of each cluster, and p_j is computed as follows:

$$p_j = \frac{1}{N_s} \sum_{s=1}^{N_s} \mathbb{I}\left(s \text{ assigned to cluster } j\right) \tag{3.33}$$

Figure 3.6 illustrates 50 generated power scenarios in blue, along with five representative cluster centroids in red. The deterministic forecast and realized power are also shown in orange and green, respectively. Compared to the 5-scenario representation in Figure 3.5, the 50-scenario set more frequently captures the realized trajectory. This suggests improved coverage of plausible outcomes, which is essential for the optimization. The divergence of clustered scenarios with time from the deterministic forecast also reflects the ARMA-based error generation, where deviations naturally grow with lead time.

However, several limitations must be acknowledged. First, the representative scenarios are notably similar, especially during the early hours of the day. This limited diversity reflects both the ARMA model's tendency to generate scenarios that concentrate around the deterministic forecast and the behavior of the k-means algorithm, which minimizes intra-cluster variance. As a result, extreme but rare events, such as large forecast deviations observed in the realized power, may be underrepresented. This underrepresentation can bias the optimization toward overly confident or aggressive market strategies, reducing resilience to adverse conditions.

Moreover, k-means clustering assumes that the central tendency (centroid) of each cluster is an adequate representation of that cluster's dynamics. While effective for capturing average behavior, this approach does not necessarily retain edge cases or non-linear transitions, especially when the original scenario set is already centered around a common deterministic baseline. Additionally, the Euclidean distance metric may underweight rare but operationally significant variations, such as sharp ramps or cut-in/cut-out conditions typical in wind generation. Despite these limitations, the use of clustering allows for a tractable yet probabilistically informed optimization model.

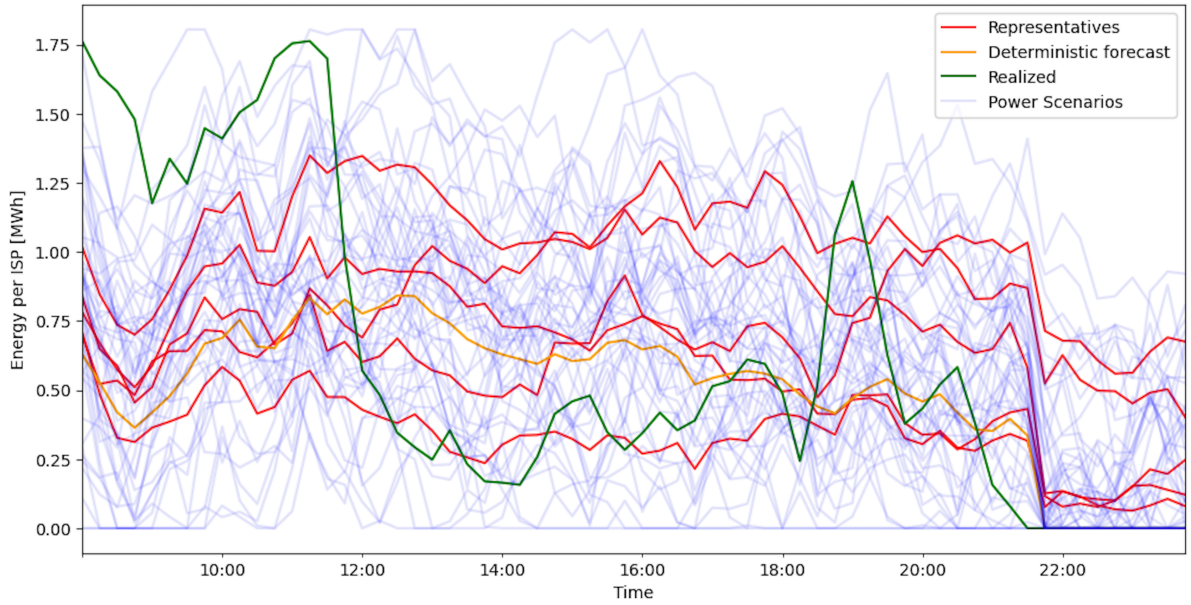

Figure 3.6: Example of 50 forecast scenarios with 5 representative scenarios. Additionally, the deterministic forecast and the realized power output are shown.

3.5. Performance Results

The optimization results in revenues generated and absolute traded energy which are calculated for each market separately. To come to the cumulative revenues, absolute traded energy and physically generated energy, the results have to be summed up over all iterations ($i = 1, \ldots, N_i$) covering the time period of the numerical experiments.

Realized Revenues

The realized revenues for day-ahead and imbalance market are calculated over the real-time operation window, as defined in Section 3.3.3 ($t = [t_{\text{current},i} - t_{\text{update}}, t_{\text{current},i}]$). During this stage the final decisions are made on imbalance positions. In this way, also the day-ahead revenue are only accounted for once. On the other hand, the decisions and thus revenues on the intraday market are made acrosss mutliple optimizations. Therefore, the revenues should be accumulated over all optimizations that cover the a specific time step.

From the day-ahead optimization stage, the accepted bid volume and clearing price are determined, and the corresponding revenue is calculated as defined in Equation 3.1. The realized day-ahead revenue ($\Pi_{\text{DA,realized}}$)is then calculated by summing the hourly revenues over the real-time window of each iteration, as shown in Equation 3.34.

$$\Pi_{\text{DA, realized}} = \sum_{i=1}^{N_i} \left(\sum_{t=t_{\text{current},i}-t_{\text{update},i}}^{t_{\text{update}}} \Pi_{\text{DA},i,t} \right) \tag{3.34}$$

Similarly, the imbalance market revenue is computed by summing the realized imbalance revenues over the real-time window across all iterations. The revenue $\Pi_{\text{IM},i,t}$ at each timestep is decided during the real-time operation stage using the pricing logic in Equations 3.25 and 3.26. The cumulative imbalance revenue is given by:

$$\Pi_{\text{IM, realized}} = \sum_{i=1}^{N_i} \left(\sum_{t=t_{\text{current},i}-t_{\text{update},i}}^{t_{\text{update}}} \Pi_{\text{IM},i,t} \right) \tag{3.35}$$

As a result of the rolling horizon approach intraday trades can be executed across multiple iterations for a single delivery period, at different prices. Therefore, intraday revenues must be accumulated over all past optimizations that contain trades affecting the current real-time window. The intraday revenue for the real-time window of iteration i is computed as:

$$\Pi_{\text{ID,realized},i} = \sum_{k=1}^{N_{\text{i-current}}} \left(\sum_{t=t_{\text{current},i}-t_{\text{update},i}}^{t_{\text{update}}} \Pi_{\text{ID},k,t} \right) \tag{3.36}$$

Here, $N_{\text{i-current}}$ represents the set of iterations k that executed trades for the delivery window covered in iteration i. The total intraday revenue across all iterations is then given by:

$$\Pi_{\text{ID,realized}} = \sum_{i=1}^{N_i} \Pi_{\text{ID,realized},i} \tag{3.37}$$

Together, these calculations yield the total realized revenue ($\Pi_{\text{total,realized}}$) for the HPP across these short-term electricity markets, which is defined by Equation 3.38.

$$\Pi_{\text{total,realized}} = \Pi_{\text{DA, realized}} + \Pi_{\text{IM, realized}} + \Pi_{\text{ID,realized}} \tag{3.38}$$

Realized Energy

In addition to financial performance, it is also important to track the absolute volume of energy traded in each market. This provides insight into the level of market participation and the operational flexibility exercised by the HPP. Here, the focus is specifically on traded energy, representing both purchases and sales, and report absolute values to capture total market activity regardless of direction.

The absolute traded energy in the day-ahead market is calculated by summing the product of committed power and time interval dt over the real-time window for each iteration. The absolute value ensures that both positive and negative trades are included. The cumulative day-ahead traded energy is given by:

$$E_{\text{DA, realized}} = \sum_{i=1}^{N_i} \left(\sum_{t=t_{\text{current},i}-t_{\text{update},i}}^{t_{\text{update}}} |P_{\text{DA},i,t} \cdot dt| \right) \tag{3.39}$$

A similar approach is applied to the imbalance market. The realized imbalance energy reflects deviations from market commitments that were settled financially in real time. It is computed as:

$$E_{\text{IM, realized}} = \sum_{i=1}^{N_i} \left(\sum_{t=t_{\text{current},i}-t_{\text{update},i}}^{t_{\text{update}}} |P_{\text{IM},i,t} \cdot dt| \right) \tag{3.40}$$

For the intraday market, trades affecting a given delivery period may be executed across multiple earlier iterations. Therefore, the realized intraday energy for iteration i aggregates trades from all relevant prior iterations $k = 1, \ldots, N_{\text{i-current}}$. The total intraday traded energy is calculated in two steps:

$$E_{\text{ID,realized,i}} = \sum_{k=1}^{N_{\text{i-current}}} \left(\sum_{t=t_{\text{current},i}-t_{\text{update},i}}^{t_{\text{update}}} |P_{\text{ID},k,t} \cdot dt| \right) \tag{3.41}$$

$$E_{\text{ID,realized}} = \sum_{i=1}^{N_i} E_{\text{ID,realized},i} \tag{3.42}$$

The total absolute traded energy is defined as the sum of the traded energy in each market (Equation 3.43).

$$E_{\text{total-traded}} = E_{\text{DA, realized}} + E_{\text{IM, realized}} + E_{\text{ID,realized}} \tag{3.43}$$

These metrics offer a comprehensive overview of the HPP's engagement across the short-term electricity markets and complement the revenue-based performance indicators. By reporting absolute energy values, the model captures both trading intensity and system responsiveness under uncertainty.

Additionally, the total physical energy that is fed into the grid as well as the energy that is lost due to curtailment are calculated. The physical energy is determined by summing the power fed into the grid per timestep ($P_{\text{HPP,i,t}}$) in the real time operation over all iterations, subtracting the difference between initial energy in the battery ($E_{\text{battery-initial}}$: $i = 1$, $t = 1$) from the energy in at the end of the optimization ($E_{\text{battery-end}}$: $i = N_i$, $t = t_{current}$). This is all reflected in Equation 3.18.

$$E_{\text{physical,realized}} = \sum_{i=1}^{N_i} \left(\sum_{t=t_{\text{current},i}-t_{\text{update},i}}^{t_{\text{update}}} P_{\text{generated},i,t} \cdot dt \right) \tag{3.44}$$

The losses associated with the battery energy storage are defined by Equation 3.45.

$$E_{\text{battery-loss},t} = \sum_{i=1}^{N_i} \left(\sum_{t=t_{\text{current},i}-t_{\text{update},i}}^{t_{\text{update}}} ((1-\eta^2_{\text{battery}}) P_{\text{charge},i,t}) \cdot dt \right) \tag{3.45}$$

Furthermore the energy lost due to curtailment is given by Equation 3.46. Subtracting the potential power that the source could provide

$$E_{\text{curtailed,realized}} = \sum_{i=1}^{N_i} \left(\sum_{t=t_{\text{current},i}-t_{\text{update},i}}^{t_{\text{update}}} (P_{\text{source,i,t}} - P_{\text{generated},i,t}) \cdot dt \right) \tag{3.46}$$

3.6. Case Studies

To validate the model and evaluate the added value of co-locating a BESS with a photovoltaic (PV) or wind asset, three case studies are conducted: HPP, stand alone RES and stand alone BESS. The specifications of the system components and simulation setup are summarized in Table 3.2, 3.3 and 3.4. The physical properties are derived from assets operated by Vandebron.

3.6.1. HPP Case

The HPP case represents the full co-located configuration, consisting of both a RES and a BESS, as modeled in detail throughout this chapter. It serves as the reference configuration for evaluating the added value of hybrid operation.

All model components, day-ahead bidding, intraday trading, and real-time balancing, are active, with both wind generation and battery flexibility contributing to market participation. This configuration forms the basis from which the RES-only and BESS-only cases are derived by selectively disabling the corresponding subsystems.

Component	Specification
Wind Power Plant (RES)	Capacity: $P_{\text{max-power-source}}$ = 7.21 MW
Battery Energy Storage System (BESS)	Capacity: $E_{\text{max-battery}}$ = 5 MWh
	Depth of discharge E_{DoD} = 0.5 MWh
	Initial SoC: $E_{\text{start},i=1}$ = 0.5$E_{\text{max-battery}}$= 2.5 MWh
	C-rate: C = 0.5 hour^{-1}
	Power: $P_{\text{max-battery}}$ = $E_{\text{max-battery}}C$ = 2.5 MW
	Battery efficiency: $\eta_{\text{battery}} = 94.9\%$
Grid Connection	Feed-in limit: $P_{\text{grid-feed-in}}$ = 7.21 MW
	Withdrawal limit: $P_{\text{grid-withdraw}}$ = 0 MW
Forecast Scenarios	Number of scenarios: N_s = 50
	Number of clusters: N_c = 5
	Time series model for error simulation: ARMA(2,2)
Simulation Parameters	Time step: dt = 0.25 hour
	Re-optimization interval: t_{update} = 1 hour
	Optimization duration: T_{sim} = 168 hour
	Optimization iterations: $N_i = \frac{T_{\text{sim}}}{t_{\text{update}}dt}$ = 168 iterations

Table 3.2: Specifications of the assets and simulation setup used in the HPP case study

3.6.2. RES Case

The RES case represents a standalone wind power plant operating without a BESS. It serves as the baseline configuration. In this case, all battery-related dynamics and constraints, specifically those defined in Equations 3.12 to 3.17, are disabled in both the intraday bidding and real-time operation stages. Additionally, battery power flows are set to zero ($P_{\text{battery}} = 0$), ensuring that only wind generation contributes to market participation. This is summarized in Table 3.3.

Component	Specification
Wind Power Plant (RES)	Capacity: $P_{\text{max-power-source}}$ = 7.21 MW
Grid Connection	Feed-in limit: $P_{\text{grid-feed-in}}$ = 7.21 MW
	Withdrawal limit: $P_{\text{grid-withdraw}}$ = 0 MW
Forecast Scenarios	Number of scenarios: N_s = 50
	Number of clusters: N_c = 5
	Time series model for error simulation: ARMA(2,2)
Simulation Parameters	Time step: dt = 0.25 hour
	Re-optimization interval: t_{update} = 1 hour
	Optimization duration: T_{sim} = 168 hour
	Optimization iterations: $N_i = \frac{T_{\text{sim}}}{t_{\text{update}}dt}$ = 168 iterations

Table 3.3: Specifications of the assets and simulation setup used in the stand-alone RES case study

3.6.3. BESS Case

The BESS case isolates the operation of a battery system participating in the electricity markets without any co-located renewable generation. The day-ahead bidding stage is omitted by setting the committed power to zero ($P_{\text{DA,t}} = 0$). RES-related constraints, namely Equation 3.11, are disabled in both the intraday and real-time stages.

Since no renewable source is modeled, (stochastic) scenarios are not required. This case is therefore solved deterministically ($N_c = 0$), with the generated power set to zero ($P_{\text{generated,t}} = 0$). To allow charging from the grid, the grid withdrawal constraint is relaxed to $P_{\text{grid-withdraw}} = P_{\text{max-battery}}$. This configuration highlights the standalone value of flexible storage capacity under current market conditions. The parameters associated with this case can be found in Table 3.4.

Component	Specification
Battery Energy Storage System (BESS)	Capacity: $E_{\text{max-battery}}$ = 5 MWh Depth of discharge E_{DoD} = 0.5 MWh Initial SoC: $E_{\text{start},i=1}$ = 0.5$E_{\text{max-battery}}$= 2.5 MWh C-rate: C = 0.5 hour^{-1} Power: $P_{\text{max-battery}}$ = $E_{\text{max-battery}}C$ = 2.5 MW Battery efficiency: $\eta_{\text{battery}} = 94.9\%$
Grid Connection	Feed-in limit: $P_{\text{grid-feed-in}}$ = 2.5 MW Withdrawal limit: $P_{\text{grid-withdraw}}$ = 2.5 MW
Simulation Parameters	Time step: dt = 0.25 hour Re-optimization interval: t_{update} = 1 hour Optimization duration: T_{sim} = 168 hour Optimization iterations: $N_i = \frac{T_{\text{sim}}}{t_{\text{update}}dt}$ = 168 iterations

Table 3.4: Specifications of the assets and simulation setup used in the stand-alone BESS case study

3.6.4. Performance Metrics

The case studies are evaluated based on their operational and economic performance over four weeks, each selected from a different season to reflect varying weather conditions and market conditions. The following performance metrics are used to quantify and compare the performance of the different system configurations:

- **Total Revenue [€]:** The realized revenue per market, as well as the total revenue, reflects the overall economic return from participation in the day-ahead, intraday, and imbalance markets. This metric serves as an indicator of the total market value captured by the system. In addition, it provides insight into the relative contribution of each market to the total earnings. The corresponding revenue calculations are defined in Equations 3.34 to 3.38.
- **Absolute Traded Energy [MWh]:** This metric quantifies the total traded energy volumes, regardless of direction (buy or sell), across all markets. It serves as a measure of trading activity and market engagement. The associated equations are given in Equations 3.39, 3.40, 3.42, and 3.43.
- **Revenue per Unit of Physical Energy [€/MWh]:** This metric evaluates the economic efficiency of each configuration by normalizing total revenue over the total physical energy delivered to the grid. It isolates the monetary value generated per unit of renewable output, offering insight into the profitability of each MWh of green energy. It is defined as:

$$\text{Revenue per Physical MWh} = \frac{\Pi_{\text{total,realized}}}{E_{\text{physical,realized}}} \tag{3.47}$$

- **Revenue per Unit of Traded Energy [€/MWh]:** This metric relates total revenue to the total traded volume, reflecting the economic efficiency of the system's market actions. It captures the effectiveness of trading strategies by indicating the return per unit of energy traded, regardless of its physical origin:

$$\text{Revenue per Traded MWh} = \frac{\Pi_{\text{total,realized}}}{E_{\text{total-traded}}} \tag{3.48}$$

- **Physical Energy Output and Utilization:** This metric includes the total renewable energy generated (Equation 3.44), the curtailed energy (Equation 3.46), and energy losses due to storage inefficiencies (Equation 3.45). Together, they characterize the system's energetic efficiency and utilization. In addition, the grid connection utilization factor is reported to assess the extent to which available export capacity is used:

$$\text{Grid Connection Utilization Factor} = \sum_{i=1}^{N_i} \left(\sum_{t=t_{\text{current},i}-t_{\text{update},i}}^{t_{\text{update}}} \frac{P_{\text{HPP,i,t}}}{P_{\text{grid-feed-in}}} \right) \tag{3.49}$$

Together, these performance metrics support a systematic comparison of the case studies and provide insight into both the operational behavior and economic impact of the proposed stochastic bidding strategy. Moreover, they enable a quantitative assessment of the value added by co-locating battery storage with renewable generation assets.

3.7. Assumption Testing and Model Sensitivity

To assess the robustness and applicability of the proposed optimization framework, the model is evaluated along two dimensions. First, the impact of key modeling assumptions is examined, focusing on how the accuracy of power and imbalance price forecasts influences system behavior, dispatch decisions, and resulting market outcomes. This includes testing cases of perfect foresight and no foresight of the imbalance price to benchmark the value of improved forecasting. Second, a sensitivity analysis is conducted on a range of design parameters that define the physical and operational characteristics of the system. These include BESS size, storage technology, grid connection constraints, and the re-optimization frequency. Together, these analyses provide insight into how forecast assumptions and system parameters shape the energetic and economic performance of the HPP under real-world market conditions.

Imbalance Price Forecasting

Imbalance prices are highly volatile and strongly influenced by real-time system conditions, making them difficult to predict accurately. In the base case of this study, the day-ahead market clearing price is used as a proxy for the imbalance price during the intraday bidding and expected imbalance stage. While this simplification does not capture sudden price spikes, it provides a useful directional estimate that supports market optimization, as explained in Section 3.2.3.

To assess the sensitivity of the model to this assumption, two alternative forecasting configurations are evaluated:

- **Perfect foresight:** The model has full knowledge of future imbalance prices during the intraday bidding and expected imbalance stage. This scenario serves as an upper bound for potential revenue and highlights the theoretical value of perfect imbalance price forecasting.
- **No foresight:** The model performs intraday bidding without any information about imbalance prices. This isolates the effect of imbalance price uncertainty on market decisions. More specifically, the model only optimizes for intraday revenues, rather than weighing them against the expected imbalance revenues.

Renewable Power Forecasting

The second assumption tested concerns the treatment of renewable generation uncertainty. In the base model, power forecasts are represented using 50 stochastic scenarios, which are clustered into five representative trajectories. To evaluate the benefit of using such scenario-based forecasting, the model is also run under a perfect foresight configuration, where the realized renewable generation is known in advance and thus one deterministic forecast is used. This comparison illustrates the operational and economic value of improved accuracy of one deterministic power forecast, compared to stochastic power forecasts.

3.7.1. Sensitivity Analysis – System Design Parameters

To evaluate the influence of key physical and operational parameters on the performance of the HPP compared to the stand-alone BESS and RES, a series of sensitivity analyses were conducted. These analyses aim to test how variations in BESS sizing, storage technology, grid connection capacity, and re-optimization frequency affect both economic and energetic outcomes under market uncertainty.

The BESS size is a fundamental design choice that directly determines the system's storage capacity and power rating, which in turn governs its flexibility to shift energy temporally and participate in multiple electricity markets. Additionally the Vanadium-Redox Flow Battery technology is also considered, as different technical characteristics such as round-trip efficiency and C-rate affect system responsiveness and energy losses.

Given the increasing relevance of grid congestion, the grid connection capacity is another critical constraint. Different configurations are assessed, including unrestricted connections and cases where

feed-in or withdrawal are individually limited, to explore how directional constraints shape market access and renewable energy utilization. Due to the asymmetrical nature of the constraints, the grid connection utilization is split into feed-in and withdrawal components, as defined in Equations 3.50 and 3.51.

$$\text{Grid Connection Utilization Factor (Feed-in)} = \sum_{i=1}^{N_i} \left(\sum_{t=t_{\text{current},\,i}-t_{\text{update},\,i}}^{t_{\text{update}}} \frac{\max(P_{HPP,i,t}, 0)}{P_{\text{grid-feed-in}}} \right) \tag{3.50}$$

$$\text{Grid Connection Utilization Factor (Withdrawal)} = \sum_{i=1}^{N_i} \left(\sum_{t=t_{\text{current},\,i}-t_{\text{update},\,i}}^{t_{\text{update}}} \frac{|\min(P_{HPP,i,t}, 0)|}{P_{\text{grid-withdraw}}} \right) \tag{3.51}$$

Finally, the frequency of re-optimization, the interval at which new market forecasts are incorporated and updated decisions are made, affects the HPP's ability to respond to changing system conditions. This rolling horizon feature of the multi-stage framework is tested across two additional update intervals to evaluate the trade-off between responsiveness and stability.

The cases tested are summarized in Table 3.5. Each parameter is varied while holding other variables constant to isolate its individual impact. Together, these tests provide insight into how design decisions influence system value creation, trading strategy, and renewable integration under uncertainty.

Table 3.5: Model Sensitivity Parameters Overview

Category	Variable	Base	Test case 1	Test case 2	Test case 3
BESS Size Sensitivity					
BESS Size	$E_{\text{battery-max}}$	5 MWh	2.5 MWh	10 MWh	
BESS Technology Characteristics - Vanadium Redox Flow Battery					
Round-trip Efficiency	η_{battery}	90%	75%		
C-rate	C_{rate}	0.5	0.25		
Depth of Discharge	E_{DoD}	0.5 MWh	0 MWh		
Grid Connection Sensitivity					
Feed-in Capacity	$P_{\text{feed-in}}$	7.21 MW	9.71 MW	7.21 MW	9.71 MW
Withdrawal Capacity	P_{withdraw}	0 MW	2.5 MW	2.5 MW	0 MW
Reoptimization Frequency Sensitivity					
Update Interval	t_{update}	4 (1h)	2 (30min)	8 (2h)	

3.8. Implementation

The implementation of the model described in this chapter is structured into three main components, as illustrated in Figure 3.7. Each step is briefly explained below.

The first step is data gathering. This model is implemented as a backward-looking simulation using historical data. Vandebron provided hourly updated power forecasts and realized power production per ISP from one of their on-shore renewable assets, located in Drenthe, the Netherlands. The processing time between the KNMI weather report publication [36] and forecast availability was also considered by introducing a 3 hour delay in forecast access. Therefore the lead time of the forecast has a minimum 3 hours for the first hour and up to maximum of 36 hours. Additionally, day-ahead and imbalance price data were supplied by Vandebron. Intraday order book data was sourced from EnAppSys [37], structured as snapshots capturing the best buy and sell orders per product type (quarter-hourly, half-hourly, hourly) and ISP.

The optimal ARMA(p, q) structure is selected by the auto_arima function of `pmdarima` package [38], determining the values of p and q. This is followed by fitting the ARMA(p, q) model to the historical forecast errors of 2024 by using the ARIMA function of the `statsmodels` [39], to generate power forecast

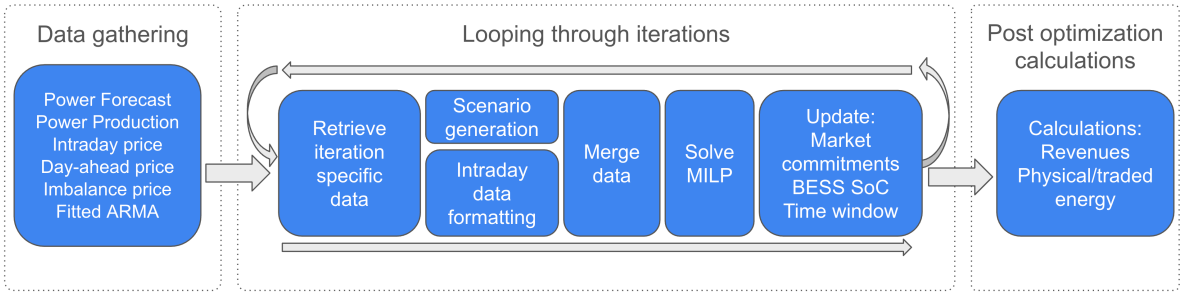

Figure 3.7: Schematic overview of model implementation

uncertainty scenarios. The resulting ARMA(2,2) model with the coefficients displayed in Table 3.6. After generating 50 scenarios, these are clustered into 5 representative clusters using a k-means clustering algorithm which is implemented using the `scikit-learn` Python package [40].

Parameter	Coefficient
ϕ_1	1.62
ϕ_2	-0.63
θ_1	-0.63
θ_2	-0.10
μ	0.0974

Table 3.6: Fitted ARMA(2,2) parameters and values

The second component is the looping structure through iterations. Each iteration begins by retrieving data specific to the current optimization window (as described in Section 3.2.3). Scenarios are then generated based on the most recent forecast and the fitted ARMA model, followed by clustering. Meanwhile, the intraday data is formatted to be compatible with the optimization process.

To prepare the intraday order book data, a tradeable resolution of 5 minutes is assumed. This reflects the assumption that the best available trades within this timeframe could realistically be captured by the plant. Consequently, not all ISPs contain a valid trading opportunity, which is encoded in the binary variables $u_{\text{sell-possible},t}$ and $u_{\text{buy-possible},t}$.

All relevant data, including market signals, power forecasts, and operational parameters, is merged into a single time zone-aware `pandas` DataFrame. This alignment ensures accurate synchronization across all inputs. Additionally, plant design parameters (e.g., BESS size, grid limits), simulation parameters (e.g., time step size, solver settings), and iteration settings (e.g., forecast update frequency) serve as input for the optimization.

The optimization problem, formulated as a MILP, is implemented using Pyomo [41] and solved with the Gurobi Optimizer [42]. Linear formulation significantly improves computational performance compared to quadratic formulations. Gurobi was selected over alternatives like Mosek due to its faster solving time and enhanced debugging features, especially useful for diagnosing infeasibility issues during development.

For each iteration, the optimizer produces two sets of results: one scenario-independent (e.g., intraday bids, intraday revenues, day-ahead commitments) and one scenario-dependent (e.g., power forecast paths, imbalance power, imbalance revenues). These outputs are stored as a list of DataFrames, with one list per iteration. The intraday market position per timestep, final battery state of charge at the end of the real-time operation stage, and updated time window are passed to the next iteration, ensuring continuity.

The final step involves performance metric calculations. Once all optimization iterations have been completed, the results are aggregated to compute key performance metrics including revenues, traded energy volumes, and physically delivered energy. These metrics are used to evaluate model behavior

and answer the research questions.

In summary, the implemented framework effectively integrates data preprocessing, scenario generation, and optimization into a robust iterative structure, enabling realistic modeling of hybrid power plant behavior under market uncertainty.

4

Results

This chapter presents the outcomes of the proposed model. Model performance is assessed on two levels. First, Section 4.1 provides an operational validation at 15-minute resolution, evaluating the system's responsiveness to market signals and its compliance with physical constraints. Second, Section 4.2 analyzes cumulative performance across the four weeks, each from a different season, on economic and energetic outcomes. Together, these analyses assess both the internal consistency of the model and the added value of the three cases. Section 4.3 further evaluates model performance by examining the effects of power and price forecast quality and conducting a sensitivity analysis. Lastly, Section 4.4 offers a critical discussion of the findings.

4.1. Model Validation

To validate the model's operation, optimization results are examined at the 15-minute resolution. This step-by-step evaluation shows how the system responds to dynamic price signals while ensuring compliance with technical and physical constraints. As the trading logic is identical for all configurations, the HPP case is used as the primary validation example. The stand-alone RES and BESS cases are included for comparison, illustrating how the absence of certain assets affects physical system behavior.

Figure 4.1 shows a stacked bar chart illustrating the energy flows per timestep for the first iteration of the HPP case, on day 06-09. The graph is constructed from the perspective of the grid connection point, where physical production, battery operation, and market interactions are aggregated. Positive values indicate feed-in to the grid, originating either from RES production, battery discharge, or net energy purchased on the market. Conversely, negative values represent energy withdrawals, including battery charging, or net sold energy. The flows displayed in Figure 4.1 are the cumulative outcome of the three-stage rolling optimization framework. Each stage contributes specific decisions.

The day-ahead bidding stage, determines commitments to the day-ahead market based solely on RES forecasts. This optimization has taken place on the day before delivery (05-09 13:00), and the optimization window covers the full day from 06-09 00:00 to 23:45. Only sell bids are allowed, represented in the graph by blue bars in Figure 4.1. These commitments remain fixed for the delivery day.

In the intraday bidding and expected imbalance stage, decisions are based on updated RES energy forecasts and updated intraday orderbook. In Figure 4.1, this optimization stage covers the period from 06-09 01:00 to 23:45. The forecast of RES production is shown in dark green. Discrepancies between updated forecasts and DA commitments lead to expected imbalance positions, represented in orange. For instance, between 03:00 and 04:00, the updated RES forecast falls short of DA commitments, resulting in an imbalance shortage (positive orange bar). At 17:30, the forecast indicates a RES surplus, reflected by a negative orange bar. It is important to note that these decisions are not fixed, but expected actions based upon forecast. Thus, these actions could change in next optimizations within the rolling horizon.

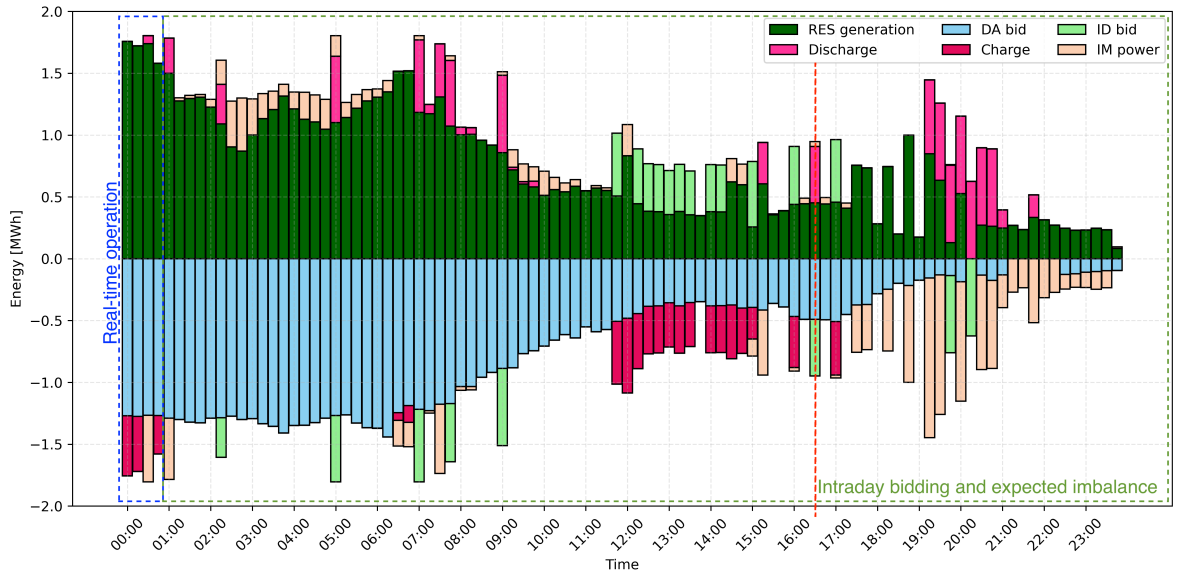

Figure 4.1: HPP case: Energy flows per timestep for the first iteration on 06-09. Positive bars indicate energy delivered or purchased; negative bars represent charging, or energy sold.

During this stage, the model also makes intraday market trades. Intraday buy actions are shown in positive bright green bars, while sell actions appear as negative bright green bars. For example, a buy trade is seen at 05:00, and a sell at 13:00. These trades are considered fixed once executed, but subsequent optimizations may adjust the net intraday position. For instance, an initial buy of +1 MWh followed by a sell of 1.5 MWh would result in a net position of -0.5 MWh (i.e., a net sell).

The model also includes forecasts for battery operation during the intraday bidding and expected imbalance stage. Charging actions are shown as negative pink bars, while discharging is represented by positive pink bars. These actions remain flexible until the start of the delivery window, at which point they are decided upon in the real-time optimization.

The final stage, real-time operation, determines and executes the actual power flows for the upcoming delivery window (e.g., 00:00–01:00 in Figure 4.1). In this stage, the realization, rather than expectation, of all variables is decided. This includes RES generation, battery (dis)charging, and imbalance volumes. The realized outcome reflects a combination of prior forecasts and committed trading actions, providing a consistent and feasible execution of the planned strategy.

Together, the decisions across all three stages result in the comprehensive flow representation in Figure 4.1. These visualizations are used throughout the results chapter to interpret and verify model behavior.

4.1.1. Energy Balance

As discussed in Chapter 3, all energy injected into the grid must be accounted for through one of the three markets: day-ahead, intraday, or imbalance. Day-ahead commitments are fixed per delivery day, while intraday trades and (expected) imbalance volumes are updated each iteration. On the physical side, energy flows are determined by RES availability, curtailment, and battery (dis)charging, subject to grid limits. These traded and physical flows must balance at every timestep.

Crucially, for every timestep, the sum of all positive and negative bars equals zero, confirming that all energy is either traded or internally balanced. This balance is illustrated at 16:30 in Figure 4.1. At this moment, power is sold on both the DA and ID markets, indicated by the negative blue and bright green bars, respectively. To fulfill these market commitments, physical energy is supplied by RES generation (dark green) and battery discharge (pink). However, the total physical output does not fully cover the sold volume, resulting in a shortage that must be settled through the imbalance market, shown as the orange bar.

Cumulatively, the volume committed in the DA and ID markets equals the sum of RES output, BESS discharge, and the imbalance shortfall. This energy balance, with equal total positive and negative contributions, is consistently maintained across the entire optimization horizon displayed.

In the RES case (Figure 4.2), the battery is disabled. As a result, less flexibility is available, which is reflected in the reduced participation in the intraday market. In contrast, the BESS case (Figure 4.3) operates without RES or day-ahead commitments. Here, the system consists solely of the battery, which charges from the grid and discharges based on price signals. In all three cases, the model maintains energy balance while operating within physical and market constraints.

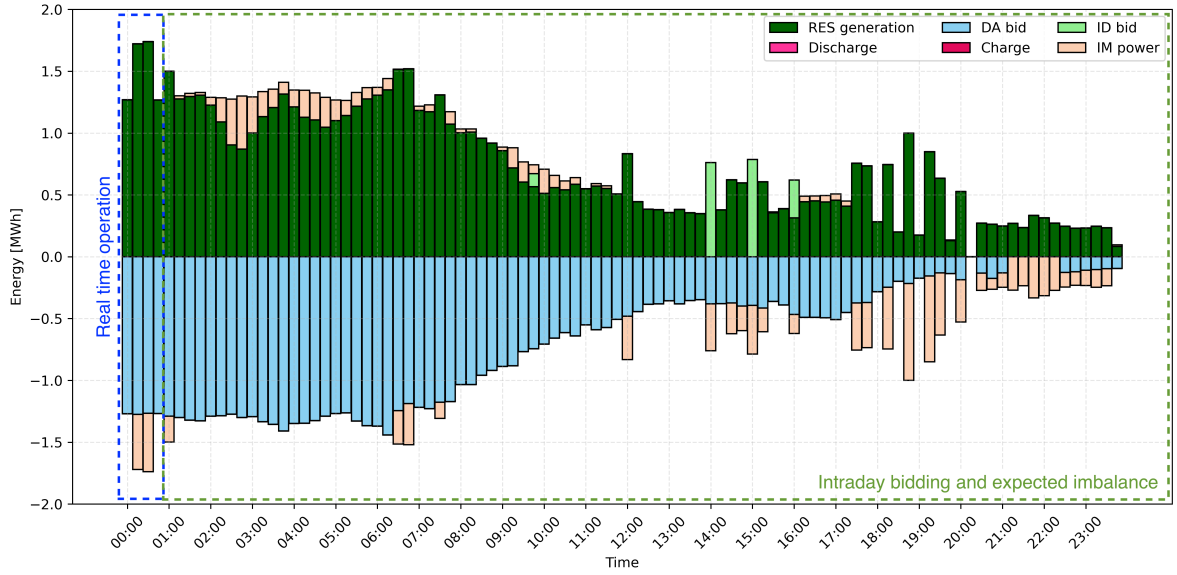

Figure 4.2: RES case: Energy flows per timestep for the first iteration on 06-09. Positive bars indicate energy delivered or purchased; negative bars represent charging, or energy sold.

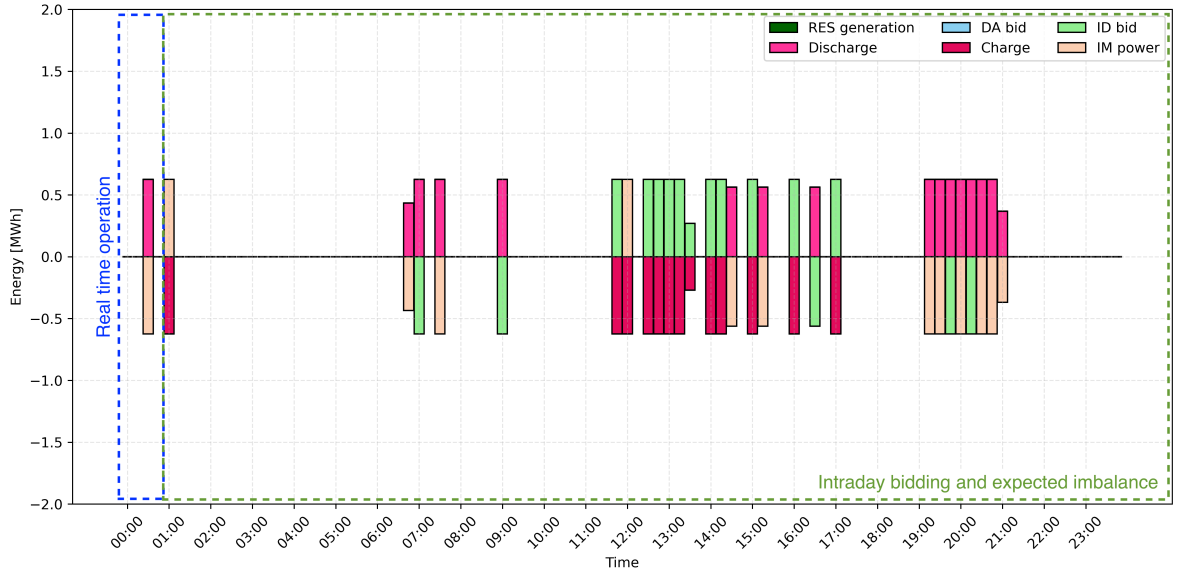

Figure 4.3: BESS case: Energy flows per timestep for the first iteration on 06-09. Positive bars indicate energy delivered or purchased; negative bars represent charging, or energy sold.

4.1.2. Price Signal Response

In addition to maintaining energy balance and respecting the physical limits of the RES, BESS, and grid connection, the model must also respond effectively to market price signals. Figure 4.4, 4.5, 4.6 illustrate one iteration of the rolling horizon optimization for the HPP case. In this iteration, the real-time operation stage spans from 00:00 to 00:45, while the intraday bidding stage covers the period from 01:00 to 23:45. During the intraday bidding stage, the model aims to maximize revenue by acting on updated forecasts and expected prices in both the intraday and imbalance markets.

Forecast Error Mitigation

A key function is to minimize the cost associated to deviations to the e-program. In the event of an oversupply, the model can curtail production, charge the battery, or sell in the most profitable market. In the case of a shortage, it can discharge the battery or purchase energy at the most economical market price.

An example of this behavior occurs between 02:30 and 03:45. The updated power and price input data for this interval of the optimization can be found in Table 4.1. As can be seen the updated power forecasts indicates a shortage relative to the day-ahead commitment. Since the intraday buy price is higher than the imbalance price forecast (Figure 4.4), the model prefers to absorb the shortage through an imbalance position rather than buy on the intraday market (Figure 4.5).

Table 4.1: Energy per ISP (15-minutes) and electricity market price input data for one optimization

Timestamp	P_{DA} [MWh/ISP]	$\mathbb{E}[P_{\text{forecast}}]$[MWh/ISP]	$\lambda_{\text{IM,forecast}}$[€/MWh]	$\lambda_{\text{ID,buy}}$[€/MWh]
02:30	1.27	0.905	50.06	156.15
02:45	1.30	0.871	50.06	198.93
03:00	1.29	1.00	48.83	897.83
03:15	1.33	1.13	48.83	368.38
03:30	1.36	1.21	48.83	131.27
03:45	1.41	1.32	48.83	842.86

In addition to error mitigation, the model exploits two types of arbitrage to generate additional revenue: arbitrage between markets and temporal arbitrage.

Arbitrage Between Markets

Revenue can be enhanced by exploiting price differences between the intraday and imbalance markets. Arbitrage is favorable when energy can be sold in one market at a higher price than it is bought in another. At 05:00, the intraday selling price (91.46 €/MWh) exceeds the expected imbalance price (70.00 €/MWh) (Figure 4.4). The model responds by executing an intraday sell (negative) while simultaneously taking a shortage position in the imbalance market (positive), as shown in Figure 4.5.

Without a constraint on speculative trading (Equation 3.9), this arbitrage opportunity could theoretically lead to unbounded trading. However, due to the uncertainty of imbalance prices, simplicity of the price forecast and uncertainty of the power forecasts, the model restricts the imbalance volume. Consequently, the intraday sell is partially backed by discharging the battery. This trade results in a positive net revenue (Figure 4.6), where the intraday gain outweighs the imbalance loss.

Temporal Arbitrage Within an Iteration

Temporal arbitrage can occur within a single optimization iteration by shifting energy dispatch through storage. For example, energy may be bought at a lower price and stored, then later discharged and sold at a higher price within the same optimization iteration window. This occurs at 16:00 to 16:30, where the battery is charged by energy bought from the intraday and later discharged at a more favorable intraday selling price, resulting in a net revenue gain (Figure 4.6). While in this example this buy and sell both happen in the intraday market, this can also be performed between markets.

Executing both the buy and sell within the intraday market has the advantage of locking in the profit, since both actions are based on known prices and commitments. In contrast, participating in the imbalance market introduces uncertainty, as no commitments are made and final outcomes depend on

real-time system conditions such as, forecast deviations, and imbalance price volatility. As a result, decisions involving imbalance positions are deferred to the real-time operation window, where delivery takes place and final decisions on the operation are made based on most recent information.

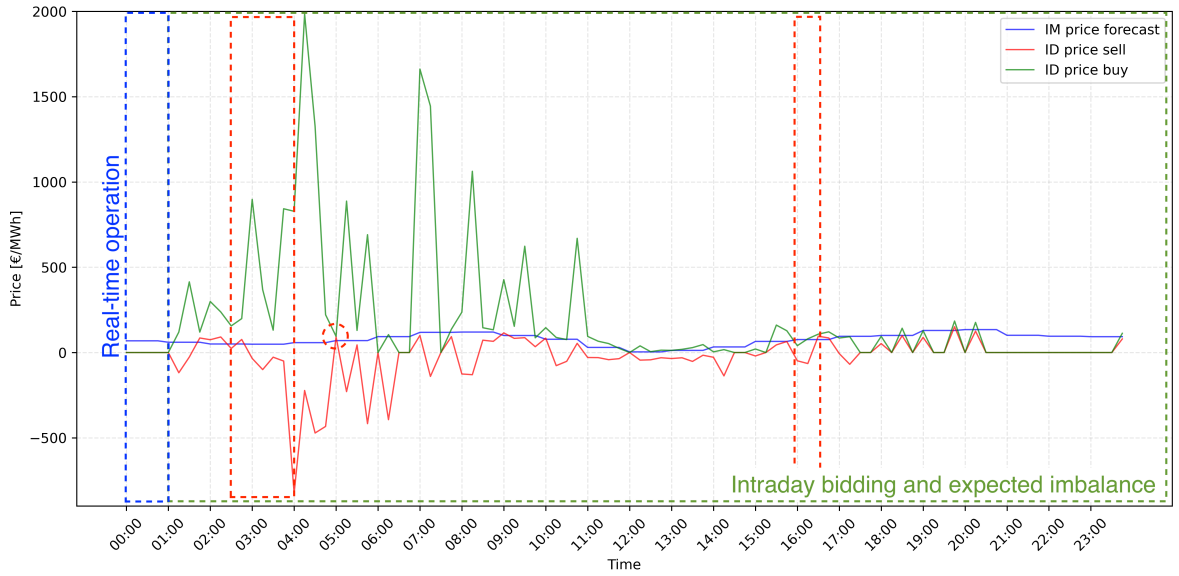

Figure 4.4: Day-ahead and intraday price signals with approximated imbalance prices. The optimization stage covering the time horizon is indicated.

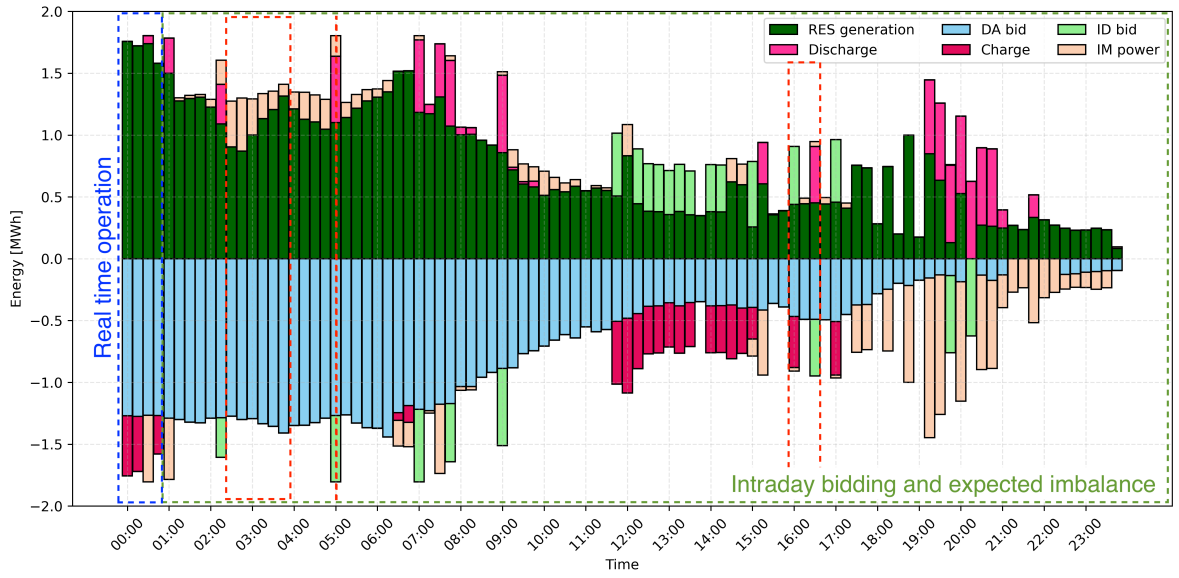

Figure 4.5: HPP traded and physical power per timestep. Positive bars indicate energy delivered or purchased; negative bars represent charging, or energy sold. The optimization stage covering the time horizon is indicated.

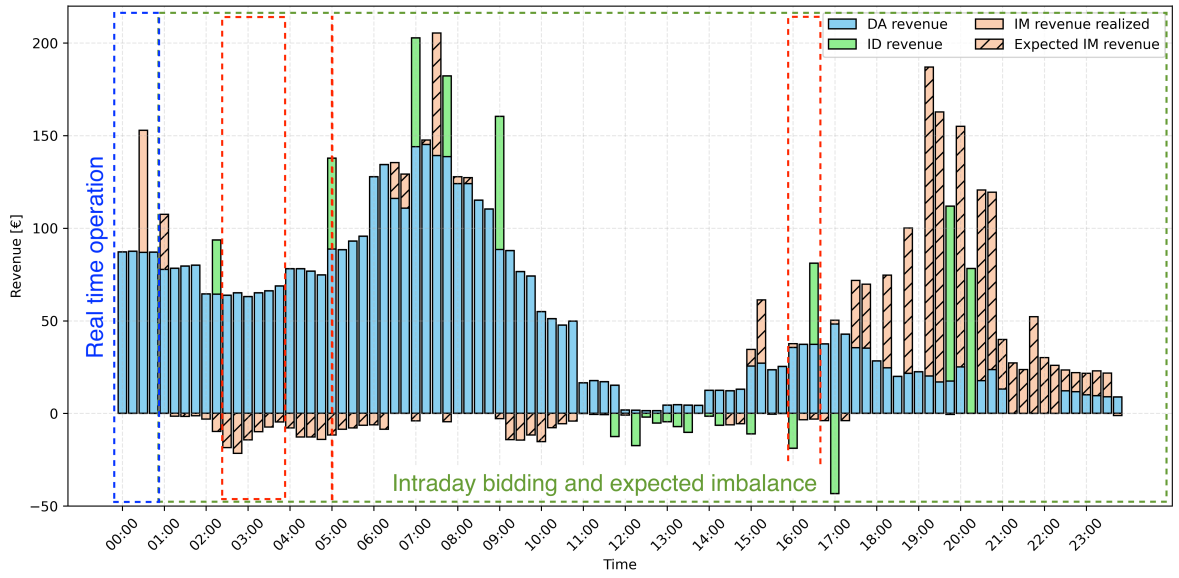

Figure 4.6: Resulting market revenues for the HPP over the optimization iteration. The optimization stage covering the time horizon is indicated.

Re-optimization Arbitrage

Arbitrage on the intraday market can also occur across multiple optimization iterations due to the rolling horizon framework. In this case, energy is bought in one iteration and sold in a subsequent one, capitalizing on price differences between intraday orderbooks retrieved at different times. This strategy is commonly referred to as asset-backed trading.

To illustrate this phenomenon, the results of two consecutive optimization iterations are shown in Figure 4.7. In iteration 8 (Figures 4.7a and 4.7c), the real-time operation window spans from 07:00 to 07:45, and the optimization window for intraday bidding and expected imbalance runs from 08:00 to 23:45. In iteration 9 (Figures 4.7b and 4.7d), these windows shift forward by one hour, covering 08:00 to 08:45 for real-time operations, and 09:00 to 23:45 for the intraday and imbalance stages. Each figure displays the optimized (expected) power flows and the corresponding (expected) revenues.

In iteration 8, at timestep 10:15, an ID buy position has been progressively built up over all preceding optimization iterations, to charge the BESS (Figure 4.7a). This stored energy is used for temporal arbitrage. Charging the BESS results in a negative ID revenue at 10:15 (Figure 4.7c), but this energy is sold at 11:15 at a higher intraday price, resulting in a net profit.

In the subsequent iteration 9, updated forecasts and an updated intraday orderbook are retrieved. Based on these, the model reverses the previous ID buy action by executing a ID sell of twice the volume previously bought. This flips the net ID position at timestep 10:15 from a buy to a sell, now supported by battery discharge (Figure 4.7b). This change yields a positive revenue at the same time (Figure 4.7d), demonstrating successful re-optimization arbitrage. Essentially, this reflects virtual charging and discharging behavior across iterations without corresponding physical delivery.

In this example, the arbitrage takes place entirely through re-optimization and virtual trading, rather than through actual energy shifting via the BESS. A similar approach could be applied using RES curtailment and later generation. However, such strategies involve greater uncertainty due to variability in renewable output.

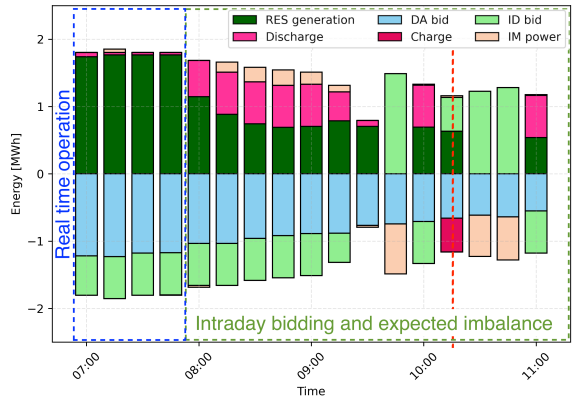

(a) Energy position resulting from optimization iteration 8

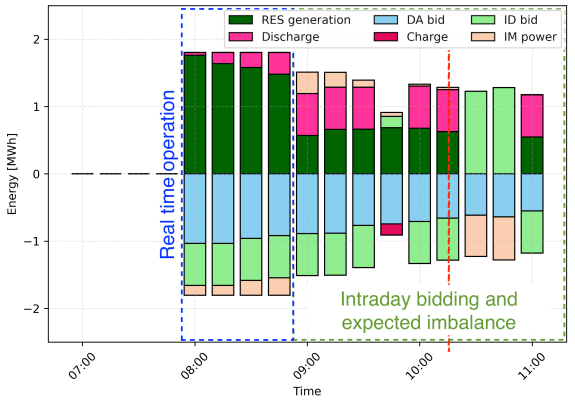

(b) Energy position resulting from optimization iteration 9

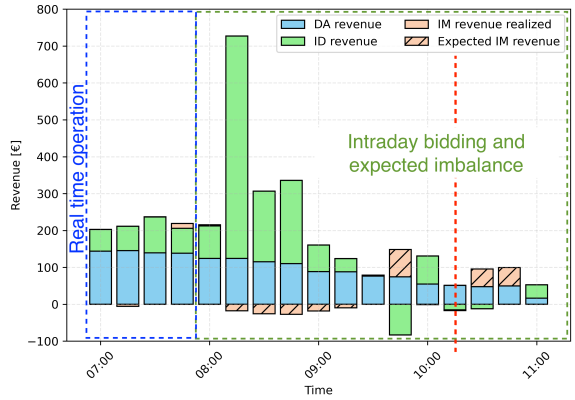

(c) Intraday revenue resulting from optimization iteration 8

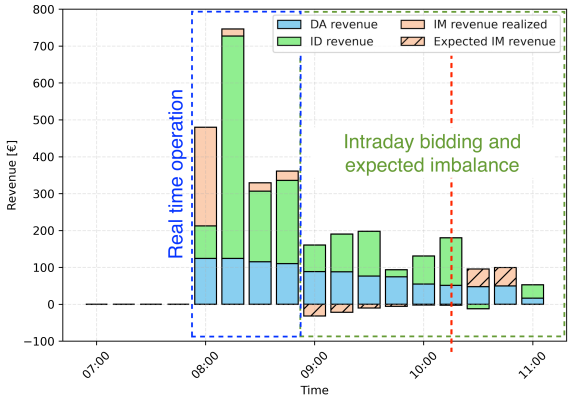

(d) Intraday revenue resulting from optimization iteration 9

Figure 4.7: Demonstration of temporal arbitrage across two iterations using rolling horizon optimization. The bars demonstrate energy flows within one ISP (15 min). Negative bars are energy sold or power consumed within the configuration from the RES. Positive bars are energy bought or power fed into the grid

Real-Time Operation Validation

In contrast to the intraday bidding and expected imbalance stage, where imbalance positions are shaped using power and price forecasts, the real-time operation stage assumes perfect foresight of imbalance prices and power forecast. During this phase, final operational adjustments are made using actual RES output and published price signals to maximize imbalance revenues.

As illustrated in Figure 4.7, the imbalance position during the real-time window of iteration 9 (08:00–08:45) differs from that of iteration 8, as shown in Figures 4.7b and 4.7a. This shift in dispatch leads to a revenue increase in iteration 9 (Figure 4.7d) compared to iteration 8 (Figure 4.7c) over this real-time operation window (08:00–08:45).

This behavior aligns with expectations based on the updated real-time conditions. As shown in Figure 4.8b, the realized RES generation (green line) exceeds the clustered forecast scenarios (red) that were used in the intraday bidding stage of iteration 8. This surplus in generation creates an opportunity to deliver additional energy to the grid. The imbalance long price is more favorable than the short price, since it results in a payment rather than a cost. In this case, the long price is also positive, meaning that creating a surplus is more profitable than avoiding an imbalance altogether. As confirmed by Figure 4.8a, favorable long prices persist throughout the delivery window. The model responds by adjusting its operation to deliver the excess energy by RES generation and battery discharge creating a surplus position in the imbalance market (Figure 4.7b), thereby capturing additional imbalance revenues. This confirms that the real-time stage reacts appropriately to updated system conditions and economic incentives.

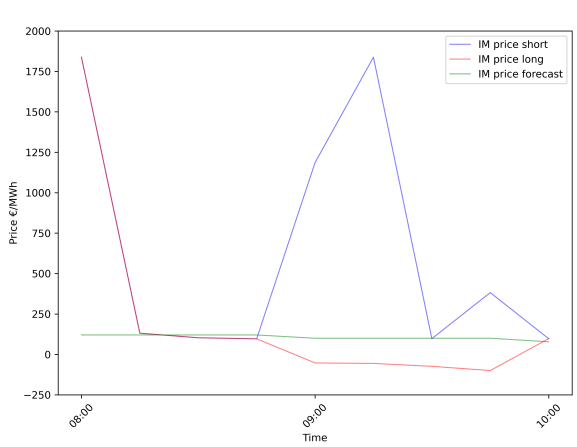

(a) Imbalance price signals during real-time operation in iteration 9.

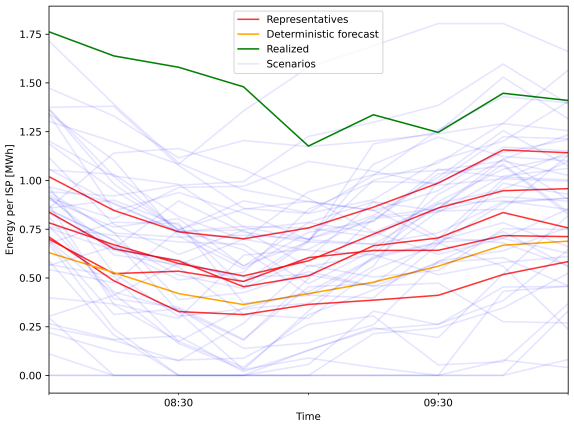

(b) Comparison of power forecasts scenarios, clusters and realized RES generation in iteration 9.

Figure 4.8: Validation of real-time operation: updated power realization and corresponding imbalance price signals.

4.2. Cumulative Results

Now that the model has been validated, the performance of the different cases over four weeks, one for each season, is assessed using the performance indicators described in Chapter 3. These metrics quantify absolute economic gain, total traded energy, physical renewable energy utilization, and normalized revenue.

4.2.1. Absolute Economic Gain

Figure 4.9a presents the cumulative revenue contributions from the DA, ID, and IM markets for each of the three configurations: HPP, RES-only, and BESS-only. The figure clearly shows that the HPP yields the highest total revenue over the four-week simulation period, totaling €164k. This represents a 29.5% increase compared to the RES-only configuration (€127k) and a 76.7% increase over the BESS-only configuration (€92.8k).

The RES case shows negative intraday revenues, which correspond to predominantly negative intraday power, indicating that the system is mostly buying energy on the intraday market. This behavior allows the RES to fulfill its day-ahead commitments or off-set expected imbalance while relying less on its own generation, as intraday purchases substitute for uncertain or scenario-dependent RES output.

Notably, the cumulative intraday position remains a net buy position throughout the horizon. Any intraday sell action is only taken to offset earlier intraday buy actions for the same time step. In this way, the RES never takes a net sell position. This conservative trading strategy stems from the inherent uncertainty in RES output across power scenarios. Since curtailment is reliably feasible across all power scenarios, whereas fulfilling a forward sell commitment with RES generation is not always guaranteed or economically viable, the model tends to favor intraday buying. This behavior is in line with an asset backed intraday trading pilot for a RES performed at Vandebron. Without the balancing capability of a BESS to back up RES availability, the model avoids forward intraday selling, resulting in lower flexibility and reduced intraday market gains.

The BESS-only case, on the other hand, earns its revenue exclusively through ID and IM markets, generating €76.6k from ID and €16.1k from IM. The BESS achieves substantial intraday (ID) revenues, primarily due to its operational flexibility and the absence of day-ahead (DA) commitment constraints. Unlike the HPP configuration, the BESS in this case is not limited by grid connection constraints. It can charge freely from the grid, making its operation independent of RES availability, and it can always discharge without competition for grid access, since there is no RES feed-in to occupy the connection. This unconstrained bidirectional access enables the BESS to respond optimally to price signals.

Despite this, the DA revenues for both RES and HPP are identical due to identical bidding strategies, while, as expected, the BESS configuration earns no DA revenue. It is important to note that the IM

revenues are optimistic, since perfect foresight on the imbalance price is assumed during real time operation.

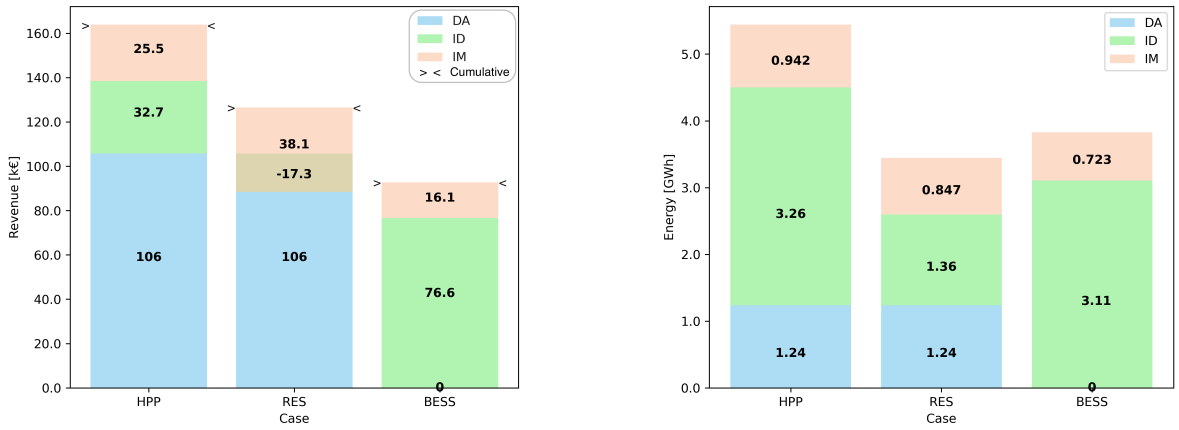

(a) Cumulative realized revenue per market for each configuration over four weeks

(b) Total absolute traded energy per market per configuration over four weeks

Figure 4.9: Cumulative results of the market revenues and absolute traded energy of the HPP, RES and BESS. In case of negative revenues, the cumulative revenue is indicated.

To validate the cumulative results of this study, the BESS results have been compared with a report by KYOS Energy Analytics. [43]. An average of €330k/MW revenue has been reported for a stand alone BESS on the intraday and imbalance market over a full year, allowing for 730 cycles. In this study the BESS revenues come from 2.5 MW power over 4 weeks with approximately 100 cycles ($\frac{\sum |P_{\text{battery}}|}{2(E_{\text{battery-max}} - E_{\text{DoD}})}$). Extrapolating these 4 weeks over a full year comes down to €480k/MW, while extrapolating over the number of cycles €270k/MW. Therefore, it can be concluded that the absolute BESS revenues are within the same order of magnitude of this benchmark.

Examining the absolute weekly revenues per case, as shown in Figure A.1, it is evident that the HPP consistently outperforms the other configurations across the different months. The RES case follows, while the BESS generates the lowest revenues.

Monthly revenues range from €23.3k in March to €59.9k in September, largely driven by market conditions given in Table A.1. In particular, higher intraday and imbalance price volatility in September, with standard deviations of €346/MWh and €301/MWh for short and long imbalance prices respectively, contributed to greater revenue opportunities compared to the more stable conditions observed in March, where standard deviations were €244/MWh and €236/MWh. Additionally, September exhibited higher average imbalance prices (short: €126/MWh, long: €66.8/MWh) compared to March (short: €106.1/MWh, long: €81.7/MWh). September also saw greater average energy production (0.507 MWh per ISP) than March (0.267 MWh per ISP), further amplifying the potential for market participation. This trend is similarly reflected in the RES and BESS cases.

For the HPP, revenues from the intraday compared to the imbalance market within one week are generally of the same order of magnitude, with the exception of the week in March. The BESS case consistently earns most of its revenue through the intraday market. In contrast, the RES configuration does not show a clear market-specific revenue pattern, reflecting its limited operational flexibility and greater exposure to forecast uncertainty due to its non-steerabel dispatch nature.

4.2.2. Trading Activity

Figure 4.9b presents the absolute traded energy per market for the three configurations over the four weeks. The HPP case exhibits the highest total traded energy at 5.44 GWh, followed by the BESS with 3.83 GWh and the RES with 3.46 GWh. This corresponds to a 57.9% increase in traded volume for the HPP compared to the RES and a 42.2% increase compared to the BESS. The HPP's engagement across the day-ahead (1.24 GWh), intraday (3.26 GWh), and imbalance (0.942 GWh) markets highlights the benefit of combining dispatchable storage with renewable generation to actively steer energy

flows and participate in multiple markets.

Notably, the intraday (ID) traded volumes of the BESS and HPP cases are similar in magnitude. However, the ID revenue for the BESS case (Figure 4.9a) is approximately 2.5 times higher than that of the HPP. This suggests that the BESS engages in more profitable intraday trades. The increased efficiency can be attributed to the absence of grid access limitations and day-ahead commitments, allowing the BESS to fully exploit intraday price fluctuations.

In the imbalance market, the BESS trades around 75% of the volume observed in the HPP case, yet only captures about 30% of the corresponding revenue. This disparity indicates less effective participation, likely due to the BESS operating without forecasted RES generation that could create larger balancing deviations and thus greater IM opportunities.

The RES case trades roughly 40% of the intraday volume compared to the HPP, reflecting a more conservative strategy driven by its limited flexibility. Without the support of storage, the RES model tends to avoid forward ID selling, relying instead on purchasing to cover potential shortfalls, resulting in a 153% decline of ID revenues. This reduced revenue highlights the challenges of participating in the ID market without the flexibility provided by a BESS, as the RES can no longer be dynamically steered. Instead, the only available control action is curtailment, which limits the ability to respond optimally to deviations in from the power forecast. However, in the imbalance market, the RES achieves 88% of the HPP's traded volume however it shows an increase of 49.4% in IM revenues. This increase in IM revenues, while reducing the traded volumes demonstrates the impact of less ID commitments, leaving more flexible dispatch capacity available during real-time operation stage.

In Appendix A the generated revenues and traded volumes per week of the HPP, RES and BESS are shown. The traded volumes in the intraday and imbalance markets for the HPP, RES, and BESS are generally of the same order of magnitude across the four weeks, with the notable exception of March, as shown in Figure A.2. In that week, all configurations exhibit noticeably lower traded volumes in both markets. This consistent drop suggests reduced market activity or fewer opportunities for adjustment. This decrease is mostly observed in the HPP and RES case and is a result of lower energy production (Table A.1).

4.2.3. Absolute Added Energetic Value

The results in Figure 4.10 show the total renewable energy utilized and curtailed for each case. Co-locating a battery with the RES, as in the HPP configuration, significantly reduces curtailment by 30.5% and thus increases the utilization of available renewable generation. Moreover, the energy lost due to storage in the BESS only accounts for 1.8% of the total energy generated RES. Additionally, the utilization of the grid connection capacity is increases from 16.3% to 18.2% when co-locating a BESS. Implying more optimal use of the grid connection capacity.

Although the HPP does not eliminate curtailment entirely, it enables improved integration of renewable energy by storing excess production that would otherwise be curtailed. As expected, the BESS case reports zero renewable output since it does not include a energy generating asset. However, about 29 MWh is lost due to storage losses, which is an 70.6% increase compared to the HPP case.

Regarding grid connection utilization, the BESS achieves the highest efficiency with a utilization factor of 0.291. This superior performance stems not only from its active trading behavior but also from its bidirectional grid access and relatively smaller connection capacity, which enhances the relative usage. In comparison, the HPP reaches a utilization of 0.182, while the RES records the lowest at 0.163. The addition of the BESS in the HPP configuration thus leads to a 10.4% increase in grid utilization over the RES alone, highlighting the benefit of co-locating storage to make more effective use of limited grid capacity.

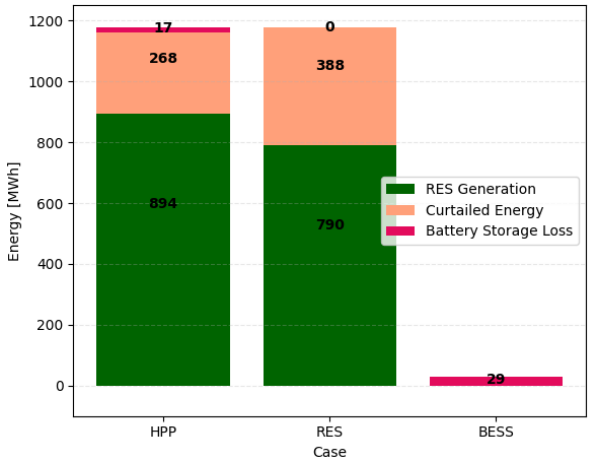

Figure 4.10: Total renewable energy utilized, curtailed and lost due to energy storage per configuration.

Table 4.2: Grid utilization factor of the three configuration cases

	HPP	RES	BESS
Utilization factor	0.182	0.163	0.291

4.2.4. Normalized Added Economic Value

Figure 4.11 presents two perspectives on cost efficiency: Figure 4.11a shows revenue per traded MWh, which is a metric for the effectiveness of a trading action. Figure 4.11b shows revenue per unit of physically delivered renewable energy, quantifying the economic value of each generated energy unit.

When normalized by traded volume, the RES case achieves the highest revenue with €36.7/MWh, followed by the HPP at €30.1/MWh and the BESS at €24.2/MWh. This means the RES outperforms the HPP by 21.9% and the BESS by 51.7%. The higher trading efficiency of the RES can be attributed to its lower number of trades, which are more selectively placed in the most profitable market windows. In contrast, the HPP performs a larger number of trades due to its flexible hybrid structure, which results in a lower efficiency but higher absolute cumulative performance.

On the other hand, when normalizing revenue by physically delivered energy, the HPP demonstrates superior performance with €183.9/MWh, compared to €160.3/MWh for the RES, an increase of 14.7%. The BESS case scores €0/MWh, as it does not produce physical energy. These results highlight the added value of co-locating storage with renewable generation, as the HPP is better able to capture revenue and reduce curtailment. The hybrid setup thus not only increases total revenue but also improves the economic return per unit of green energy.

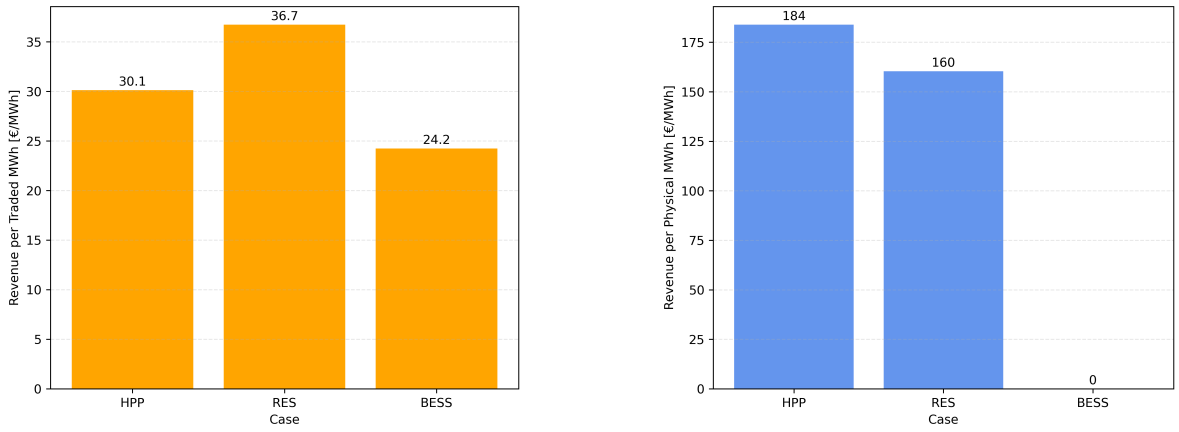

(a) Revenue per traded energy.

(b) Revenue per physical energy.

Figure 4.11: Normalized economic performance across all three configurations: HPP, RES and BESS.

4.3. Assumption Testing and Model Sensitivity

This section evaluates the robustness and realism of the proposed optimization framework by analyzing how different assumptions influence economic and energetic outcomes. Key model components, including assumptions on imbalance price forecasting, power forecasting, and system design parameters such as battery size, technology, and grid constraints, are tested through a series of sensitivity analyses. Each subsection isolates a specific factor to assess its impact on bidding decisions, traded volumes, curtailment, and overall revenue. These insights are essential for understanding the performance limits and design trade-offs of hybrid power plants operating under uncertainty in short-term electricity markets. An overview of the results of all the analysis performed can be found in Appendix B. Showing the absolute performance metrics (Table B.1, B.3 and B.5) and relative change compared to the base case (Table B.2, B.4 and B.6) .

4.3.1. Imbalance Price Forecasting

Figure 4.12 presents the impact of imbalance price forecast quality on both revenue and traded energy volumes for each configuration: HPP, RES, and BESS. Since the DA bidding phase is independent of the imbalance price forecast, the revenue and traded energy in this market is not considered in this analysis. The three tested forecasting strategies include: (1) a base case using day-ahead prices as a proxy for imbalance forecasts, (2) perfect foresight of imbalance prices, and (3) no imbalance price forecast. Subfigures 4.12a, 4.12c, and 4.12e show the revenue breakdown between ID and IM market per configuration, while subfigures 4.12b, 4.12d, and 4.12f show the corresponding traded volumes in the ID and IM market. Additional results can be found in Appendix B.

In the base case, the DA clearing price is used as a forecast for the IM price during the intraday bidding and expected imbalance stage. This approach allows some anticipation of imbalance value without relying on perfect future knowledge. In the perfect foresight scenario, the actual IM price is assumed to be known during bidding, which leads to speculative yet highly profitable market behavior. The no-forecast case removes IM price forecasting altogether: IM revenues are excluded from the objective function during ID bidding, leaving them to be considered only in the real-time operation stage.

Across all configurations, perfect foresight of the IM price consistently yields the highest total revenue. Although speculative behavior was limited through constraints, market benchmarks consider the resulting imbalance revenues to be unrealistically high [43]. For the HPP, total revenue increases from €58.2k in the base case to €130k under perfect foresight, a 123% improvement (Figure 4.12a). Interestingly, the revenue gains under perfect foresight stem primarily from increased IM revenues, while ID revenues remain relatively constant. This suggests that perfect foresight enables more effective inter-market arbitrage, allowing the model to strategically balance intraday positions against more favorable imbalance prices. The RES configuration shows the most dramatic relative increase, with combined ID and IM revenues rising from €20.8k to €68.6k, a 230% gain, again mainly due to improved perfor-

mance in the IM market (Figure 4.12c). The BESS configuration also benefits substantially, with total revenue growing from €92.8k to €195k, a 111% increase (Figure 4.12e). For the BESS, both IM and ID revenues increase under perfect foresight, though the majority of the improvement is attributed to the IM market. Logically following from the improved price forecast and no exposure to power forecast uncertainty.

By contrast, excluding any IM forecasts leads to significantly lower revenues. The RES case is particularly impacted, with total negative revenue dropping by 130% relative to the base case and turning negative due to poor imbalance market performance. The HPP sees a 33.4% decline in revenue compared to the base case, while the BESS revenue falls by only 12.3%, indicating its lower dependence on imbalance forecasting due to the absence of RES-related forecast deviations and ability to adjust positions during the real-time operation stage with perfect foresight on the imbalance price.

The trading actions on the ID are decided upon, based on this imbalance price forecast, while the final decision on imbalance position is made during real-time operation stage (with perfect imbalance foresight). Therefore, the ID traded energy is most relevant to analyze with respect to the imbalance price forecast. From the results shown in Figures 4.12b, 4.12d, and 4.12f, it is evident that traded volumes vary less significantly than revenues and do not consistently increase with improved forecast accuracy. For the HPP, intraday traded energy decreases slightly from 3.26 GWh in the base case to 3.07 GWh under perfect foresight, and increases to 3.72 GWh without any forecast. A similar trend is observed for the BESS, where traded volume drops from 3.11 GWh in the base case to 2.77 GWh under perfect foresight and rises to 3.70 GWh in the no forecast scenario. The RES case also shows a decline in intraday trading volumes for both cases: from 1.36 GWh in the base case to 1.15 GWh under perfect foresight, and down to 0.565 GWh without any forecast. These results suggest that for the HPP and BESS better price foresight enables more selective, higher-value trades rather than increasing trading volume. In contrast, the absence of a forecast may trigger excessive or inefficient trading in an attempt to hedge uncertainty. The RES is unable to respond similarly due to the lack of flexible dispatchable capacity from a BESS.

Apart from a reduction in curtailment for the HPP and RES configurations under the no imbalance price forecast scenario (−15.5% and −11.3%, respectively), the energetic performance is not significantly impacted by the quality of the imbalance price forecast (Appendix B). For the BESS configuration, grid utilization decreases by 20.2% under perfect imbalance price foresight, indicating fewer but more targeted and effective trading actions.

In summary, better imbalance price forecasting enhances economic performance across all configurations, with the greatest value realized by the HPP. The HPP and RES are especially sensitive to forecast quality due to their exposure to variability and deviation penalties, whereas the BESS demonstrates more robust performance but still benefits in its ID bidding strategy from improved foresight.

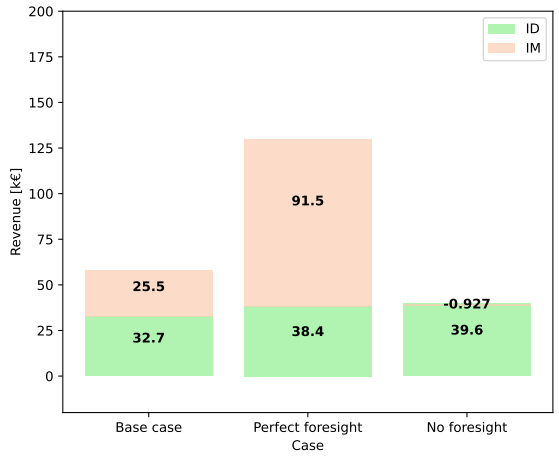

(a) HPP — Revenue breakdown

(b) HPP — Absolute traded energy

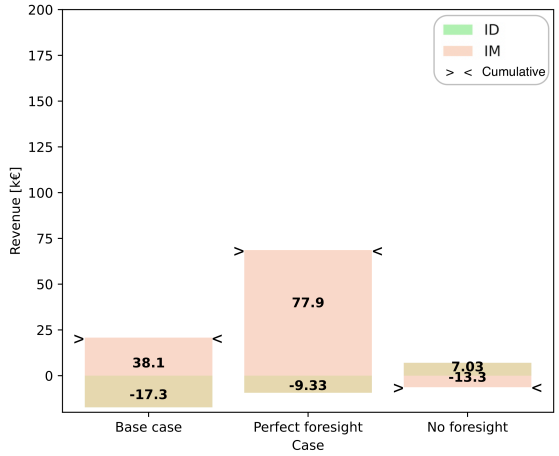

(c) RES — Revenue breakdown

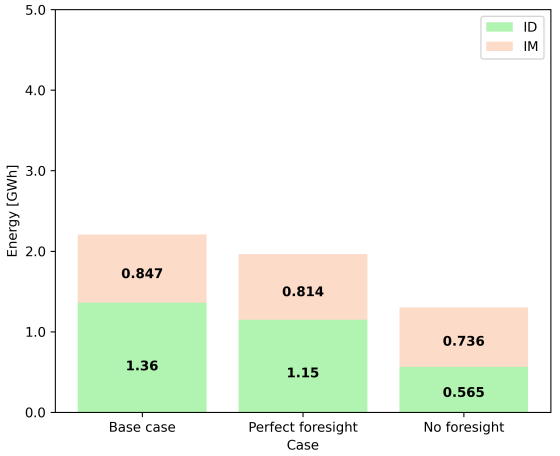

(d) RES — Absolute traded energy

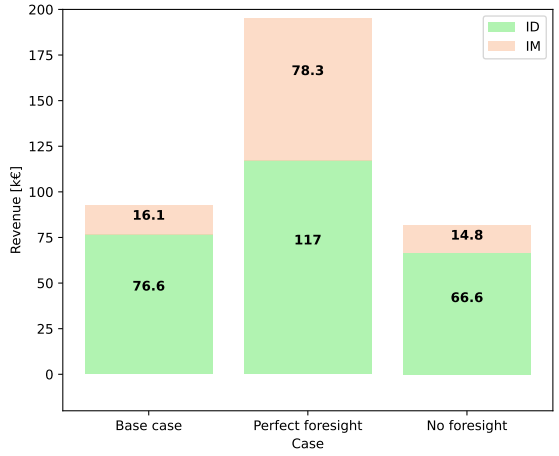

(e) BESS — Revenue breakdown

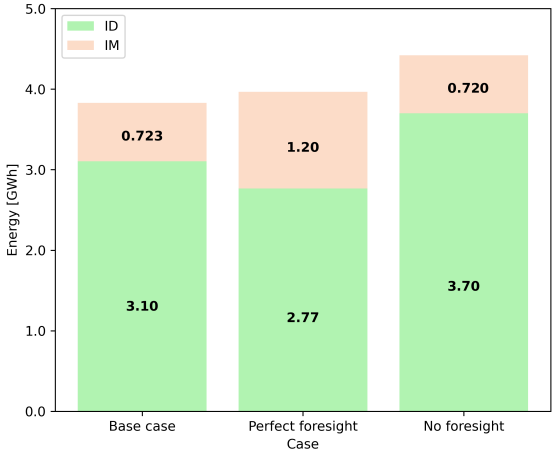

(f) BESS — Absolute traded energy

Figure 4.12: Impact of imbalance price forecasting strategy on revenue and traded energy for HPP, RES, and BESS configurations. Three forecasting assumptions are compared: day-ahead prices (base), perfect foresight, and no forecast. In case of negative revenues, the cumulative revenue is indicated.

4.3.2. Power Forecast Assumption

The impact of using multiple stochastic power forecasts is assessed by comparing the model's performance to a case with perfect power foresight. In this alternative setup, only one power forecast is used, where $\hat{P}_{\text{source}} = P_{\text{realized}}$. Only the HPP and RES case are evaluated, since the BESS operations are independent of power forecasts. The results of realized revenue and absolute traded energy of this analysis are presented in Figure 4.13a and 4.13b. The additional results are given in Appendix B.

For the HPP case, the combined ID and IM revenue is €65.7k which is an 13.0% increase, driven primarily by a rise in IM market revenue, while ID revenues decline slightly. The traded energy volumes show a similar trend. Energetic performance remains constant, with no change in RES generation or curtailed energy. As a result, both the revenue per traded volume and revenue per unit of physical energy increase. This improvement is explained by the enhanced ability to take more accurate positions in the intraday market and the BESS's flexibility to respond to real-time imbalance prices.

In contrast, the RES case shows a decline in both ID and IM revenues under perfect power foresight. The cumulative ID and IM revenue is €1.43k which is a 93.1% decline from the stochastic scenarios revenues. While this outcome may appear counterintuitive, it is driven by the rigid bidding strategy necessitated by relying on a single deterministic forecast. Since all constraints must be satisfied for this single forecast scenario, rather than across multiple stochastic ones, the intraday market bidding becomes more aggressive. However, these bids are made against an imbalance price forecast whose uncertainty is not explicitly considered during the optimization process.

As a result of this reduced forecast uncertainty, the RES configuration commits more volume in the intraday market, reflected by a 16.0% increase in traded ID energy, which is often offset by subsequent imbalance positions. When the actual imbalance prices deviate from the forecast, these positions can lead to unfavorable costs, as intraday commitments are fixed and cannot be adjusted. Moreover, without a BESS, the RES lacks the operational flexibility to respond effectively to real-time imbalance signals, further reducing its economic performance despite a perfectly accurate generation forecast.

From these findings, it can be concluded that perfect power forecast information adds economic value for the HPP, particularly in the imbalance market, where flexibility through the BESS enables better real-time imbalance price response. However, in the RES case, perfect foresight does not improve and even reduces economic value due to increased ID commitments and lack of flexibility. In both cases, the energetic performance remains relatively unaffected.

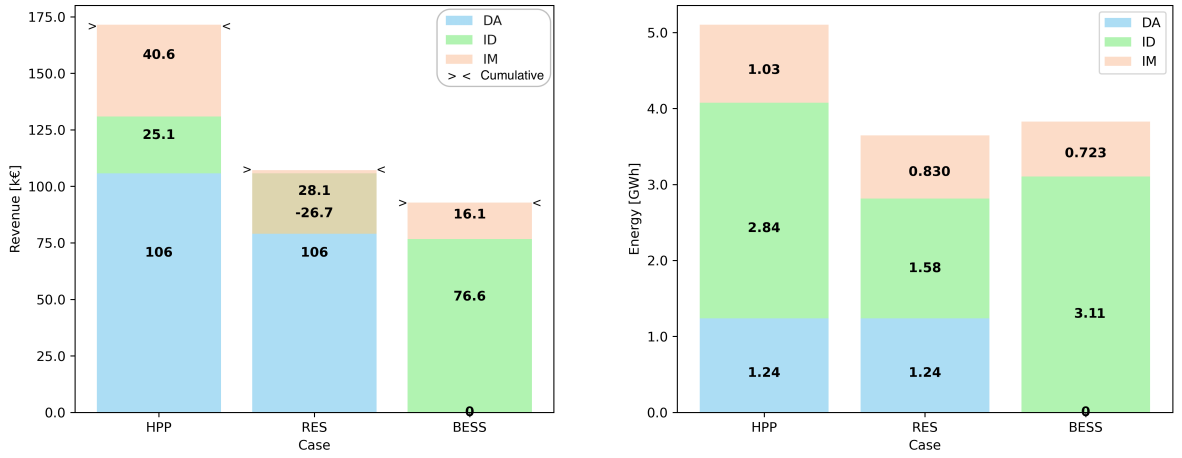

(a) Perfect power forecast — Revenue

(b) Perfect power forecast — Absolute traded energy

Figure 4.13: Sensitivity of the model performance to power forecasting assumptions. Revenue and traded energy outcomes are shown for each configuration case. In case of negative revenues, the cumulative revenue is indicated.

4.3.3. Sensitivity Analysis

To evaluate the robustness of the proposed optimization framework, a series of sensitivity analyses are conducted. These analyses isolate key model parameters and assumptions, such as BESS size,

technology type, grid connection capacity, and re-optimization frequency, to assess their impact on economic performance, traded energy volumes, and physical system behavior. By systematically varying these inputs, the analysis provides insights into the model's responsiveness and highlights critical design trade-offs for hybrid power plant operation under uncertainty.

BESS Size Sensitivity

The size of the BESS, denoted as $E_{\text{battery-max}}$, is a key design parameter in the HPP. Since the C-rate is kept constant, an increase in storage capacity also leads to a proportional increase in the maximum power output. As the RES configuration does not include a BESS, only the HPP and stand-alone BESS configurations are evaluated for this sensitivity.

Table 4.3: Design Parameters for BESS Size Sensitivity

	Variable	Base	Smaller	Larger
BESS Size	$E_{\text{battery-max}}$	5 MWh	2.5 MWh	10 MWh

Table 4.4: Results of sensitivity analysis for BESS size cases for the HPP and stand-alone BESS case

	Absolute Revenue [k€]			Traded Energy [GWh]			Physical [GWh]			Grid Utilization [-]	Normalized [€/MWh]	
Scenario	ID	IM	ID + IM	ID	IM	ID + IM	Generated	Curtailed	Battery Loss		Rev/Traded	Rev/Physical
HPP case												
Base Case	32.7	25.5	58.2	3.26	0.942	4.20	0.891	0.271	0.016	0.182	30.1	184
BESS Size 10 MWh	64.5	33.6	98.1	4.17	1.06	5.22	0.924	0.229	0.026	0.190	31.6	221
BESS Size 2.5 MWh	10.8	21.2	32.0	2.47	0.870	3.34	0.854	0.315	0.010	0.175	30.1	161
BESS case												
Base Case	76.6	16.1	92.8	3.11	0.723	3.83	–	–	0.029	0.291	24.2	–
BESS Size 10 MWh	153	32.2	185	6.21	1.45	7.66	–	–	0.055	0.292	24.2	–
BESS Size 2.5 MWh	38.4	8.08	46.5	1.55	0.362	1.92	–	–	0.014	0.292	24.3	–

Table 4.4 presents the absolute values and relative change in performance metrics for two alternative BESS sizes: 10 MWh and 2.5 MWh, as reported in Table 4.3. The relative change compared to the base case are reported in Appendix B. In the 10 MWh configuration, both traded energy volumes and revenues increase by approximately 100%, whereas they decrease by approximately 50% in the 2.5 MWh case. These results show that for the stand-alone BESS, the relationship between storage capacity and economic performance is nearly linear. This can be explained by the fact that more power becomes available due to the higher energy content and unchanged C-rate, allowing similar trading patterns with doubled or halved volume. This is further supported by the near-zero change in revenue per traded MWh, indicating stable trading efficiency.

In contrast, this linearity does not fully hold for the HPP configuration. When the BESS size is doubled to 10 MWh, ID revenues nearly double to €64.5k, while IM revenues increase by about 32% (€33.6k). This results in a total combined revenue increase of 68.7% from these two markets. A similar pattern can be observed for traded energy volumes, where ID trades increase more significantly than IM trades. Additionally, curtailment is reduced by around 15%, which improves the energetic performance of the HPP. Overall, the revenue per unit of physically generated renewable energy increases by 20%, indicating a higher economic return on green energy.

When the BESS capacity is reduced to 2.5 MWh in the HPP configuration, a stronger impact is also observed on intraday revenues and traded energy compared to the imbalance market. The combined revenues from the intraday and imbalance markets decrease by 45%. Due to the associated increase in curtailment, the revenue per unit of physically delivered energy falls by only 12.3%. Notably, trading efficiency remains unaffected, as reflected by the unchanged revenue per traded MWh.

In conclusion, the size of the BESS has the greatest influence on the ID revenues and traded volumes in the HPP configuration. In contrast, the stand-alone BESS configuration exhibits a proportional and uniform effect across all performance metrics. Increasing the BESS size enhances both the economic and energetic value of the system, while reducing the size leads to lower flexibility, higher curtailment, and a corresponding decline in value.

BESS Technology Sensitivity

To assess the impact of different storage technologies, a Vanadium Redox Flow Battery (VRFB) was tested as an alternative to the lithium-ion battery. The VRFB configuration is based on specifications from E22 Energy Storage Solutions. [44], of which the values are shown in Table 4.5. The results for both the HPP and BESS configurations are presented in Table 4.6. The relative change in results compared to the base case can be found in Appendix B.

Table 4.5: Design Parameters for BESS Technology Characteristics

Technology	Variable	Base: Li-ion Battery	Vanadium Redox Flow Battery
Round-trip Efficiency	η_{battery}	90%	75%
C-rate	C_{rate}	0.5	0.25
Depth of Discharge	E_{DoD}	0.5 MWh	0 MWh

Table 4.6: Results of sensitivity analysis for an alternative BESS technology (Vanadium Redox Flow Battery) for the HPP and stand-alone BESS case

	Absolute Revenue [k€]			Traded Energy [GWh]			Physical [GWh]			Grid Utilization [-]	Normalized [€/MWh]	
Scenario	ID	IM	ID + IM	ID	IM	ID + IM	Generated	Curtailed	Battery Loss		Rev/Traded	Rev/Physical
HPP case												
Base Case	32.7	25.5	58.2	3.26	0.942	4.20	0.891	0.271	0.016	0.182	30.1	184
VRFB	19.0	19.0	38.0	2.29	0.858	3.14	0.869	0.297	0.014	0.174	32.8	166
BESS case												
Base Case	76.6	16.1	92.8	3.11	0.723	3.83	–	–	0.029	0.291	24.2	–
VRFB	42.4	8.41	50.8	1.46	0.353	1.81	–	–	0.019	0.291	28.1	–

In the BESS case, traded volumes and revenues decline by approximately 50%. This is primarily due to the lower C-rate, which limits the maximum power output, and the reduced round-trip efficiency, which increases energy losses.

For the HPP configuration, the combined intraday and imbalance revenues fall by 34.7% and 24.2%, respectively, with the intraday market showing the largest loss in both revenue and trading activity. Additionally, curtailed energy increases, indicating a decline in energetic performance.

In summary, both the economic and energetic performance of the BESS and HPP are negatively impacted by the lower C-rate and round-trip efficiency of the Vanadium Redox Flow Battery. This underscores the importance of carefully selecting storage technologies when designing hybrid systems, as technical specifications directly influence both value creation and renewable energy utilization. However, the overall performance of the HPP still surpasses that of the standalone RES and BESS cases, indicating that other storage technologies also add value to the system.

Grid Connection Capacity Sensitivity

The grid connection capacity is a limiting parameter only for the HPP configuration case. Therefore, the sensitivity of HPP performance with respect to grid connection limits is evaluated. Since grid constraints can differ for withdrawal and feed-in directions, three cases are considered: an unconstrained grid connection, a feed-in constrained grid, and a withdrawal constrained grid, the values associated with these cases are reported in Table 4.7. The results for these cases are presented in Table 4.8. For the relative change in results compared to the base case please refer to Appendix B.

Table 4.7: Design Parameters for Grid Connection Sensitivity

	Variable	Base	Unconstrained	Feed-in Constrained	Withdrawal Constrained
Feed-in Capacity	$P_{\text{feed-in}}$	7.21 MW	9.71 MW	7.21 MW	9.71 MW
Withdrawal Capacity	P_{withdraw}	0 MW	2.5 MW	2.5 MW	0 MW

Table 4.8: Results of sensitivity analysis for three alternative grid connection capacity constraints for the HPP.

	Absolute Revenue [k€]			Traded Energy [GWh]			Physical [GWh]			Grid Utilization [-]		Normalized [€/MWh]	
Scenario	ID	IM	ID + IM	ID	IM	ID + IM	Generated	Curtailed	Battery Loss	Feed-in	Withdraw	Rev/Traded	Rev/Physical
HPP case													
Base Case	32.7	25.5	58.2	3.26	0.942	4.20	0.891	0.271	0.016	0.182	–	30.1	184
Grid Unconstrained	65.9	45.0	111	4.40	1.57	5.97	0.785	0.365	0.029	0.189	0.285	30.0	276
Grid Feed-in Constrained	67.0	32.4	99.4	4.37	1.49	5.87	0.761	0.389	0.028	0.247	0.277	28.9	270
Grid Withdrawal Constrained	31.2	34.8	66.0	3.32	0.982	4.30	0.919	0.242	0.018	0.140	–	31.0	187

In the unconstrained grid connection case, the battery is allowed to both charge from the grid and discharge without restriction from RES feed-in. This increased operational flexibility leads to substantial gains in ID and IM market revenues, increasing by 90.6% and 42.6%, respectively. However, because the BESS can now charge from the grid, less energy from the RES is used, resulting in a 34.7% increase in curtailed energy. The revenue per traded volume remains nearly constant, while the revenue normalized by the physically produced energy increases by 50.1%, due to higher revenues and reduced RES generation.

In the case with only a feed-in constraint, revenues and traded volumes also rise significantly, by 70.9% and 39.5%, respectively. Compared to the unconstrained case, intraday revenues are similar, while imbalance revenues and traded volumes are lower. Energetic performance is worse than in both the base and unconstrained cases, as indicated by a 43.5% increase in curtailed energy. While the revenue normalized by traded volume shows a slight decrease (4.0%), the revenue per unit of physical RES-generated energy increases by 46.6%.

When the HPP is constrained only in its withdrawal capacity, meaning the BESS can charge only from the RES, a more modest improvement is observed: total revenue grows by 13.5% while traded volumes remain rather stable (+2.4%). While intraday revenues decrease slightly, they are offset by a rise in imbalance market revenues. Notably, this configuration results in improved energetic performance, with curtailed energy reduced by 10.7%. Moreover, both revenue per traded volume and revenue per physical energy show a insignificant changes (<3%).

In the unconstrained case, feed-in utilization remains constant. Meanwhile, withdrawal capacity utilization increases to 0.285, representing 151% of the original feed-in utilization. In the feed-in constrained case, feed-in capacity utilization increases by 35.5%, while withdrawal utilization, previously zero, rises to 0.277, equal to 148% of the original feed-in reference. By contrast, increasing only the feed-in capacity results in a 23.5% decrease in utilization, indicating less efficient use of available infrastructure.

In summary, economic value increases with greater grid connection capacity, regardless of the direction. However, allowing withdrawal capacity contributes more than five times the additional revenue compared to unconstraining only the feed-in capacity. Overall, the unconstrained configuration yields the highest revenue. From an energy perspective, restricting only the withdrawal capacity leads to improved RES energy utilization and reduced curtailment. In contrast, expanding feed-in capacity or fully removing grid constraints increases curtailment and battery losses, which diminishes the energetic contribution of the HPP. Moreover, the most efficient utilization of the grid connection occurs in the case where only the feed-in capacity is constrained.

Re-optimization Frequency

The implemented multi-stage optimization framework uses a rolling horizon approach, where both the intraday bidding and expected imbalance stage and the real-time operation stage are iteratively solved. The time window shifts forward by t_{update} timesteps after each iteration. This timestep interval not only defines the frequency of re-optimization but also sets the length of each real-time operation phase. To evaluate the impact of this parameter, two additional configurations were tested: a shorter interval of 30 minutes ($t_{\text{update}} = 2$) and a longer interval of 2 hours ($t_{\text{update}} = 8$), as showed in Table 4.9. Results are presented in Table 4.10. The relative change compared to the base case can be found in Appendix B.

Table 4.9: Design Parameters for Reoptimization Frequency Sensitivity

	Variable	Base: 1 hour	30 minutes	2 hours
Update Interval	t_{update}	4	2	8

Table 4.10: Results of sensitivity analysis for two alternative re-optimization frequencies for the HPP, the stand-alone RES and stand-alone BESS.

	Absolute Revenue [k€]			Traded Energy [GWh]			Physical [GWh]			Grid Utilization [-]	Normalized [€/MWh]		
Scenario	ID	IM	ID + IM	ID	IM	ID + IM	Generated	Curtailed	Battery Loss		Rev/Traded	Rev/Physical	
HPP case													
Base Case	32.7	25.5	58.2	3.26	0.942	4.20	0.891	0.271	0.016	0.182	30.1	184	
Re-optimization Every 30 min	38.8	22.8	61.6	5.29	0.961	6.25	0.877	0.290	0.022	0.187	22.4	191	
Re-optimization Every 2 Hours	19.9	24.4	44.2	2.07	0.902	2.97	0.918	0.248	0.013	0.181	35.7	163	
RES case													
Base Case	-17.3	38.1	20.8	1.36	0.847	2.21	0.789	0.390	–	0.163		36.7	160
Re-optimization Every 30 min	-8.74	14.2	5.42	2.21	0.847	3.05	0.781	0.398	–	0.166	25.9	142	
Re-optimization Every 2 Hours	-10.3	-3.50	-13.8	0.884	0.785	1.67	0.803	0.376	–	0.161	31.6	114	
BESS case													
Base Case	76.6	16.1	92.8	3.11	0.723	3.83	–	–	0.029	0.291	24.2	–	
Re-optimization Every 30 min	87.6	6.47	94.1	4.53	0.702	5.24	–	–	0.043	0.301	18.0	–	
Re-optimization Every 2 Hours	63.5	23.3	86.8	2.15	0.768	2.92	–	–	0.019	0.294	29.7	–	

For the case with a 30-minute re-optimization interval, the HPP configurations show an increase in combined ID and IM revenue of 5.96%. This improvement is primarily driven by increased activity in the ID market, where more frequent updates allow for quicker response to changing forecasts and market prices. This increase in ID revenue partially cannibalizes IM revenues, however the net effect remains positive. Moreover, the higher ID activity reduces the revenue per traded volume, indicating a decline in trading efficiency. The curtailed energy rises slightly by 7.0%, and the gain in revenue more than compensates, resulting in an improved revenue per unit of RES-generated energy. When the re-optimization interval is extended to 2 hours, the opposite trend is observed for the HPP. Combined ID and IM revenues decline by a factor roughly four times greater than the increase achieved with the 30-minute case (-24.0%). Although the drop in traded volume is less pronounced, the total economic performance declines. Interestingly, curtailed energy decreases in this scenario, improving the energetic performance of the HPP.

For the BESS case, increasing the optimization frequency does not significantly affect the total combined revenues. However, the composition of revenue sources shifts notably. ID revenue increases by 14.3%, accompanied by a 46.0% rise in traded volume, while IM revenue and traded volume decline by 59.9% and 2.9%, respectively. This shift indicates a transition toward more secure and predictable revenue streams, as the BESS becomes less reliant on the uncertainty associated with imbalance prices. An opposite effect is observed when the re-optimization interval is extended to two hours. In this setting, ID market participation decreases in both activity and revenue, while IM revenues rise. Unlike the higher-frequency optimization, the 2-hour interval results in a reduction in total revenue from ID and IM markets, showing a 6.5% overall decline. This suggests that lower update frequencies limit the system's ability to respond effectively to evolving ID market conditions, reducing overall economic efficiency.

The RES case responds differently to changes in re-optimization frequency. The highest combined revenue is achieved in the baseline case with an hourly re-optimization. In both the 30-minute and 2-hour configurations, intraday revenues increase only marginally, but imbalance revenues fall significantly. This imbalance underperformance outweighs any intraday market gains, leading to net revenue decreases of 73.9% and 166.5%, respectively. However, traded volumes show similar trends to the HPP and BESS cases, with ID activity increasing slightly while IM volumes remain stable. Also the physical RES generated energy remains stable over the three cases.

In summary, increasing the re-optimization frequency improves economic performance for configurations with storage (HPP and BESS), mainly by enabling more responsive and effective ID trading. This shift toward the ID market supports more stable and predictable revenue streams, while slightly reducing trading efficiency and increasing curtailment. In contrast, longer update intervals limit responsiveness and reduce overall revenue, particularly for the HPP. The RES-only case performs best at the

default 1-hour interval, with both shorter and longer intervals leading to lower revenues due to its lack of operational flexibility. Overall, the impact on energetic performance is modest across all configurations.

4.4. Discussion

The results presented in this study provide valuable insight into the operational potential of HPPs under uncertainty in market prices and renewable generation forecasts. However, several simplifications and assumptions have been made in the modeling framework that influence the interpretation of the outcomes. This section critically evaluates the key modeling choices, such as the exclusion of battery degradation, simplifications in scenario generation, the treatment of imbalance prices, and the definition of economic value as revenue. The implications of these assumptions on the results are discussed, along with recommendations for improving model accuracy and extending the analysis in future research.

4.4.1. Battery Degradation

Value has been added by the integration of a storage in the HPP and BESS case. However, in this model the degradation of the battery is not considered, nor are associated costs incorporated in the economic optimization. This assumption introduces an important simplification that impacts both the energetic and economic interpretation of the results.

Battery degradation occurs as a result of charge and discharge cycles, depth of discharge, temperature fluctuations, and calendar aging. Physically, the capacity of a battery deteriorates over time, reducing its ability to store and dispatch energy effectively. Operationally, this means that a battery's performance, and therefore its contribution to reducing RES curtailment, diminishes over its lifetime.

Economically, degradation imposes a cost that should be factored into any dispatch decision. Each charging or discharging action effectively consumes a portion of the battery's useful life, representing a hidden operational cost. Ignoring degradation in the optimization model allows for more frequent and aggressive battery cycling, which overestimates both the frequency and economic viability of trading actions. As a result, the model likely produces an optimistic estimate of the added value of co-locating a BESS.

In terms of energetic value, the absence of degradation constraints enables the BESS to capture more curtailed RES generation than would be feasible under realistic operating conditions. If battery wear were considered, the system would need to prioritize higher-value charging and discharging events, reducing the total energy throughput from RES to the grid.

From an economic perspective, including degradation costs would require that each battery cycle yields a net profit that exceeds the associated wear cost. This would reduce the number of economically justified dispatch actions. Consequently, the added economic value observed in the HPP and BESS cases may be overstated under the current modeling assumptions.

Future research should incorporate a battery degradation model. This could be achieved by including a degradation cost function, based on empirical cycle aging models or manufacturer data, within the optimization. Another approach would be to limit the cycles per day, reducing the number of cycles. Doing so would enable a more realistic assessment of long-term profitability and operational sustainability. Furthermore, assessing the trade-off between short-term arbitrage gains and long-term degradation costs would provide valuable insight for investment and operational strategy in hybrid power plant development.

4.4.2. Power Forecast Scenarios

To capture the uncertainty inherent in renewable power generation forecasts, this study adopts a scenario-based approach using an ARMA(2,2) model to generate forecast errors. These synthetic errors are sampled and superimposed onto deterministic power forecasts to produce multiple forecast trajectories, which feed into the stochastic optimization model. The ARMA model is trained on historical forecast errors with a lead time of 15 to 39 hours, representative of the typical range between the day-ahead forecast and delivery.

While this approach captures some statistical features of historical forecast errors, it introduces several

important limitations that affect the realism of the resulting scenarios and, by extension, the optimization outcomes. First, ARMA models are linear and assume stationarity, meaning they cannot fully capture the nonlinear, regime-dependent behavior of wind or solar power forecast errors. In reality, error characteristics are not constant but vary with the forecasted power level, atmospheric conditions, and time of day. For instance, low wind power regimes typically show higher relative forecast uncertainty, which ARMA tends to underestimate. This may lead to an overly narrow distribution of scenarios in these regimes, underrepresenting curtailment risk and operational variability.

Secondly, the use of a fixed lead time range (15–39 hours) across all optimization stages simplifies the temporal structure of forecast uncertainty. Forecasts made closer to real-time (e.g., during intraday bidding) generally exhibit lower errors and reduced volatility. By training the ARMA model on a broad lead time window and applying it uniformly, the model may overstate uncertainty closer to delivery while understating it for delivery times further away, thereby distorting the expected value of trading flexibility.

A further simplification lies in the method of scenario construction itself. Errors are imposed on the power output rather than on the input variables to the power forecasting process (e.g., wind speed). While convenient, this approach does not preserve physical consistency. In reality, the transformation from wind speed to power output is nonlinear, especially between the rated and cut-out wind speed. For example, imposing a ±1 m/s wind speed error between cut-in and rated wind speed causes a much larger deviation in output power than the same error near the between rated wind and cut out speed. This effect is not captured when errors are applied directly to the power forecast. As a result, the scenario set may misrepresent forecast uncertainty depending on the operating regime of the renewable asset.

Additionally, Figure 4.14 shows that the historical error distribution has a non-zero mean, indicating a systematic bias in the deterministic forecast model. This suggests that, on average, the forecast tends to overpredict wind power. Since this bias is not explicitly corrected in the scenario generation process, it may skew optimization outcomes toward overly optimistic expectations of available renewable energy, thereby overstating both energetic and economic value, particularly for BESS dispatch and curtailment reduction in HPP configuration.

To reduce the number of scenarios while preserving their statistical characteristics, Euclidean distance-based clustering is applied to the set of forecast errors generated by the ARMA model. These simulated errors follow a normal distribution, which is a typical property of ARMA processes. However, as shown in Figure 4.14, the clustered error distribution approximates the historical error profile more closely than the underlying normal distribution. While the normal distribution captures the central tendencies well, it fails to account for the heavier tails observed in reality, where rare but high-impact forecast deviations occur. Consequently, the clustering approach improves realism, but some skewness remains, and extreme under- or overproduction events may still be underrepresented in the optimization.

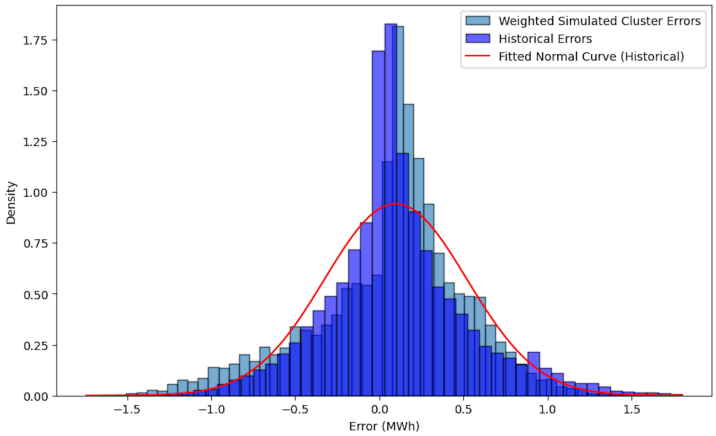

Figure 4.14: Error distribution of historical and clustered sampled errors, with a fitted normal distribution

The implications of these assumptions are twofold. On the energetic side, the underrepresentation of low-probability but high-impact deviations can result in an overestimation of the curtailment reduction

potential of the BESS, as the model does not fully explore worst-case misalignment between production and dispatch. On the economic side, if uncertainty is understated, particularly early intraday stages, then the optimization may over-commit energy sales, leading to optimistic revenue projections. Conversely, if uncertainty is overstated during short lead times, the model may become too conservative in leveraging intraday opportunities, thereby missing profitable actions.

Despite these limitations, the clustered ARMA-based scenario generation provides a tractable and transparent method for representing uncertainty. However, it falls short of capturing the full conditional and temporal dynamics of forecast errors. Future work should explore non-linear, heteroskedastic models, such as GARCH or machine learning-based probabilistic forecasting techniques (e.g., quantile regression forests), which allow forecast uncertainty to vary with forecast value and lead time. Furthermore, adopting lead time-specific error models could significantly improve the realism of scenario generation across the multi-stage optimization framework.

Finally, a promising direction for future research is the representation of scenarios as a scenario tree rather than independent scenarios. A scenario tree allows for conditional branching at decision stages and can represent a greater number of possible future outcomes with fewer nodes, for example combining probabilistic power and price scenarios. This improves computational efficiency and realism in sequential decision-making contexts. An example of this concept is described by Heredia, Cuadrado, and Corchero [10]. However, such a structure has not been implemented in the current study.

4.4.3. Imbalance Price Forecast

In this study, the day-ahead market clearing price is used as a forecast for imbalance prices in the stochastic optimization framework. This simplification enables the model to estimate potential imbalance revenues without relying on complex real-time price forecasting. However, it introduces significant limitations that impact both the realism of price dynamics and the validity of the optimization results.

Figure 4.15 shows the time series of the day-ahead price alongside the imbalance prices in both surplus (long) and shortage (short) directions over one simulation week. While the day-ahead price follows the general trend of the imbalance prices, due to shared underlying system conditions, it fails to capture the short-term volatility and extreme price excursions that occur under system stress, particularly during regulation state 2 events.

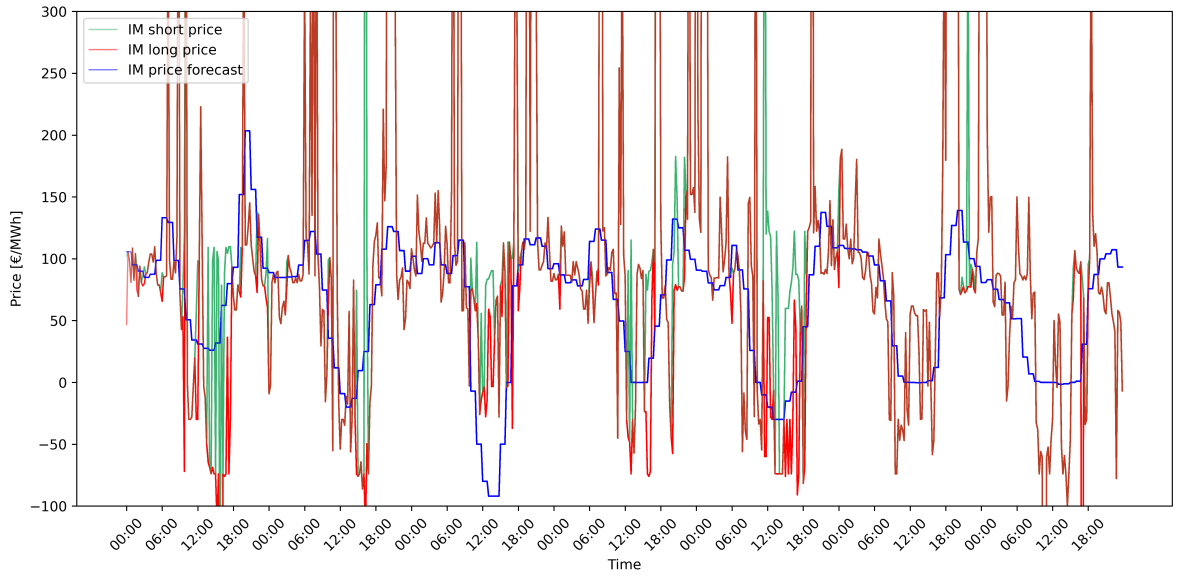

Figure 4.15: Day-ahead, imbalance long and imbalance short prices [€/MWh] over one simulation week. While trends align, large deviations and spikes in imbalance prices are not captured by the day-ahead proxy.

This observation is supported quantitatively in Figure 4.16, which presents the distribution of forecast errors when using the day-ahead price as a forecast for imbalance settlement, over the four weeks experimented in this sturdy. The distribution is sharply peaked around zero but exhibits heavy tails,

indicating the presence of large errors during a limited number of high-impact events. The mean forecast error over the simulation period is –65.76 €/MWh, reflecting a consistent underestimation bias. Furthermore, the root mean square error (RMSE) for the combined long and short imbalance prices is 372.59 €/MWh, highlighting that the forecast errors are not only biased, but also large in magnitude.

This high RMSE points to the inherent unpredictability of imbalance prices and the inadequacy of day-ahead prices as reliable proxies. The inability to anticipate sharp imbalance price peaks leads to an underrepresentation of arbitrage opportunities in the optimization model. As a result, the economic value of dispatch flexibility, particularly from BESS assets, is underestimated, especially during periods of market imbalance when the potential gains are most significant.

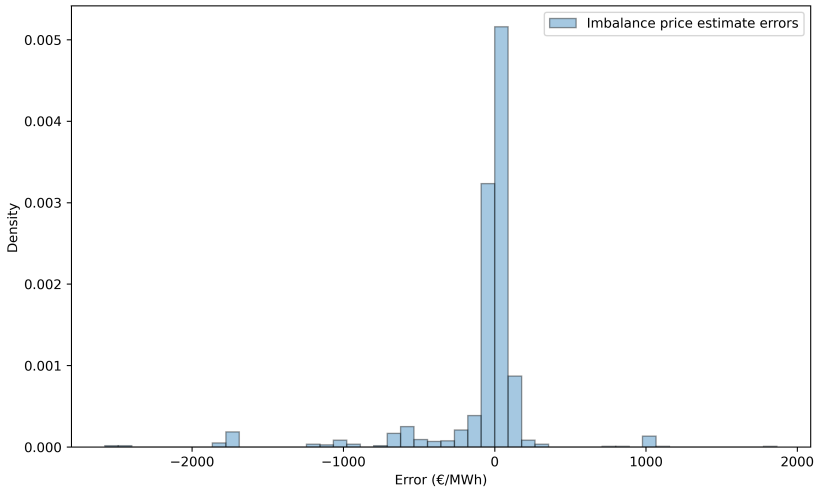

Figure 4.16: Histogram of the error between imbalance price forecasts (based on day-ahead price) and realized imbalance prices over the simulation period. Note the heavy-tailed distribution and underestimation bias. RMSE (combined): 372.59 EUR/MWh.

As demonstrated in Section 4.3, enhanced imbalance price forecasting yields a substantial improvement in economic performance, validating the importance of this modeling component. Capturing the value of extreme price signals is critical for optimal participation in the imbalance market.

Future research should therefore focus on developing more accurate and dynamic imbalance price forecasting methods. One direction is to incorporate additional explanatory variables such as real-time system load, renewable infeed levels, BRP positions, or the aFRR bid ladder. These variables could provide better context for short-term price volatility and regulation needs. Another avenue is the use of machine learning techniques, including recurrent neural networks, gradient boosting trees, or hybrid models, that can learn complex temporal and nonlinear relationships in the data. In addition, probabilistic forecasting approaches that explicitly account for regulation state uncertainty and its impact on pricing would offer more robust insights into price risk. Integrating such methods would enable the optimization framework to more effectively anticipate market behavior, improving both the economic valuation of flexibility and the robustness of scheduling decisions.

Improving imbalance price predictions would allow the optimization to better anticipate high-reward events, resulting in more effective use of BESS flexibility and more realistic profitability assessments.

4.4.4. Revenue Optimization

In this study, the objective function of the optimization model is formulated to maximize total operational revenue from participation in electricity markets, including the day-ahead, intraday, and imbalance markets. While this provides insight into the trading potential of different system configurations, the revenue definition used in the model introduces several simplifying assumptions that limit its applicability for assessing true economic viability.

First and foremost, no cost components are included in the revenue calculation. The results are therefore based solely on gross revenues from market participation, without accounting for capital expenditures (CAPEX), operational and maintenance costs (OPEX), or battery degradation costs. Additionally, the model does not incorporate discounting of future cash flows, implicitly assuming that revenues generated at any point in the time horizon are equally valuable. These assumptions are suitable for assessing the relative flexibility and market participation behavior of different configurations, but they can lead to misleading conclusions when interpreted in an investment or business case context.

The absence of costs is particularly relevant when comparing the standalone RES system to hybrid configurations with co-located BESS. As the results show, the HPP configuration consistently generates higher operational revenue due to its ability to reduce curtailment and perform market arbitrage. However, without incorporating the significantly higher capital and operational costs associated with BESS systems, this conclusion cannot be interpreted as evidence of superior economic performance. In scenarios with high battery costs or limited support schemes, the net profitability of the HPP could fall below that of a simpler RES-only setup.

Beyond direct capital and operating costs, several other financial factors influence the real-world economic viability of hybrid energy systems. For example, grid connection and reinforcement costs can be substantial for large-scale systems, particularly when high-power charging and discharging is involved. Similarly, the eligibility for and value of subsidies (e.g., feed-in tariffs, investment grants, or capacity payments) can materially alter the revenue landscape, particularly for emerging technologies such as BESS. These external revenues or charges are not considered in the current model but may significantly affect technology choice and system sizing.

In summary, while the revenue-maximizing approach used in this study offers useful insights into the operational potential of HPPs under uncertainty, it does not constitute a full techno-economic assessment. Future research should extend the current model by incorporating cost structures, investment decision-making frameworks, and possibly multi-objective formulations that jointly consider profit, risk, and system performance. Only then can a comprehensive conclusion be drawn regarding the net value and long-term feasibility of hybrid energy systems.

5

Conclusion

This study set out to quantify the added economic and energetic value of co-locating a Battery Energy Storage System (BESS) with a renewable energy source (RES), forming a Hybrid Power Plant (HPP), in the context of the Dutch electricity markets. Motivated by increasing shares of intermittent renewable generation, evolving electricity market structures, and growing grid congestion, the research aimed to evaluate how hybrid systems can improve system flexibility and support a more efficient and sustainable energy transition. The research intends to answer the following research question:

What is the added energetic and economic value of BESS co-location for a Hybrid Power Plant participating in the Dutch day-ahead, intraday, and imbalance markets, when using a bidding strategy that accounts for power forecasting uncertainty?

To answer this question, a multi-stage stochastic mixed-integer linear programming (MILP) model with a rolling horizon was developed, that quantifies the economic and energetic value. The model simulates the sequential market participation of an HPP in the day-ahead (DA), intraday (ID), and imbalance (IM) markets. It incorporates renewable power forecast uncertainty through scenario modeling and applies realistic market rules and technical constraints, including grid connection limits. A model validation has been performed, demonstrating the validity of the model in its response to price signals and adherence of physical limits. Three system configurations were compared: a stand-alone RES, a stand-alone BESS, and a co-located HPP. Additionally the response of the model to several assumptions and design variables have been tested, such as imbalance price forecasts, power forecast accuracy, BESS size, BESS technology, grid constraints and optimization frequency of the rolling horizon.

The results demonstrate that the HPP configuration consistently outperforms the standalone RES and BESS cases in terms of total revenue and traded volume. The HPP generated 29.5% more revenue than the RES system and 76.7% more than the standalone BESS, demonstrating the added economic value of the HPP. While the standalone BESS excelled in intraday market trading due to its flexibility, it lacked the base revenue contribution from RES generation and associated DA market participation. Conversely, the standalone RES shows to be more dependent on the uncertainty of the power forecast, creating a more conservative ID bidding strategies required to avoid imbalance penalties, leading to underutilization of market opportunities. The hybrid configuration enabled coordinated bidding that capitalized on the generation potential of the RES and the flexibility of the BESS.

The results further show that the HPP's economic performance is highly sensitive to assumptions about imbalance price forecasting. Perfect foresight of imbalance prices during the intraday bidding stage yielded the highest revenue, but using day-ahead prices as a forecast still enabled substantial gains. Grid connection design also plays a crucial role: enabling grid withdrawal significantly improved profitability by increasing trading opportunities, while larger BESS sizes and higher re-optimization frequencies contributed positively to market responsiveness and revenue.

Beyond economic performance, the HPP also demonstrated energetic benefits. The inclusion of a BESS reduced curtailment of RES generation by 30.5%, and storage-related losses were limited to

only 1.8% of total renewable output. This led to a more efficient use of green energy, demonstrating the added economic value. The hybrid configuration also improved grid utilization: feed-in capacity was used more consistently, and overall utilization rates increased by 12%. This is particularly relevant in the Dutch context, where net congestion is a growing concern, and acquiring grid connection is becoming a bottleneck for the green transition. The ability to withdraw energy from the grid increased flexibility of energy dispatch and utilization of the grid connection capacity for energy feed-in as well as withdrawal.

Notably, this study reveals that economic and energetic objectives can be in tension. Allowing grid withdrawal significantly enhances economic value by unlocking new trading opportunities, but it also results in increased curtailment, thereby reducing the energetic performance of the system. A similar pattern is observed with changes in the re-optimization frequency: shorter intervals improve revenue through faster intraday market responses, yet lead to higher levels of curtailment. Conversely, longer intervals reduce economic value but improve energy utilization. These opposing effects highlight a fundamental tension between maximizing profitability and optimizing the use of renewable energy. As such, energy producers, traders, and system operators must carefully balance these objectives in operational strategies and policy design.

The findings of this study are highly relevant in light of current societal, political, economic, and technological developments shaping the energy transition. Societally, the transition toward a carbon-neutral energy system hinges on the effective integration of RES. HPPs, by reducing curtailment and enhancing market responsiveness, enable a more efficient use of green electricity and thereby contribute to decarbonization goals. Their ability to dispatch renewable energy more flexibly strengthens both the sustainability and reliability of the electricity system.

From a political and regulatory perspective, this research underscores the importance of revisiting grid connection policies and market access rules. In particular, the study demonstrates that permitting grid withdrawal for HPP, even without expanding total grid capacity, unlocks considerable economic value. Policy makers aiming to stimulate BESS investment and optimize renewable integration could consider targeted reforms. For example, enabling grid connection upgrades that allow bi-directional flow, without increasing contracted capacity, may accelerate HPP deployment without exacerbating congestion. Conversely, if the policy goal is to maximize green energy utilization rather than market value, restricting grid charging while promoting co-located BESS capacity offers a better pathway. The findings therefore provide concrete input for designing differentiated policy instruments that align with specific regulatory objectives.

Economically, the model results reveal that the co-location of BESS and RES can substantially enhance revenue potential and market responsiveness, suggesting improved monetization of renewable energy under current market structures. The added flexibility of the HPP increases revenue streams, particularly in the ID and IM markets. This makes HPPs attractive to private investors and commercial aggregators, provided that market structures reward flexibility and uncertainty management. Traders and market participants should note that much of the HPP's added value is derived from short-term market responsiveness, particularly the ability to anticipate and react to ID and IM price signals. Investments in price forecasting and bidding automation are likely to be financially beneficial in this context.

For grid operators, the study provides insight into how grid connection points can be used more efficiently. A key recommendation is to prioritize the regulatory adaptation of existing RES grid connection points to accommodate co-located storage. This may involve allowing bi-directional flows or granting partial additional access for storage components. Doing so could defer the need for costly grid reinforcements while enabling local flexibility and supporting system stability. Moreover, HPPs equipped with appropriately sized BESS can play a key role in congestion management and balancing services, provided that market mechanisms and grid codes evolve to allow for such participation.

Technologically, this research highlights the growing need for advanced tools that support real-time optimization under uncertainty. The demonstrated model framework integrates multi-market decision-making, stochastic power forecasting, and rolling re-optimization tools that are increasingly essential in an electricity system dominated by variable renewables. To fully leverage this technological potential, future developments should focus on improving forecast accuracy, reducing model runtimes, and enabling integration with live market data streams.

In conclusion, the value of HPPs lies not only in their market performance but also in their potential to support the structural transformation of the electricity system. To realize this potential, stakeholders across the energy sector, including policy makers, investors, grid operators, and technology providers, must act in coordination to create an enabling environment for flexible and integrated energy solutions.

While this study demonstrates the added value of hybrid power plants under uncertainty, several opportunities remain for further research. Incorporating battery degradation would allow for a more realistic assessment of long-term operational strategies and economic viability. More advanced methods for power and imbalance price forecasting, potentially using machine learning or probabilistic approaches, could enhance the model's responsiveness to short-term market dynamics. Additionally, extending the revenue-based analysis to include investment costs, subsidies, grid fees, and battery wear would enable a more comprehensive techno-economic evaluation. Lastly, future studies could explore the system-level impact of HPPs on grid stability and congestion, informing regulatory frameworks that support their deployment.

References

[1] International Energy Agency. *Renewables 2021 – Analysis and Forecast to 2026*. Technical Report. Paris, France: International Energy Agency, 2021.

[2] K. Das et al. “Recommendations for balancing requirements for future North Sea countries towards 2050”. In: *Proceedings of the 19th Wind Integration Workshop 2020*. Energynautics GmbH. Online, Nov. 11–12, 2020.

[3] H. Schermeyer et al. “Understanding Distribution Grid Congestion Caused by Electricity Generation from Renewables”. In: *Smart Energy Research. At the Crossroads of Engineering, Economics, and Computer Science*. Springer International Publishing, 2017, pp. 78–89. ISBN: 978-3-319-66553-5. DOI: 10.1007/978-3-319-66553-5_6.

[4] A. Jarrett. *The Duck Curve*. MGA Thermal. Mar. 3, 2023. URL: https://www.mgathermal.com/blog/the-duck-curve (visited on 12/17/2024).

[5] M. K. Mehta et al. “Technical and economic value of utility-scale wind-storage hybrid power plants”. In: *Proceedings of Hybrid Power Systems Workshop*. 2021.

[6] Q. Li et al. “On the determination of battery energy storage capacity and short-term power dispatch of a wind farm”. In: *IEEE Transactions on Sustainable Energy* 2.2 (2011), pp. 148–158. DOI: 10.1109/TSTE.2010.2073056.

[7] EPEX SPOT. *Trading Products*. Accessed: 2025-01-09. EPEX SPOT. URL: https://www.epexspot.com/en/tradingproducts.

[8] Next Kraftwerke. *From Hours to Quarter-Hours: The Day-Ahead Market Gets a Facelift*. Accessed: 2025-06-05. Next Kraftwerke. 2023. URL: https://www.next-kraftwerke.com/energy-blog/day-ahead-switch-15-min.

[9] I. Gomes et al. “Stochastic coordination of joint wind and photovoltaic systems with energy storage in day-ahead market”. In: *Energy* 124 (Apr. 2017), pp. 310–320. ISSN: 03605442. DOI: 10.1016/j.energy.2017.02.080. URL: https://linkinghub.elsevier.com/retrieve/pii/S0360544217302542 (visited on 01/04/2025).

[10] F. J. Heredia, M. D. Cuadrado, and C. Corchero. “On optimal participation in the electricity markets of wind power plants with battery energy storage systems”. In: *Computers & Operations Research* 96 (Aug. 1, 2018), pp. 316–329. ISSN: 0305-0548. DOI: 10.1016/j.cor.2018.03.004. URL: https://www.sciencedirect.com/science/article/pii/S030505481830073X (visited on 12/10/2024).

[11] R. Zhu et al. “Optimal Participation of Co-Located Wind–Battery Plants in Sequential Electricity Markets”. In: *Energies* 16.15 (2023), p. 5597. DOI: 10.3390/en16155597.

[12] M. Ledro et al. “Day-ahead trading of wind-battery hybrid power plants: wind forecast uncertainty and limited feed-in grid connection”. In: *IET Conference Proceedings* 2024.2 (June 13, 2024), pp. 210–219. ISSN: 2732-4494. DOI: 10.1049/icp.2024.1840. URL: http://digital-library.theiet.org/doi/10.1049/icp.2024.1840 (visited on 01/06/2025).

[13] K. Das et al. “Optimal battery operation for revenue maximization of wind-storage hybrid power plant”. In: *Electric Power Systems Research* 189 (Dec. 2020), p. 106631. ISSN: 03787796. DOI: 10.1016/j.epsr.2020.106631. URL: https://linkinghub.elsevier.com/retrieve/pii/S037877962030434X (visited on 12/09/2024).

[14] J. Martinez-Rico et al. “Forecast Error Sensitivity Analysis for Bidding in Electricity Markets with a Hybrid Renewable Plant Using a Battery Energy Storage System”. In: *Sustainability* 12.9 (Apr. 28, 2020), p. 3577. ISSN: 2071-1050. DOI: 10.3390/su12093577. URL: https://www.mdpi.com/2071-1050/12/9/3577 (visited on 01/03/2025).

[15] X. Ayón, M. Moreno, and J. Usaola. “Aggregators’ Optimal Bidding Strategy in Sequential Day-Ahead and Intraday Electricity Spot Markets”. In: *Energies* 10.4 (Apr. 1, 2017), p. 450. ISSN: 1996-1073. DOI: 10.3390/en10040450. URL: https://www.mdpi.com/1996-1073/10/4/450 (visited on 01/03/2025).

[16] J. L. Crespo-Vazquez et al. “A machine learning based stochastic optimization framework for a wind and storage power plant participating in energy pool market”. In: *Applied Energy* (Dec. 2018), pp. 341–357. DOI: 10.1016/j.apenergy.2018.09.195. URL: https://linkinghub.elsevier.com/retrieve/pii/S0306261918315150 (visited on 01/02/2025).

[17] A. R. Silva, H. Pousinho, and A. Estanqueiro. “A multistage stochastic approach for the optimal bidding of variable renewable energy in the day-ahead, intraday and balancing markets”. In: *Energy* 258 (Nov. 2022). ISSN: 03605442. DOI: 10.1016/j.energy.2022.124856. URL: https://linkinghub.elsevier.com/retrieve/pii/S0360544222017595 (visited on 02/04/2025).

[18] A. Gonzalez-Garrido et al. “Annual Optimized Bidding and Operation Strategy in Energy and Secondary Reserve Markets for Solar Plants With Storage Systems”. In: *IEEE Transactions on Power Systems* 34.6 (Nov. 2019), pp. 5115–5124. ISSN: 0885-8950, 1558-0679. DOI: 10.1109/TPWRS.2018.2869626. URL: https://ieeexplore.ieee.org/document/8458439/ (visited on 01/03/2025).

[19] X. A. Sun and A. J. Conejo. *Robust Optimization in Electric Energy Systems*. Vol. 313. International Series in Operations Research & Management Science. Cham: Springer International Publishing, 2021. ISBN: 978-3-030-85127-9 978-3-030-85128-6. DOI: 10.1007/978-3-030-85128-6. URL: https://link.springer.com/10.1007/978-3-030-85128-6 (visited on 02/26/2025).

[20] Y. Wang, H. Zhao, and P. Li. “Optimal Offering and Operating Strategies for Wind-Storage System Participating in Spot Electricity Markets with Progressive Stochastic-Robust Hybrid Optimization Model Series”. In: *Mathematical Problems in Engineering* 2019.1 (2019), p. 2142050. ISSN: 1563-5147. DOI: 10.1155/2019/2142050. URL: https://onlinelibrary.wiley.com/doi/abs/10.1155/2019/2142050 (visited on 12/12/2024).

[21] M. A. Mohamed, T. Jin, and W. Su. “An effective stochastic framework for smart coordinated operation of wind park and energy storage unit”. In: *Applied Energy* 272 (Aug. 2020). ISSN: 03062619. DOI: 10.1016/j.apenergy.2020.115228. URL: https://linkinghub.elsevier.com/retrieve/pii/S0306261920307406 (visited on 12/20/2024).

[22] M. Rahimiyan and L. Baringo. “Strategic Bidding for a Virtual Power Plant in the Day-Ahead and Real-Time Markets: A Price-Taker Robust Optimization Approach”. In: *IEEE Transactions on Power Systems* 31 (July 2016). ISSN: 0885-8950, 1558-0679. DOI: 10.1109/TPWRS.2015.2483781. URL: http://ieeexplore.ieee.org/document/7307233/ (visited on 12/19/2024).

[23] G. C. Pflug and A. Pichler. *Multistage Stochastic Optimization*. Springer Series in Operations Research and Financial Engineering. Cham: Springer International Publishing, 2014. ISBN: 978-3-319-08842-6 978-3-319-08843-3. DOI: 10.1007/978-3-319-08843-3. URL: https://link.springer.com/10.1007/978-3-319-08843-3 (visited on 02/17/2025).

[24] H. Khaloie et al. “Offering and bidding for a wind producer paired with battery and CAES units considering battery degradation”. In: *International Journal of Electrical Power & Energy Systems* 136 (Mar. 2022), p. 107685. ISSN: 01420615. DOI: 10.1016/j.ijepes.2021.107685. URL: https://linkinghub.elsevier.com/retrieve/pii/S0142061521009145 (visited on 12/13/2024).

[25] A. Fusco et al. “A multi-stage stochastic programming model for the unit commitment of conventional and virtual power plants bidding in the day-ahead and ancillary services markets”. In: *Applied Energy* 336 (Apr. 2023). ISSN: 03062619. DOI: 10.1016/j.apenergy.2023.120739. URL: https://linkinghub.elsevier.com/retrieve/pii/S0306261923001034 (visited on 01/30/2025).

[26] A. J. Conejo, M. Carrión, and J. M. Morales. *Decision Making Under Uncertainty in Electricity Markets*. Vol. 153. International Series in Operations Research & Management Science. Boston, MA: Springer US, 2010. ISBN: 978-1-4419-7420-4 978-1-4419-7421-1. DOI: 10.1007/978-1-4419-7421-1. URL: https://link.springer.com/10.1007/978-1-4419-7421-1 (visited on 02/17/2025).

[27] F. Gulotta et al. “Short-term uncertainty in the dispatch of energy resources for VPP: A novel rolling horizon model based on stochastic programming”. In: *International Journal of Electrical Power & Energy Systems* 153 (Nov. 1, 2023), p. 109355. ISSN: 0142-0615. DOI: 10.1016/j.ijepes.2023.109355. URL: https://www.sciencedirect.com/science/article/pii/S014206152300412X (visited on 12/30/2024).

[28] D. Wozabal and G. Rameseder. “Optimal bidding of a virtual power plant on the Spanish day-ahead and intraday market for electricity”. In: *European Journal of Operational Research* 280.2 (2020). ISSN: 03772217. DOI: 10.1016/j.ejor.2019.07.022. URL: https://linkinghub.elsevier.com/retrieve/pii/S0377221719305867 (visited on 12/18/2024).

[29] TenneT. *Marktrollen in de Nederlandse elektriciteitsmarkt*. Accessed: 2024-12-23. Dec. 23, 2024. URL: https://www.tennet.eu/nl/de-elektriciteitsmarkt/nederlandse-markt/marktrollen.

[30] X. Yan and N. A. Chowdhury. “Mid-term electricity market clearing price forecasting: A multiple SVM approach”. In: *International Journal of Electrical Power Energy Systems* 58 (2014), pp. 206–214. ISSN: 0142-0615. DOI: https://doi.org/10.1016/j.ijepes.2014.01.023. URL: https://www.sciencedirect.com/science/article/pii/S0142061514000362.

[31] EPEX SPOT. *Single Intraday Coupling (SIDC) Information Package*. Accessed: 2025-01-09. Oct. 2019. URL: https://www.epexspot.com/sites/default/files/2019-10/20191001_SIDC%20%28XBID%29%20Information%20Package.pdf.

[32] Nord Pool AS. *Product Specifications: Belgian and the Netherlands Market Areas*. Accessed: 2025-01-09. July 2024. URL: https://www.nordpoolgroup.com/4a787a/globalassets/download-center/rules-and-regulations/product-specifications-belgium-and-the-netherlands-18.07.2024.pdf.

[33] TenneT. *Market Types*. Accessed: 2024-12-23. Dec. 23, 2024. URL: https://www.tennet.eu/market-types.

[34] TenneT. *aFRR Manual for BSPs*. Tech. rep. Accessed: 2024-12-28. TenneT TSO B.V., 2024. URL: https://tennet-drupal.s3.eu-central-1.amazonaws.com/default/2024-12/aFRR%20manual%20for%20BSPs%20en.pdf.

[35] TenneT. *Imbalance Pricing System*. Tech. rep. Accessed: 2024-12-28. TenneT TSO B.V., 2024. URL: https://tennet-drupal.s3.eu-central-1.amazonaws.com/default/2024-10/Imbalance%20Pricing%20System.pdf.

[36] Royal Netherlands Meteorological Institute (KNMI). *KNMI Data Platform*. Accessed: 2025-06-02. 2025. URL: https://www.knmidata.nl/.

[37] EnAppSys Ltd.. *EnAppSys – Decision Support for Energy Markets*. Accessed: 2025-06-02. 2025. URL: https://www.enappsys.com/.

[38] T. G. Smith et al. *pmdarima: ARIMA estimators for Python*. [Online; accessed <today>]. 2017–. URL: http://www.alkaline-ml.com/pmdarima.

[39] J. P. Halchenko et al. *statsmodels/statsmodels: Release 0.14.2*. Version v0.14.2. Apr. 2024. DOI: 10.5281/zenodo.10984387. URL: https://doi.org/10.5281/zenodo.10984387.

[40] F. Pedregosa et al. “Scikit-learn: Machine Learning in Python”. In: *Journal of Machine Learning Research* 12 (2011), pp. 2825–2830.

[41] W. E. Hart, J.-P. Watson, and D. L. Woodruff. “Pyomo: modeling and solving mathematical programs in Python”. In: *Mathematical Programming Computation* 3.3 (2011), pp. 219–260.

[42] Gurobi Optimization, LLC. *Gurobi Optimizer Reference Manual*. 2024. URL: https://www.gurobi.com.

[43] KYOS Energy Analytics. *Energy Storage Report: Benchmark Assessments of Battery Energy Storage Value*. Accessed: 2025-05-28. KYOS Energy Analytics, May 2025. URL: https://www.kyos.com/wp-content/uploads/2025/01/KYOS-Energy-storage-report-May-2025-website.pdf.

[44] E22 Energy Storage Solutions. *Vanadium Redox Flow Battery 250-kW (1,000-kWh) Datasheet*. Tech. rep. Accessed: 2025-05-28. E22 Energy Storage Solutions, 2025. URL: https://www.energystoragesolutions.com/documents/Datasheet-E22-250kW.pdf.

A

Appendix

Table A.1: Summary statistics of imbalance prices and power production, grouped by the month in which each week falls

Month	Short Price Mean [€/MWh]	Short Price Std Dev [€/MWh]	Long Price Mean [€/MWh]	Long Price Std Dev [€/MWh]	Energy Production Mean [MWh/15 min]
March	106.11	243.62	81.73	236.49	0.267
June	114.66	174.87	97.67	182.72	0.271
September	126.02	345.83	66.83	300.51	0.507
December	174.84	288.77	145.80	290.03	0.710

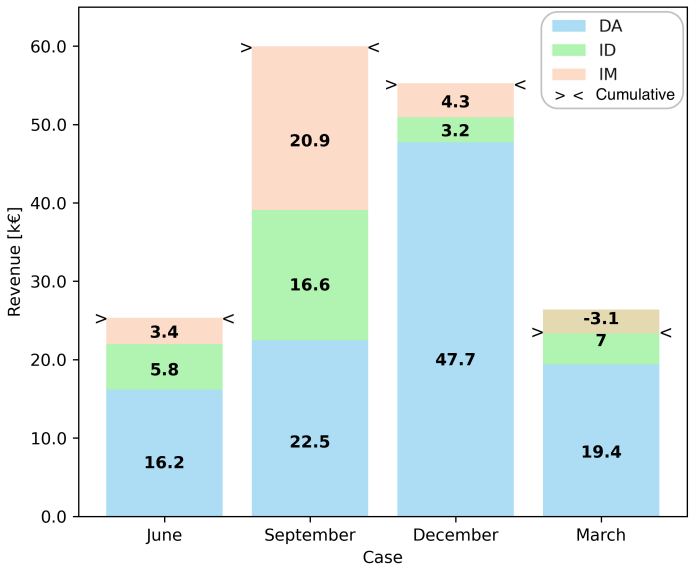

(a) Weekly breakdown of HPP revenues, grouped by the month in which each week falls.

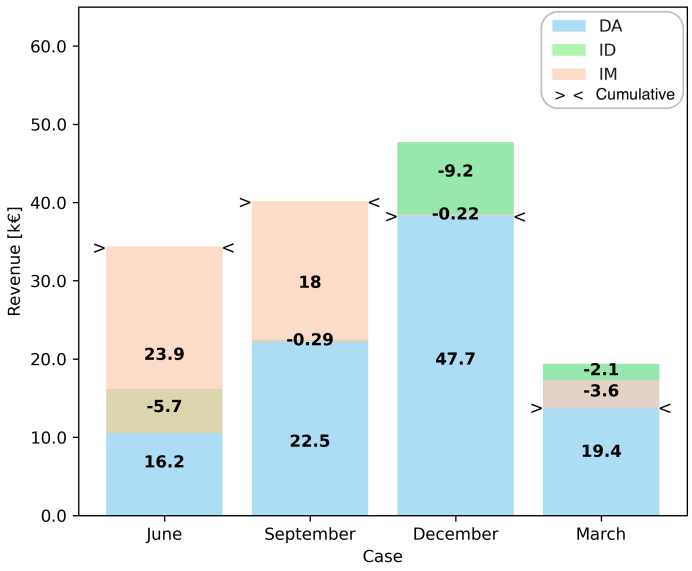

(b) Weekly breakdown of RES revenues, grouped by the month in which each week falls.

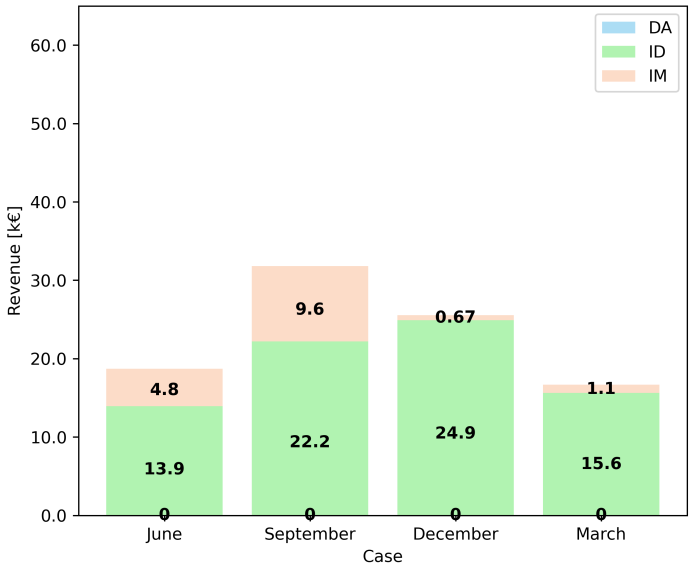

(c) Weekly breakdown of BESS revenues, grouped by the month in which each week falls.

Figure A.1: Per week revenue (in a month) for the three different cases: HPP, RES and BESS. Broken down by the three electricity markets: day-ahead (DA), intraday (ID) and imbalance (IM). In case of negative revenues, the cumulative revenue is indicated

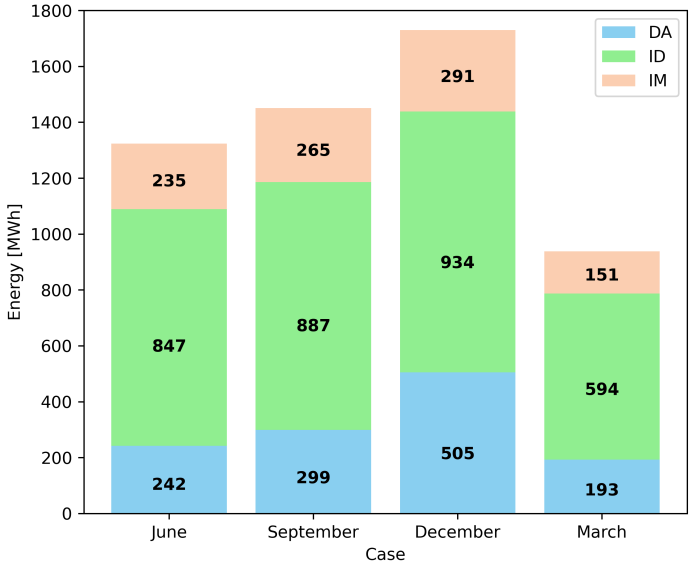

(a) Weekly breakdown of HPP absolute traded energy, grouped by the month in which each week falls.

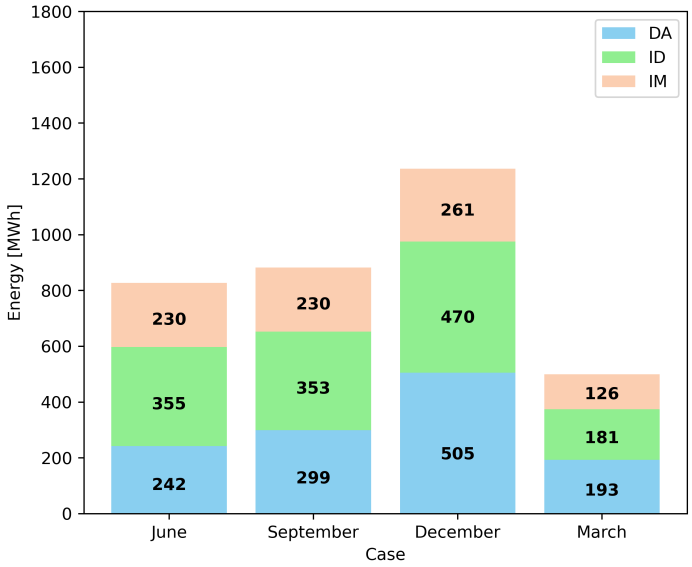

(b) Weekly breakdown of RES absolute traded energy, grouped by the month in which each week falls.

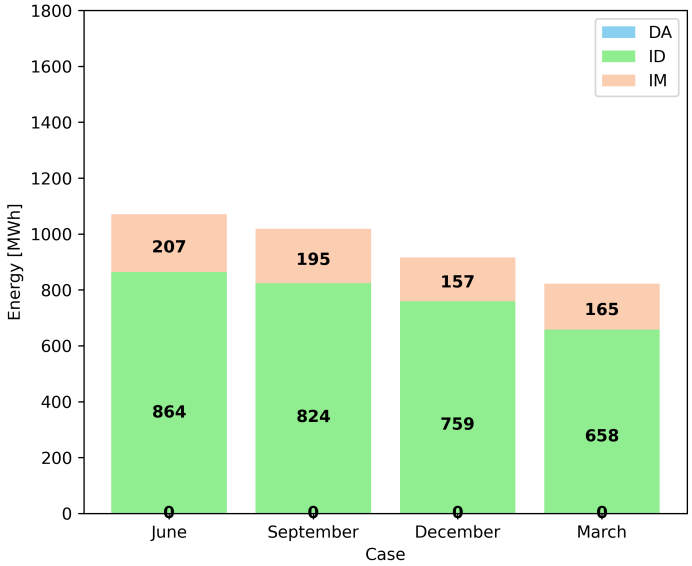

(c) Weekly breakdown of BESS absolute traded energy, grouped by the month in which each week falls.

Figure A.2: Per week absolute traded energy (in a month) for the three different cases: HPP, RES and BESS. Broken down by the three electricity markets: day-ahead (DA), intraday (ID) and imbalance (IM)

B

Assumption Testing and Model Sensitivity Results

Table B.1: Sensitivity analysis for HPP case: comparison of scenarios based on absolute revenue, traded energy, physical metrics, and normalized performance.

	Absolute Revenue [k€]			Traded Energy [GWh]			Physical [GWh]			Grid Utilization [-]		Normalized [€/MWh]	
Scenario	ID	IM	ID + IM	ID	IM	ID + IM	Generated	Curtailed	Battery Loss	Feed-in	Withdraw	Rev/Traded	Rev/Physical
BASE CASE	32.7	25.5	58.2	3.26	0.942	4.20	0.891	0.271	0.016	0.182	–	30.1	184
BESS Size 10 MWh	64.5	33.6	98.1	4.17	1.06	5.22	0.924	0.229	0.026	0.190	–	31.6	221
BESS Size 2.5 MWh	10.8	21.2	32.0	2.47	0.870	3.34	0.854	0.315	0.010	0.175	–	30.1	161
Grid Unconstrained	65.9	45.0	111	4.40	1.57	5.97	0.785	0.365	0.029	0.189	0.285	30.0	276
Grid Feed-in Constrained	67.0	32.4	99.4	4.37	1.49	5.87	0.761	0.389	0.028	0.247	0.277	28.9	270
Grid Withdrawal Constrained	31.2	34.8	66.0	3.32	0.982	4.30	0.919	0.242	0.018	0.140	–	31.0	187
Imbalance Price - Perfect Foresight	38.4	91.5	130	4.72	0.926	5.65	0.900	0.261	0.017	0.185	–	44.8	262
Imbalance Price - No Foresight	39.6	-0.927	38.7	3.07	0.960	4.03	0.932	0.229	0.018	0.191	–	24.5	155
Perfect Power Forecast	25.1	40.6	65.7	2.84	1.03	3.86	0.893	0.270	0.016	0.183	–	33.6	192
Reoptimization Every 30 mins	38.8	22.8	61.6	5.29	0.961	6.25	0.877	0.290	0.022	0.187	–	22.4	191
Reoptimization Every 2 Hours	19.9	24.4	44.2	2.07	0.902	2.97	0.918	0.248	0.013	0.181	–	35.7	163
Vanadium Redox Storage	19.0	19.0	38.0	2.29	0.858	3.14	0.869	0.297	0.014	0.174	–	32.8	166

Table B.2: Sensitivity analysis for HPP case: comparison of scenarios based on absolute revenue, traded energy, physical metrics, and normalized performance.

	Absolute Revenue			Traded Energy			Physical			Grid Utilization		Normalized	
Scenario	ID	IM	ID + IM	ID	IM	ID + IM	Generated	Curtailed	Battery Loss	Feed-in	Withdraw	Rev/Traded	Rev/Physical
BESS Size 10 MWh	97.4%	31.9%	68.7%	27.7%	12.1%	24.2%	3.70%	-15.5%	62.5%	4.06%	–	4.98%	20.0%
BESS Size 2.5 MWh	-67.0%	-16.7%	-45.0%	-24.2%	-7.64%	-20.5%	-4.15%	16.2%	-37.5%	-4.00%	–	0.00%	-12.3%
Grid Unconstrained	102%	76.5%	90.6%	35.0%	66.7%	42.1%	-11.9%	34.7%	81.2%	3.57%	–	-0.33%	50.1%
Grid Feed in Constrained	105%	27.1%	70.9%	34.0%	58.6%	39.5%	-14.6%	43.5%	75.0%	35.5%	–	-4.00%	46.6%
Grid withdrawal Constrained	-4.49%	36.6%	13.5%	1.84%	4.25%	2.38%	3.14%	-10.7%	12.5%	-23.5%	–	2.99%	1.58%
Imbalance price - perfect foresight	17.5%	259%	123%	44.8%	-1.70%	34.4%	1.01%	-3.69%	6.25%	1.26%	–	48.8%	42.4%
Imbalance price - no foresight	21.4%	-104%	-33.5%	-6.04%	1.91%	-4.26%	4.60%	-15.5%	12.5%	4.94%	–	-18.6%	-15.8%
Perfect power forecast	-23.1%	59.2%	13.0%	-13.0%	8.92%	-8.09%	0.22%	-0.37%	0.00%	0.33%	–	11.6%	4.40%
Reoptimization every 30 mins	18.9%	-10.6%	5.96%	62.0%	2.02%	48.6%	-1.57%	7.01%	37.5%	2.47%	–	-25.6%	3.75%
Reoptimization every 2 hours	-39.1%	-4.50%	-23.9%	-36.7%	-4.25%	-29.4%	3.03%	-8.49%	-18.8%	-0.88%	–	18.6%	-11.2%
Vanadium Redox storage	-41.7%	-25.7%	-34.7%	-30.0%	-8.92%	-25.2%	-2.47%	9.59%	-12.5%	-4.61%	–	8.97%	-10.0%

Table B.3: Sensitivity analysis for RES case: absolute revenue, traded energy, physical metrics, and normalized performance.

	Revenue [k€]			Traded Energy [GWh]			Physical [GWh]			Grid Utilization [-]	Normalized [€/MWh]	
Scenario	ID	IM	ID + IM	ID	IM	ID + IM	Generated	Curtailed	Battery Loss		Rev/Traded	Rev/Physical
BASE CASE	-17.3	38.1	20.8	1.36	0.847	2.21	0.789	0.390	–	0.163	36.7	160
BESS Size 10 MWh	–	–	–	–	–	–	–	–	–	–	–	–
BESS Size 2.5 MWh	–	–	–	–	–	–	–	–	–	–	–	–
Grid Constrained	–	–	–	–	–	–	–	–	–	–	–	–
Grid Feed-in Constrained	–	–	–	–	–	–	–	–	–	–	–	–
Grid Withdrawal Constrained	–	–	–	–	–	–	–	–	–	–	–	–
Imbalance Price - Perfect Foresight	-9.33	77.9	68.6	0.565	0.736	1.30	0.795	0.384	–	0.164	54.5	219
Imbalance Price - No Foresight	7.03	-13.3	-6.31	1.15	0.814	1.96	0.832	0.347	–	0.172	39.2	120
Perfect Power Forecast	-26.7	28.1	1.43	1.58	0.830	2.41	0.792	0.386	–	0.163	29.4	135
Reoptimization Every 30 mins	-8.74	14.2	5.42	2.21	0.847	3.05	0.781	0.398	–	0.166	25.9	142
Reoptimization Every 2 Hours	-10.3	-3.50	-13.8	0.884	0.785	1.67	0.803	0.376	–	0.161	31.6	114
Vanadium Redox Storage	–	–	–	–	–	–	–	–	–	–	–	–

Table B.4: Sensitivity analysis for RES case: percentage change relative to base case, across revenue, traded energy, physical metrics, and normalized performance.

	Revenue			Traded Energy			Physical			Grid Utilization	Normalized	
Scenario	ID	IM	ID + IM	ID	IM	ID + IM	Generated	Curtailed	Battery Loss		Rev/Traded	Rev/Physical
BESS Size 10 MWh	–	–	–	–	–	–	–	–	–	–	–	–
BESS Size 2.5 MWh	–	–	–	–	–	–	–	–	–	–	–	–
Grid Unconstrained	–	–	–	–	–	–	–	–	–	–	–	–
Grid Feed-in Constrained	–	–	–	–	–	–	–	–	–	–	–	–
Grid Withdrawal Constrained	–	–	–	–	–	–	–	–	–	–	–	–
Imbalance Price - Perfect Foresight	-46.0%	105%	230%	-58.4%	-13.1%	-41.0%	0.76%	-1.54%	–	0.68%	48.5%	36.9%
Imbalance Price - No Foresight	-141%	-135%	-130%	-15.5%	-3.90%	-11.0%	5.45%	-11.0%	–	5.41%	6.81%	-25.5%
Perfect Power Forecast	54.5%	-26.1%	-93.1%	16.0%	-2.01%	9.07%	0.38%	-1.03%	–	0.37%	-19.9%	-15.6%
Reoptimization Every 30 mins	-49.4%	-62.8%	-73.9%	62.3%	0.00%	38.4%	-1.01%	2.05%	–	1.72%	-29.4%	-11.2%
Reoptimization Every 2 Hours	-40.2%	-109%	-167%	-35.0%	-7.32%	-24.3%	1.77%	-3.59%	–	-1.04%	-13.9%	-28.6%
Vanadium Redox Storage	–	–	–	–	–	–	–	–	–	–	–	–

Table B.5: Sensitivity analysis for BESS case: absolute revenue, traded energy, physical metrics, and normalized performance.

	Revenue [k€]			Traded Energy [GWh]			Physical [GWh]			Grid Utilization [-]	Normalized [€/MWh]	
Scenario	ID	IM	ID + IM	ID	IM	ID + IM	Generated	Curtailed	Battery Loss		Rev/Traded	Rev/Physical
BASE CASE	76.6	16.1	92.8	3.11	0.723	3.83	–	–	0.029	0.291	24.2	–
BESS Size 10 MWh	153	32.2	185	6.21	1.45	7.66	–	–	0.055	0.292	24.2	–
BESS Size 2.5 MWh	38.4	8.08	46.5	1.55	0.362	1.92	–	–	0.014	0.292	24.3	–
Grid Unconstrained	–	–	–	–	–	–	–	–	–	–	–	–
Grid Feed-in Constrained	–	–	–	–	–	–	–	–	–	–	–	–
Grid Withdrawal Constrained	–	–	–	–	–	–	–	–	–	–	–	–
Imbalance Price - Perfect Foresight	117	78.3	195	3.70	0.720	4.42	–	–	0.025	0.233	49.2	–
Imbalance Price - No Foresight	66.6	14.8	81.4	2.77	1.20	3.97	–	–	0.029	0.297	18.4	–
Perfect Power Forecast	–	–	–	–	–	–	–	–	–	–	–	–
Reoptimization Every 30 mins	87.6	6.47	94.1	4.53	0.702	5.24	–	–	0.043	0.301	18.0	–
Reoptimization Every 2 Hours	63.5	23.3	86.8	2.15	0.768	2.92	–	–	0.019	0.294	29.7	–
Vanadium Redox Storage	42.4	8.41	50.8	1.46	0.353	1.81	–	–	0.019	0.291	28.1	–

Table B.6: Sensitivity analysis for BESS case: percentage change relative to base case, across revenue, traded energy, physical metrics, and normalized performance.

	Revenue			Traded Energy			Physical			Grid Utilization	Normalized	
Scenario	ID	IM	ID + IM	ID	IM	ID + IM	Generated	Curtailed	Battery Loss		Rev/Traded	Rev/Physical
BESS Size 10 MWh	100%	99.2%	99.9%	99.9%	101%	100%	–	–	89.7%	0.07%	0.00%	–
BESS Size 2.5 MWh	-49.9%	-49.9%	-49.9%	-50.0%	-49.9%	-50.0%	–	–	-51.7%	0.10%	0.41%	–
Grid Unconstrained	–	–	–	–	–	–	–	–	–	–	–	–
Grid Feed-in Constrained	–	–	–	–	–	–	–	–	–	–	–	–
Grid Withdrawal Constrained	–	–	–	–	–	–	–	–	–	–	–	–
Imbalance Price - Perfect Foresight	52.8%	385%	111%	19.2%	-0.41%	15.5%	–	–	-13.8%	-20.2%	103%	–
Imbalance Price - No Foresight	-13.2%	-8.11%	-12.3%	-10.9%	66.0%	3.66%	–	–	0.00%	1.96%	-24.0%	–
Perfect Power Forecast	–	–	–	–	–	–	–	–	–	–	–	–
Reoptimization Every 30 mins	14.3%	-59.9%	1.41%	46.0%	-2.90%	36.8%	–	–	48.3%	3.26%	-25.6%	–
Reoptimization Every 2 Hours	-17.2%	44.2%	-6.48%	-30.7%	6.22%	-23.7%	–	–	-34.5%	0.96%	22.7%	–
Vanadium Redox Storage	-44.7%	-47.9%	-45.3%	-53.1%	-51.2%	-52.8%	–	–	-34.5%	-0.17%	16.1%	–